Consistency Between Liquefaction Prediction Based on SPT, CPT, and V_S Measurements at the Same Sites

by

James Calvin Chrisley, B.S.

Report

Presented to the Faculty of the Graduate School

of The University of Texas at Austin

in Partial Fulfillment

of the Requirements

for the Degree of

Master of Science in Engineering

The University of Texas at Austin

December 1999

REPORT DOCUMENTATION PAGE	Form Approved OMB No. 0704-0188

1. AGENCY USE ONLY *(Leave blank)*	2. REPORT DATE	3. REPORT TYPE AND DATES COVERED
	27.Jan.00	MAJOR REPORT

4. TITLE AND SUBTITLE
MAJOR REPORT: CONSISTENCY BETWEEN LIQUEFACTION PREDICTION BASED ON SPT, CPT, AND VS MEASUREMENTS AT THE SAME SITES

5. FUNDING NUMBERS

6. AUTHOR(S)
CAPT CHRISLEY JAMES C

7. PERFORMING ORGANIZATION NAME(S) AND ADDRESS(ES)
UNIVERSITY OF TEXAS AUSTIN

8. PERFORMING ORGANIZATION REPORT NUMBER

9. SPONSORING/MONITORING AGENCY NAME(S) AND ADDRESS(ES)
THE DEPARTMENT OF THE AIR FORCE
AFIT/CIA, BLDG 125
2950 P STREET
WPAFB OH 45433

10. SPONSORING/MONITORING AGENCY REPORT NUMBER
FY00-40

11. SUPPLEMENTARY NOTES

12a. DISTRIBUTION AVAILABILITY STATEMENT
Unlimited distribution
In Accordance With AFI 35-205/AFIT Sup 1

12b. DISTRIBUTION CODE

13. ABSTRACT *(Maximum 200 words)*

DISTRIBUTION STATEMENT A
Approved for Public Release
Distribution Unlimited

14. SUBJECT TERMS	15. NUMBER OF PAGES
	131
	16. PRICE CODE

17. SECURITY CLASSIFICATION OF REPORT	18. SECURITY CLASSIFICATION OF THIS PAGE	19. SECURITY CLASSIFICATION OF ABSTRACT	20. LIMITATION OF ABSTRACT

Consistency Between Liquefaction Prediction Based on SPT, CPT, and V_S Measurements at the Same Sites

APPROVED BY

SUPERVISING COMMITTEE:

_____

_____

_____

ACKNOWLEDGEMENTS

The author would like to thank Dr. Kenneth H. Stokoe II for his never ending support during the initial, research, and writing phases of this report. The author would also like to thank Dr. Ronald D. Andrus for providing references for sites that could not be located locally. Finally, the author would like to thank Dr. Alan F. Rauch for reviewing this manuscript.

TABLE OF CONTENTS

LIST OF TABLES

LIST OF FIGURES

CHAPTER 1

INTRODUCTION

1.1 BACKGROUND

Liquefaction induced ground failure is a major cause of damage during earthquakes. Liquefaction is a phenomenon that is not limited to one specific region in the world, but occurs worldwide. Liquefaction has not only caused major financial property loss but also has been attributed to the loss of lives throughout the world. Since the early 1970's, the prediction of liquefaction potential has been an area of high interest throughout the engineering community. The ability to predict whether or not a site in an active seismic zone will liquefy has the potential of saving a tremendous amount of money in property losses and more importantly the potential to save lives.

The key to predicting liquefaction potential is to have a simple, low cost, accurate method. In the early 1970's, a procedure was developed by Seed and Idriss (1971) to predict liquefaction potential by using blow counts from the Standard Penetration Test (SPT). The method was termed the *simplified procedure* and is currently used in the United States and throughout the world. The original procedure correlated blow-count measurements with Cyclic Stress Ratio (CSR). CSR is a parameter that represents the seismic loading on the soil during an earthquake. Since 1971, the procedure has been updated and improved. In addition, other investigators have produced similar correlations using tip resistance measurements from the Cone Penetration Test (CPT) (Robertson and Wride 1998), and shear wave velocity (V_S) measurements (Andrus et al. 1997). Measured values from the CPT and V_S methods have also been correlated with CSR. The correlations between each of the measured values and CSR consist of boundary curves that are used to predict whether or not a specific site will liquefy under a specific earthquake loading.

Until recently each method was generally used independently to predict the liquefaction potential of a specific site. Few attempts have been made to present correlations between the three methods and, in general, these attempts have lacked enough data to show definite, indisputable correlations. By making comparisons between the three different methods, future investigators will be able to improve predictions of liquefaction potential. When two or more methods are used on the same site, one's confidence in the prediction of whether the site will or will not liquefy is certainly increased when the different approaches agree.

To establish confidence in any attempted correlation between the three methods, real field data must be presented as evidence. The data must be from a wide range of sites that have been subjected to different earthquake loadings. The data set must have similar numbers of sites that liquefied and sites that did not liquefy. In addition, sites used in a particular correlation must have had at least two types of measurements made in close proximity on the site. In this report, an attempt is made to present correlations between the three field investigation techniques based on a large number of sites from around the world. This data represents the largest data set to date with which an attempt has been made to correlate predicted liquefaction performance between the three different field techniques.

1.2 PURPOSE

This report uses the Vs data set compiled by Andrus, Stokoe, and Chung (1999) and presents SPT and CPT measurements from the same sites. In general, each site has experienced at least one earthquake, determination of field liquefaction has been made, at least one V_S measurement has been made in the critical layer, and at least one of the other field measurements, SPT or CPT, has been performed in the same critical layer. To begin, each type of measured field data is plotted with the presently accepted correlation for that particular technique and evaluated for accuracy. For sites that had at least two different measurements, a comparison of the

methods is made. It is shown, for this particular data set, which current method was able to most accurately predict liquefaction. Changes to the currently accepted correlations, made to obtain better agreement between the different methods, are then discussed. Finally, correlations between the three different field measurement techniques are presented; that is, $V_{S1} - N_{1,60}$, $V_{S1} - q_{c1,N}$, and $q_{c1,N} - N_{1,60}$ relationships are presented for the potentially liquefiable materials in this data set.

1.3 REPORT OVERVIEW

In Chapter 2 the background information on predicting liquefaction utilizing the three different methods and correlations used in this report are presented. The data set and sources used for this report are presented in Chapter 3. The V_S, SPT, and CPT correlations are discussed in Chapters 4, 5, and 6, respectively. Each correlation is presented with the respective data set and the performance of each method is evaluated. The consistencies and inconsistencies between the different methods are discussed in Chapter 7. Finally, recommendations for possible changes in the database and correlations between the three different methods are also presented in Chapter 7.

CHAPTER 2

BACKGROUND ON PREDICTION OF LIQUEFACTION POTENTIAL

2.1 OVERVIEW OF LIQUEFACTION

Liquefaction is a phenomenon that has most often been associated with saturated loose sand layers. During an earthquake, the soil is subjected to dynamic stresses, which cause excess positive pore water pressures to develop rapidly. The dynamic loading on the soil occurs so quickly that the soil does not have enough time to drain and, in a liquefiable deposit, the pore pressures increase thereby reducing the effective stresses. Simultaneously, the strength of the soil is greatly reduced and the soil begins to act like a liquid, and any structure relying on the strength of the sand layer can be damaged severely due to the loss of support.

Liquefiable layers of soil are generally located beneath the ground water table and relatively close to the surface (typically within 15 m of the ground surface). Loose non-plastic soils are the most susceptible to liquefaction, but under certain circumstances clays and silts have been known to show 'liquefaction-like' effects (Seed and Idriss, 1982).

2.2 OVERVIEW OF LIQUEFACTION PREDICTION METHODS

Three field methods used to evaluate liquefaction potential are based on shear wave velocity, SPT blow counts, and CPT tip resistance. Other methods have been developed using different field measurement techniques, but only these three methods are considered in this report. All methods are based on the concept of obtaining the specific field measurement and plotting it against the estimated cyclic stress ratio (CSR). The plotted value is then compared with a pre-determined boundary curve. If the plotted value is on one side of the boundary, the site is predicted to liquefy. If the plotted value is on the opposite side of the boundary, the

site is predicted to not liquefy. The boundary curves were determined by compiling observations of field performance of various sites under actual earthquake loading. The techniques used to predict liquefaction potential sound simple, but some analysis is required to determine the most critical values within a particular soil deposit.

When comparing one method to another at a particular site, the only difference between the methods should be the type of field value measured. The depth of the measurement and the calculation of CSR should be identical in both methods. In an ideal case, all methods used at a site should predict the same result. In this chapter, the identical portions of all three methods are described. The analysis and evaluation of the specific field measurements are discussed in Chapters 4, 5, and 6.

Andrus, Stokoe and Chung (1999) presented all sites used in this report in a report from the National Institute of Standards and Technology entitled, "Draft Guidelines for Evaluating Liquefaction Resistance Using Shear Wave Velocity Measurements and Simplified Procedures."

2.2.1 Determination of The Critical Layer

The first step in performing a simplified liquefaction analysis is to determine whether or not the proper soil conditions are present that would allow liquefaction to occur. Field investigations must be accomplished to determine the soil profile of the site and to determine the most critical layer of soil within the soil profile. The critical layer is the layer within a soil profile that is most susceptible to liquefaction. Since liquefaction has been observed to occur in saturated loose sand deposits, Andrus et al. (1999) defined the critical layer as the layer of non-plastic soil beneath the groundwater table where values of V_S and values of penetration resistance were generally the least, and where the cyclic stress ratio relative to V_S was the greatest. The key point for determining the critical layer is finding the layer of loose granular soil within the deposit that has the lowest measured value of V_S, SPT or CPT, and

the highest CSR relative to the field measured value. This relative comparison determines the proper depth to perform the liquefaction hazard analysis. Obviously, measured field values and estimated values for CSR are calculated throughout the soil profile before the critical layer can be designated.

In this report, the critical layers for each site are the ones that were calculated by Andrus et al. (1999). To be consistent, the critical layer defined by Andrus et al. (1999) for a particular site was also used as the critical layer for the SPT and CPT profiles.

2.2.2 Calculation of Cyclic Stress Ratio

The cyclic stress ratio, CSR, is calculated at each depth in the soil profile based on a specific or estimated earthquake loading. The larger the cyclic shear stresses generated by an earthquak, the larger the CSR. Seed and Idriss (1971) defined CSR as:

$$CSR = \tau_{av} / \sigma'_V = 0.65 \{a_{max} / g\} \{\sigma_V / \sigma'_V\} r_d \qquad (2.1)$$

where

τ_{av} = the average equivalent shear stress generated by the earthquake (assumed to be 0.65 of the maximum induced stress),

a_{max} = the peak horizontal ground surface acceleration,

σ'_V = the initial effective overburden stress at the specific depth,

σ_V = the total overburden stress at the same depth,

g = the acceleration of gravity, and

r_d = the shear stress reduction coefficient.

In this report, the CSR for each site was calculated and presented by Andrus et al. (1999). This value was also used for the SPT and CPT correlations so that the three

methods could be compared on an equal basis. Even though each parameter of CSR was not specifically calculated in this report, the following is presented for informational purposes.

2.2.2.1 Peak Horizontal Ground Surface Acceleration

Peak horizontal ground surface acceleration is a measured value of earthquake intensity. Youd et al. (1997) defined it as the peak value in a horizontal ground acceleration record that would occur at the site without the influence of excess pore-water pressures or liquefaction that might develop. Horizontal accelerations can be estimated by using empirical attenuation relationships that estimate a_{max} based on earthquake magnitude, distance from the earthquake source, and local site conditions. Horizontal accelerations can also be estimated by utilizing data from previous earthquakes of similar size and distance.

2.2.2.2 Total and Effective Overburden Stresses

Total and effective overburden stresses are calculated at an average depth within the critical layer using the density of the particular soils above and below the ground water table. In cases where the density of the soil cannot be measured, estimates are made based on previous experience with similar soils. The use of estimated soil densities does not cause an adverse impact on the calculations, since the CSR is not sensitive to changes in soil density.

The most important aspect for calculation of CSR is determination of the depth of the ground water table. Effective overburden stress and CSR are sensitive to the ground water table depth. To calculate a realistic CSR, the ground water table depth must be known accurately (assumed to be within about one meter in this report).

2.2.2.3 Stress Reduction Coefficient

The stress reduction coefficient, r_d, is a term used to model the soil column as a deformable body rather than a rigid body. Values for r_d have been presented by various sources, including Seed and Idriss (1971), Liao and Whitman (1986), Robertson and Wride (1997), and revised values by Idriss (1998; 1999). The value of r_d depends on the depth (z) below the surface and the magnitude of the earthquake, M_W. As z increases and M_W decreases, r_d decreases. Values of r_d plotted in Figure 2 were determined analytically using various earthquake magnitudes and differing soil conditions. For depths below 15 m, there is not enough to data assure that the presented values are correct. Therefore, caution should be used when making a CSR calculation for depths below 15 m. In the calculation of the CSR values used in this report, Andrus et al. (1999) used the revised r_d values proposed by Idriss (1998; 1999) as shown in Figure 2.1.

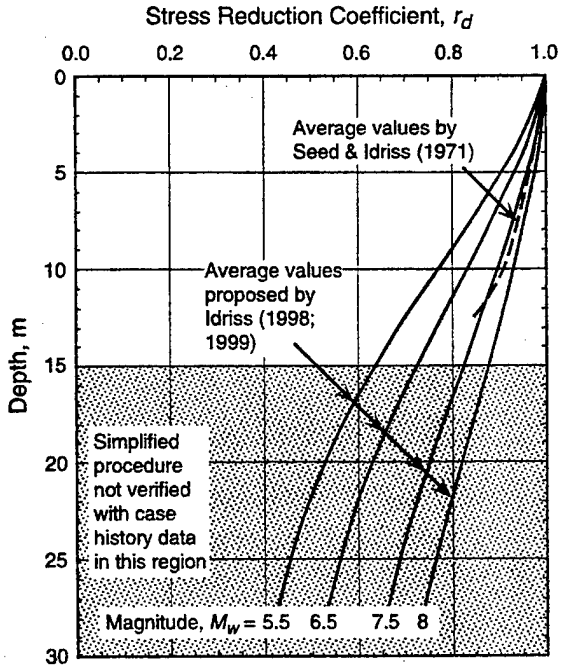

Fig. 2.1 - Relationship Between Average Stress Reduction Coefficient and Depth Proposed by Idriss (1998; 1999) with Average of Range Determined by Seed and Idriss (1971) (from Andrus et al., 1999).

2.2.3 Calculation of the Equivalent Cyclic Stress Ratio for $M_W = 7.5$

When developing the simplified procedure, Seed and Idriss (1971) based the original SPT correlation upon data collected from earthquakes that had approximate magnitudes equal to 7.5. To use the same correlations, different earthquake magnitudes must be corrected to an equivalent $M_W = 7.5$ value. Therefore, a CSR induced by an earthquake with a M_W equal to something other than 7.5 must be adjusted to an equivalent value. The equivalent value is termed $CSR_{7.5}$. $CSR_{7.5}$ is defined as:

$$CSR_{7.5} = (CSR)/(MSF) \tag{2.2}$$

where

MSF = Magnitude Scaling Factor, and

CSR = Calculated Cyclic Stress Ratio.

Seed and Idriss (1982) first presented the magnitude scaling factor to create equivalent earthquake loadings for earthquakes with magnitudes other than 7.5. Throughout the 1980's and 1990's, other investigators have calculated different values for MSF. In this report, MSF is calculated using the equation presented by Youd et al. (1997):

$$MSF = \{M_w/7.5\}^n \tag{2.3}$$

where

M_w = moment magnitude of the earthquake of interest, and

n = an exponent.

The 1996 NCEER workshop recommended that n = -2.56 (Idriss, personal communication to T.L. Youd, 1995) as the lower bound for earthquakes with $M_w \leq$ 7.5 and Andrus and Stokoe (1997) recommended an upper bound with n = -3.3 for earthquakes with $M_w \leq 7.5$. The use of the lower bound value produces more

conservative values for MSF. Therefore, the $CSR_{7.5}$ values, calculated by Andrus et al. 1999, reported in this study were determined using the lower bound value, n = -2.56.

2.2.4 Boundary Curves Used to Predict Liquefaction Potential

Throughout the previous three decades, there have been many correlations based on the simplified procedure developed by Seed and Idriss (1971). The three most commonly used are the V_S, SPT, and CPT based correlations.

All three correlations require that the field value be corrected before the respective correlation is used. V_S field measurements are corrected for overburden stress and the corrected values are termed V_{S1} values in units of meters per second. Equation 4.1, presented in Chapter 4, is used to correct V_S values to V_{S1} values. In addition to being corrected for overburden stresses, SPT field values (N-Values) require additional corrections that account for variations in SPT testing techniques. The corrected values for the SPT test are termed $N_{1,60}$ values and are in units of blows per foot. Equation 5.1, presented in Chapter 5, is used to calculate $N_{1,60}$ values. CPT field values (q_c values) are also corrected for overburden stress, and additionally, are normalized to one atmosphere of pressure. Overburden stress corrected normalized q_c values are termed $q_{c1,N}$ values. Due to the normalization, $q_{c1,N}$ values are unitless. Equation 6.1, presented in Chapter 6, is used to correct q_c values to $q_{c1,N}$ values. The following is an overview of the different boundaries used by different investigators over the past three decades.

2.2.4.1 V_{S1} Boundary Curves

Figure 2.2 shows seven boundary curves that have been proposed to evaluate a site using overburden stress corrected shear wave velocity. These curves are based on V_{S1} values, earthquakes with $M_W = 7.5$, and only apply to clean sands.

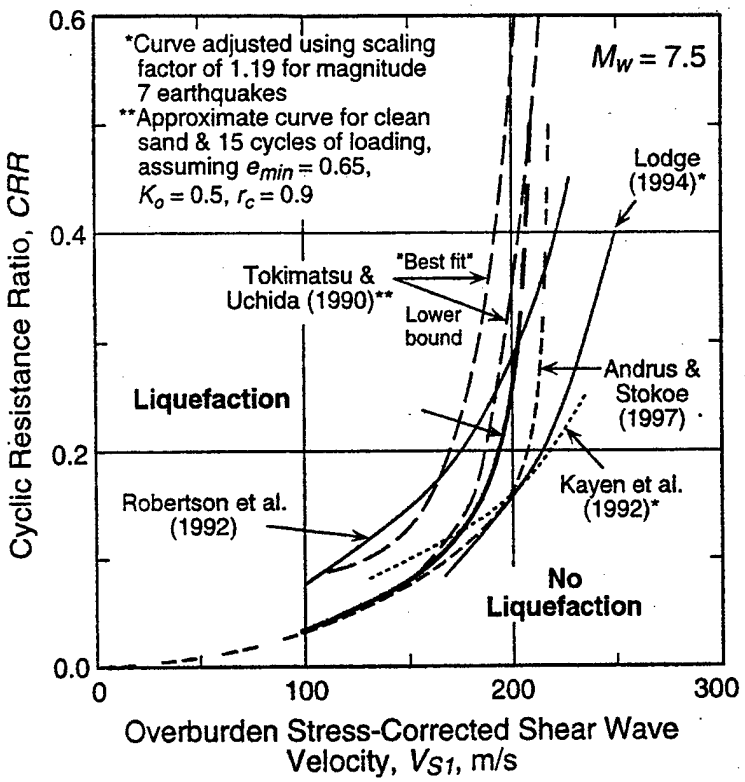

Fig. 2.2 - Comparison of Seven Relationships Between Liquefaction Resistance and Corrected Shear Wave Velocity for Clean Granular Soils (from Andrus et al., 1999).

2.2.4.2 SPT Boundary Curves

Figure 2.3 shows the Seed et al. (1985) curve, the most widely used correlation for evaluating potentially liquefiable sites. The boundaries were determined using $N_{1,60}$ values in conjunction with the fines content of the soil. Figure 2.4 depicts other boundaries that have been developed to evaluate liquefaction potential. These boundaries are based on equivalent SPT N-values and the mean grain size (D_{50} value) for the soil. All boundaries shown have been used throughout the world.

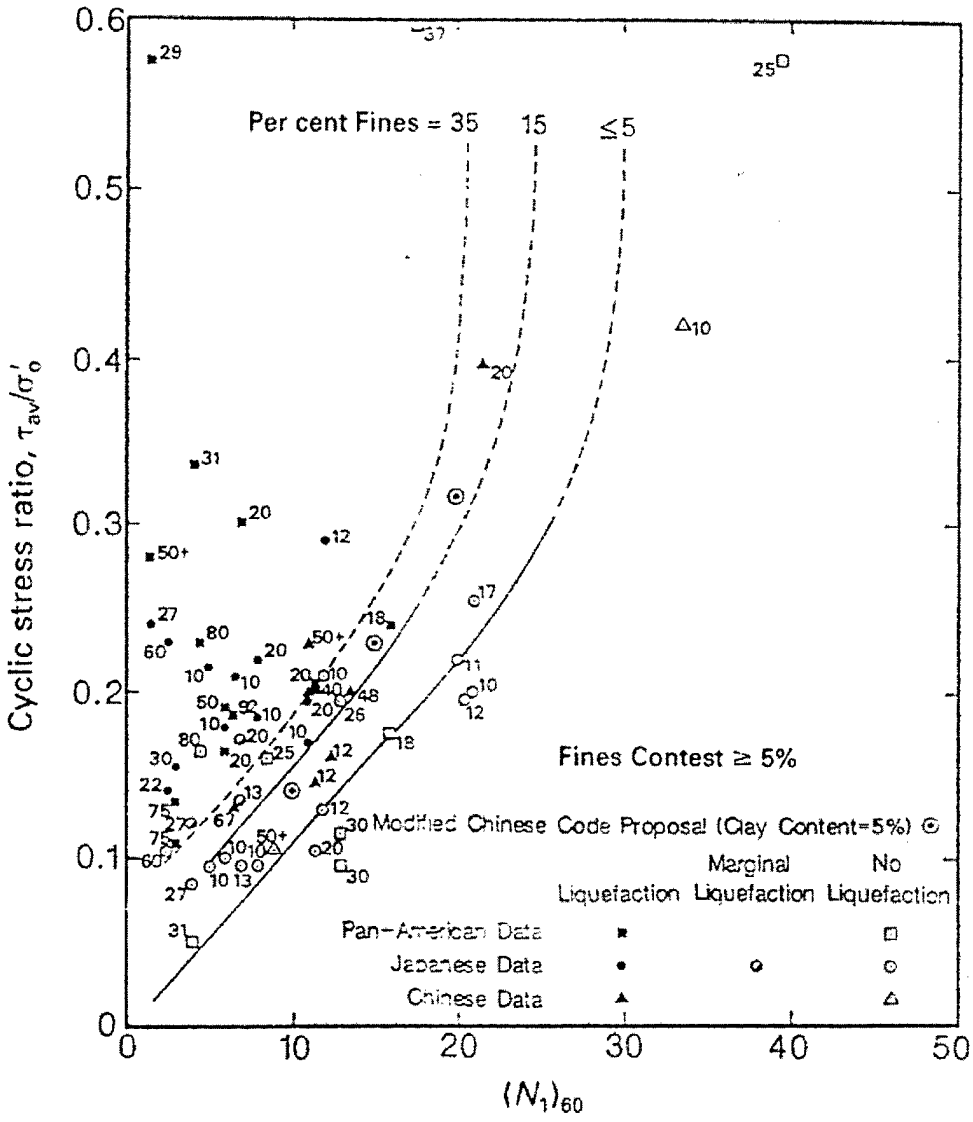

Fig. 2.3 – Correlation of CSR and SPT $N_{1,60}$ Values for Sands Based on Field Performance Data (from Seed et al., 1985).

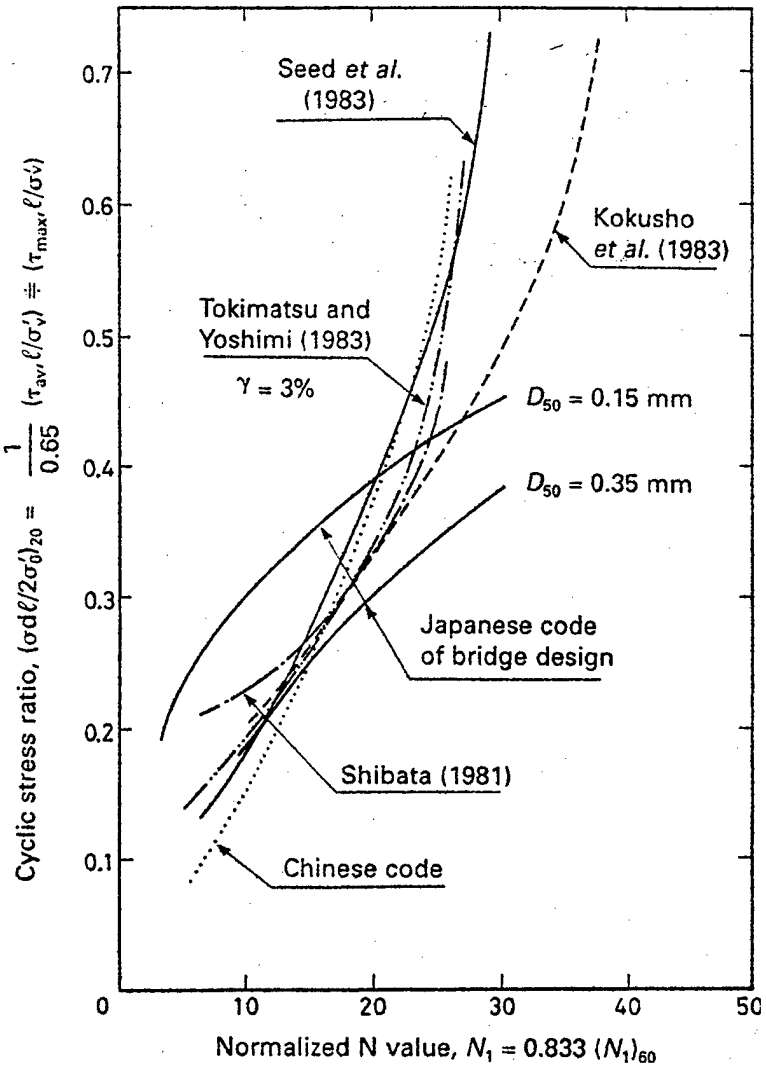

Fig. 2.4 – Other Liquefaction Correlations Based on Normalized N-Value (from Ishihara, 1996).

2.2.4.3 CPT Boundary Curves

Figure 2.5 shows some of the most widely used correlations to evaluate sites based on CPT cone resistance, q_c. These correlations are based on overburden stress corrected CPT cone resistance, q_{c1}, and the D_{50} value for the soil. Figure 2.6 presents the boundary curves presented by Stark and Olson (1995). These curves are

based on normalized overburden stress corrected CPT tip resistance, $q_{c1,N}$, the D_{50} value, and the average fines content.

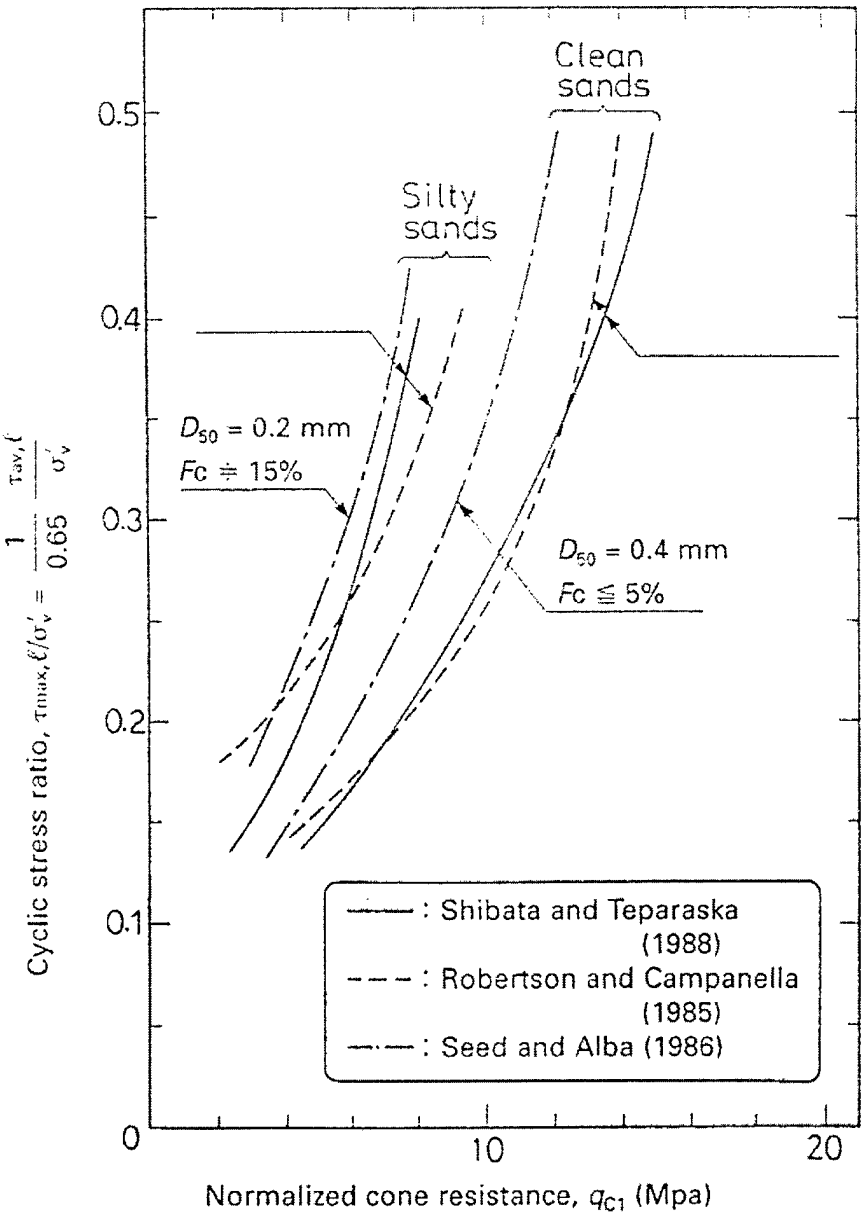

Fig. 2.5 – Various Boundaries in Use to Correlate Overburden Stress Corrected CPT Cone Resistance, q_{c1}, with Liquefaction Resistance (from Ishihara, 1996).

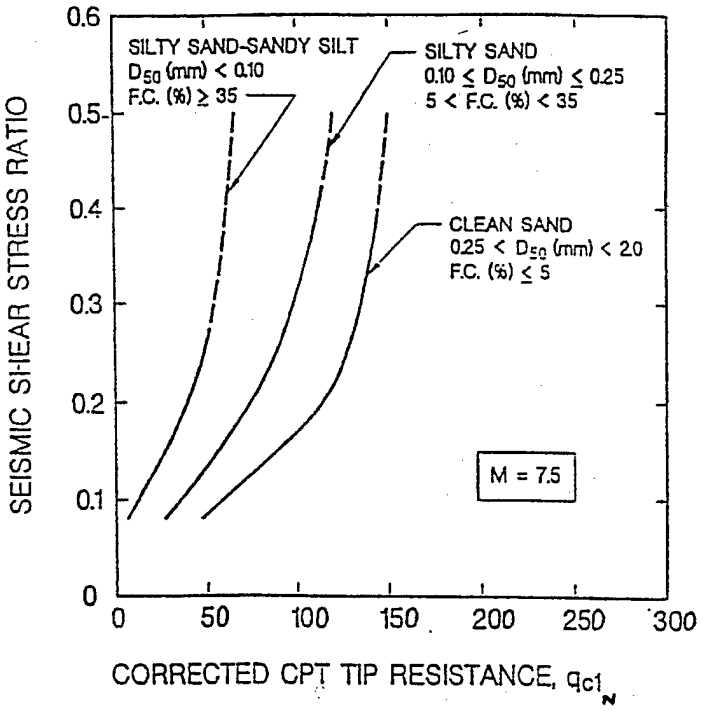

Fig 2.6 – Liquefaction Boundaries Developed by Stark and Olson (1995) for Normalized Overburden Stress Corrected CPT Tip Resistance, $q_{c1,N}$, D_{50}, and Fines Content.

2.3 Correlations Used In This Report

To analyze the database in this report, specific curves were chosen as the best correlations to use in evaluating each of the sites contained within the database. Since the use of different bounding curves will result in different results, which curves to choose was an important aspect of this study. Each of the three methods utilized herein have all been widely used.

The shear wave correlation used was presented by Andrus, Stokoe, and Chung (1999). The boundary curves used for this correlation are shown in Figure 2.7. The boundary curves in this correlation were chosen because the curves are based on the database presented in this study. This allows the shear wave velocity curves to be compared to the other two methods used in the study.

The boundary curves presented by Seed et al. (1985) and shown in Figure 2.3 were used to correlate the SPT database. These curves were chosen for this study because they have been widely and successfully used for many years.

The Stark and Olson (1995) curves were chosen to analyze the CPT data. Figure 2.6 depicts these curves. These curves are based on fines content of the subject soil. Other boundary curves, based on CPT, are based on q_c and D_{50}. In general, no D_{50} data were available for the case histories in this study, so boundary curves based on D_{50} could not be applied to the entire database. The Stark and Olson boundaries were chosen because they could be applied to every case history within the CPT database.

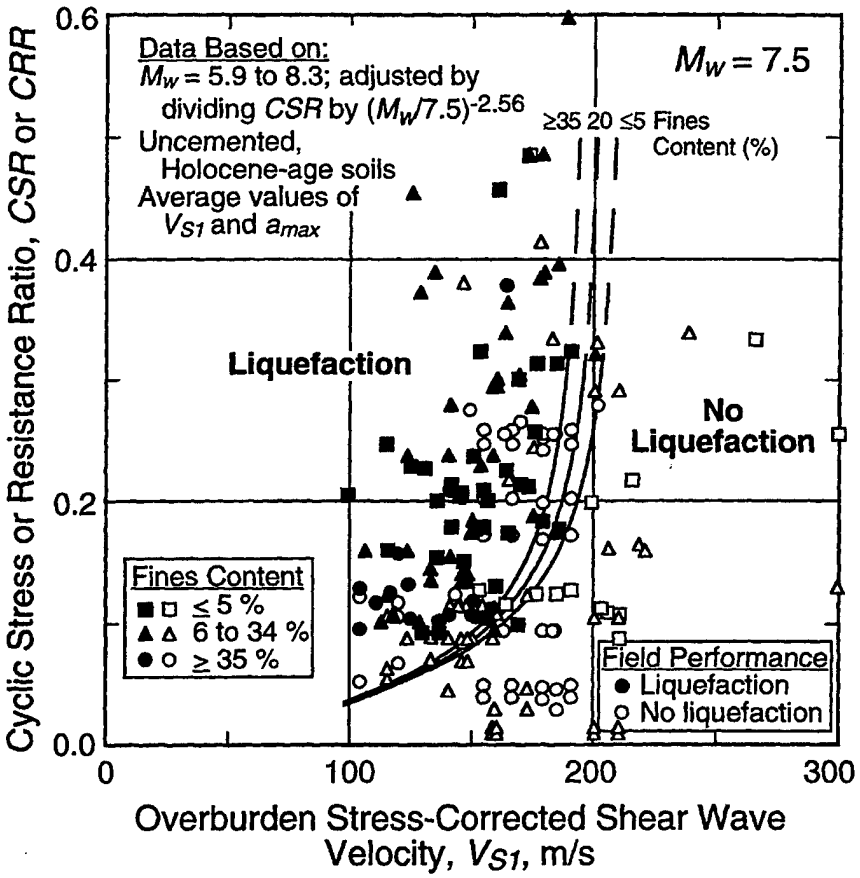

Figure 2.7 – V_S Liquefaction Boundary Curves Recommended by Andrus et al. (1999).

CHAPTER 3

DESCRIPTION OF DATABASE

Shear wave velocity, SPT blow counts, and CPT resistance measurements have been made for various field liquefaction studies throughout the world. In many cases more than one method was used at a particular site. This report is based on the database compiled by Andrus et al. (1999), which forms the basis for the most current and widely used liquefaction correlation based on shear wave velocity. The database presented in this report utilizes all the data from Andrus et al. (1999) and adds all available SPT and CPT data from the sites in that data base. Therefore, every site in the database has at least one shear wave velocity measurement, some sites have additional SPT data, some sites have additional CPT data, and in some cases a particular site has V_S, SPT, and CPT data. The augmented database was created by researching each individual site reported by Andrus et al. (1999) and determining what other in situ tests were performed at the site. In this chapter, the sources of data and variability in site conditions are discussed and the characteristics of the augmented database are described.

3.1 SHEAR WAVE VELOCITY DATABASE STATISTICS

3.1.1 Earthquake Magnitude and Location

The shear wave velocity database includes data from 84 sites and 26 earthquakes that have been previously investigated. Table 3.1 lists the sites, earthquakes, and references in the shear wave velocity database. Of the 26 earthquakes listed in Table 3.1, nine occurred in the United States, seven occurred in Japan, one occurred in China, and nine occurred in Taiwan. Earthquake magnitudes for these earthquakes ranged from 5.3 to 8.3, based on the moment magnitude scale.

Table 3.1 - Earthquakes and Sites Used in the Shear Wave Velocity Database.

Earthquake (1)	Moment Magnitude (2)	Site (3)	Reference (4)
1906 San Francisco California	7.7	Coyote Creek; Salinas River (North, South)	Youd and Hoose (1978); Barrow (1983); Bennett & Tinsley (1995)
1957 Daly City California	5.3	Marina District (2, 3, 4, 5, School)	Kayen et al. (1990); Tokimatsu et al. (1991b); T. L. Youd (personal communication to R. D. Andrus, 1999)
1964 Niigata Japan	7.5	Niigata City (A1, C1, C2, Railway Station)	Yoshimi et al. (1984; 1989); Tokimatsu et al. (1991a)
1975 Haicheng China	7.3	Chemical Fiber; Construction Building; Fishery & Ship Building; Glass Fiber; Middle School; Paper Mill	Arulanandan et al. (1986)
1979 Imperial Valley California 1981 Westmorland California 1987 Elmore Ranch California 1987 Superstition Hills California	6.5 5.9 5.9 6.5	Heber Road (Channel fill, Point bar); Kornbloom; McKim; Radio Tower; Vail Canal; Wildlife	Bennett et al. (1981; 1984); Sykora & Stokoe (1982); Youd & Bennett (1983); Bierschwale & Stokoe (1984); Stokoe & Nazarian (1984); Dobry et al. (1992); Youd & Holzer (1994)
1980 Mid-Chiba Japan 1985 Chiba-Ibaragi-Kenkyo Japan	5.9 6.0	Owi Island No. 1	Ishihara et al. (1981; 1987)

Table 3.1 (cont.) - Earthquakes and Sites Used in the Shear Wave Velocity Database.

Earthquake (1)	Moment Magnitude (2)	Site (3)	Reference (4)
1983 Borah Peak Idaho	6.9	Anderson Bar; Goddard Ranch; Mackay Dam Downstream Toe; North Gravel Bar; Pence Ranch	Youd et al. (1985); Stokoe et al. (1988a); Andrus et al. (1992); Andrus (1994)
1986 Event LSST2 1986 Event LSST3 1986 Event LSST4 1986 Event LSST6 1986 Event LSST7 1986 Event LSST8 1986 Event LSST12 1986 Event LSST13 1986 Event LSST16 Taiwan	5.3 5.5 6.6 5.4 6.6 6.2 6.2 6.2 7.6	Lotung LSST Facility	Shen et al. (1991); EPRI (1992)
1987 Chiba-Toho-Oki Japan	6.5	Sunamachi	Ishihara et al. (1989)
1989 Loma Prieta California	7.0	Bay Bridge Toll Plaza; Bay Farm Island (Dike, South Loop Road); Port of Oakland; Port of Richmond	Stokoe et al. (1992) Mitchell et al. (1994)
		Coyote Creek; Salinas River (North, South)	Barrow (1983); M. J. Bennett (personal communication to R. D. Andrus, 1995); Bennett and Tinsley (1995)
		Marina District (2, 3, 4, 5, school)	Kayen et al. (1990); Tokimatsu et al. (1991b)
		Moss Landing (Harbor Office, Sandholdt Road, State Beach)	Boulanger et al. (1995); Boulanger et al. (1997)

Table 3.1 (cont.) - Earthquakes and Sites Used in the Shear Wave Velocity Database.

Earthquake (1)	Moment Magnitude (2)	Site (3)	Reference (4)
1989 Loma Prieta (cont.) California	7.0	Santa Cruz (SC02, SC03, SC04, SC05, SC13, SC14)	Hryciw (1991); Hryciw et al. (1998)
		Treasure Island Fire Station	Hryciw et al. (1991); Redpath (1991); Gibbs et al. (1992); Furhriman (1993); Andrus (1994); de Alba et al. (1994)
		Treasure Island Perimeter (Approach to Pier, UM03, UM05, UM06, UM09)	Geomatrix Consultants (1990); Hryciw (1991); R. D. Hryciw (personal communication to R. D. Andrus, 1998); Hryciw et al. (1998); Andrus et al. (1998a, 1998b)
1993 Kushiro-Oki Japan	8.3	Kushiro Port (2, D)	Iai et al. (1995); S. Iai (personal communication to R. D. Andrus, 1997)
1993 Hokkaido-Nansei-Oki Japan	8.3	Pension House	Kokusho et al. (1995a, 1995b, 1995c)
		Hakodate Port	S. Iai (personal communication to R. D. Andrus, 1997)
1994 Northridge California	6.7	Rory Lane	Abdel-Haq & Hryciw (1998)
1995 Hyogo-Ken Nanbu Japan	6.9	Hanshin Expressway 5 (3, 10, 14, 25, 29); Kobe-Nishinomiya Expressway (3, 17, 23, 28)	Hamada et al. (1995); Hanshin Expressway Corporation (1998)
		KNK; Port Island Downhole Array); SGK	Sato et al. (1996); Shibata et al. (1996)

Table 3.1 (cont.) - Earthquakes and Sites Used in the Shear Wave Velocity Database.

Earthquake (1)	Moment Magnitude (2)	Site (3)	Reference (4)
1995 Hyogo-Ken Nanbu (cont.) Japan	6.9	Port Island (Common Factory)	Ishihara et al. (1997); Ishihara et al. (1998)
		Kobe Port (7C); Port Island (1C, 2C)	Inatomi et al. (1997); Hamada et al. (1995)
		Kobe Port (LPG Tank Yard)	S. Yasuda (personal communication to R. D. Andrus, 1997)

3.1.2 Shear Wave Velocity Measurement

Shear wave velocities were measured with 139 test arrays at over 80 investigation sites listed in Table 3.1. A test array, as defined by Andrus et al. (1999), is the two boreholes used for crosshole seismic measurements, the borehole and source used for downhole seismic measurements, the cone sounding and source used for seismic cone measurements, the borehole used for suspension logging measurements, or the line of receivers used for Spectral-Analysis-of-Surface-Waves (SASW) measurements. Of the 139 test arrays, 39 are crossholes, 21 downhole, 27 seismic cones, 15 suspension logger, 36 SASW, and one is unknown.

3.1.3 Case History

For the shear wave velocity database, a V_S case history is defined as a seismic event and a test array. If one site with an individual test array has been subjected to a number of earthquakes, each time the site was subjected to an earthquake is considered one case history. By combining the 26 seismic events and the 139 test arrays, a total of 225 case histories are obtained. Of the 225 case histories, 149 are from the United States, 36 are from Taiwan, 34 are from Japan, and six are from China. Each of the 225 case histories is assigned an individual number that will remain consistent throughout the V_S, SPT, and CPT databases.

3.1.4 Liquefaction Occurrence

The occurrence of liquefaction for each site was reported by Andrus et al. (1999). The liquefaction determination was based on the appearance of surface evidence, such as sand boils, ground cracks and fissures, and ground settlement. Case histories are classified as non-liquefaction when no liquefaction effects were observed at the ground surface. Figure 3.1 shows the distribution of case histories with earthquake magnitude and liquefaction performance. Of the 225 V_S case

histories, 96 are liquefaction case histories and 129 are non-liquefaction case histories.

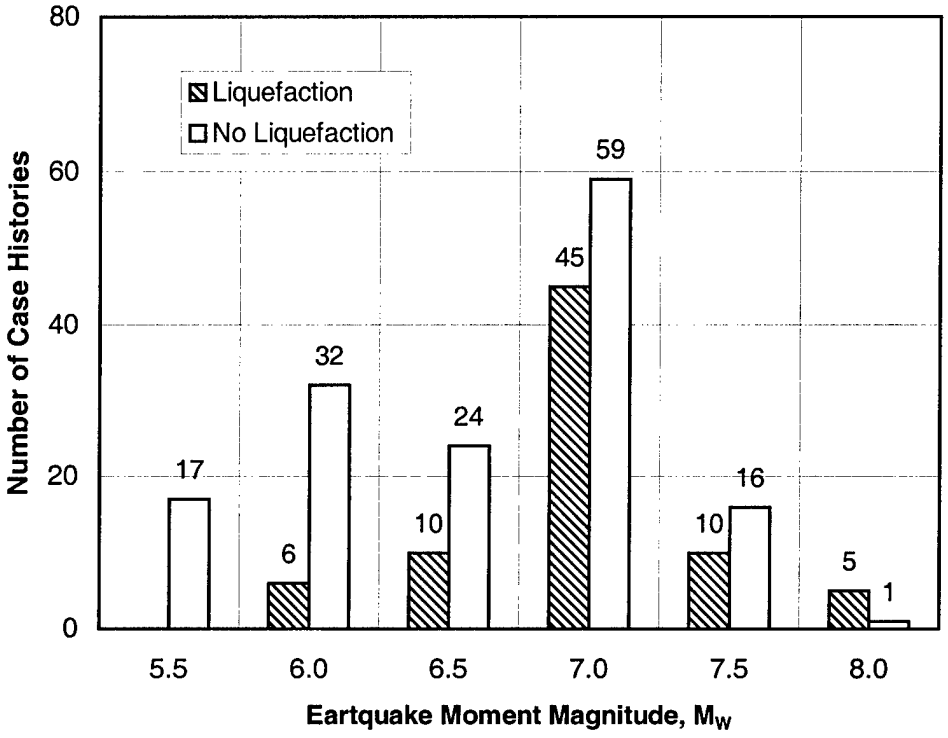

Fig. 3.1 – Distribution of Liquefaction and Non-Liquefaction Case Histories by Earthquake Magnitude for the V_S Database (from Andrus et al., 1999).

3.1.5 Fines Content

Another important site characteristic that influences the liquefaction performance of a particular site is the average fines content of the soil in the critical layer. Liquefiable soils with higher average fines content are less susceptible to liquefaction than soils with lower values. Figure 3.2 shows the distribution of V_S case histories with earthquake moment magnitude and fines content. Of the 225 case histories, 57 had average fines content less than 5%, 98 had a value between 6% and 34%, and 70 had values greater than 35%.

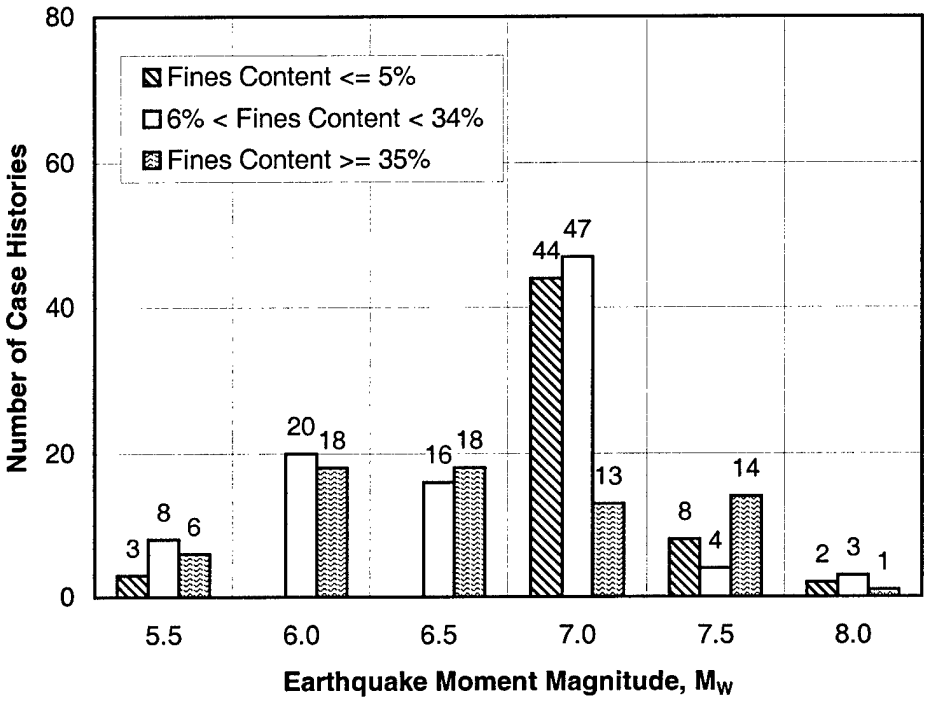

Fig. 3.2 – Distribution of Case Histories by Earthquake Magnitude and Average Fines Content for the V_S Database (from Andrus et al., 1999).

3.1.6 Data Quality

All V_S values presented in the database are identical to the values reported by Andrus et al. (1999). No changes to the original database were made in this study. Each site has at least one stress-corrected V_S value within the critical layer, depending on the type of test array used at the site.

The variability of the V_S measurements in the critical layer is a critical aspect in determining the quality of the data for the site. Andrus et al. (1999) only reported one, averaged V_S measurement for each case history, so a determination of the variability for individual case histories could not be calculated in this study. However, sixteen sites within the V_S database contained more than one V_S case history. Therefore, a comparison between case histories located at the same site

could be made. The variability of V_S measurements for case histories at the same site was determined by calculating the coefficient of variability (CV). CV, in percent, is defined as (Devore 1995):

$$CV = (\sigma/\mu)*100\% \quad (3.1)$$

where

σ = Standard deviation of V_S measurements at the site, and

μ = Mean of the V_S measurements at the site.

A calculated CV of 50% was the initial base line for determining the quality of data at the site. Critical layers at sites that had a CV less than 50% through the critical layer were noted to be high quality data and sites that had a CV greater than 50% were marked as questionable. Sixteen sites had more than one reported shear wave velocity and all 16 exhibited a CV value less than 50%. These 16 sites represent 101 of the 225 V_S case histories in the V_S database.

3.2 SPT DATABASE STATISTICS

3.2.1 Earthquake Magnitude and Location

The SPT database includes data from 70 sites and 24 earthquakes that have been previously investigated. Table 3.2 lists the sites, earthquakes, and references in the SPT database. Of the 24 earthquakes listed in Table 3.2, eight occurred in the United States, six occurred in Japan, one occurred in China, and nine occurred in Taiwan. Earthquake magnitudes ranged from 5.3 to 8.3, based on the moment magnitude scale.

3.2.2 SPT Blow Count Measurement

The SPT tests performed at the sites in the database were reported by various investigators throughout the world and were reported in various languages. In many

Table 3.2 - Earthquakes and Sites Used in the SPT Database.

Earthquake (1)	Moment Magnitude (2)	Site (3)	Reference (4)
1906 San Francisco California	7.7	Coyote Creek; Salinas River (South)	Barrow (1983)
1957 Daly City California	5.3	Marina District (2, 3, 4, 5)	Kayen et al. (1990)
1964 Niigata Japan	7.5	Niigata City (Railway Station)	Yoshimi et al. (1984)
1975 Haicheng China	7.3	Chemical Fiber; Construction Building; Fishery & Ship Building; Glass Fiber; Middle School; Paper Mill	Arulanandan et al. (1986)
1979 Imperial Valley California 1981 Westmorland California 1987 Elmore Ranch California 1987 Superstition Hills California	6.5 5.9 5.9 6.5	Heber Road (Channel fill, Point bar) Kornbloom; McKim; Radio Tower; Vail Canal; Wildlife	Youd & Bennett (1983) Bierschwale & Stokoe (1984)
1980 Mid-Chiba Japan 1985 Chiba-Ibaragi-Kenkyo Japan	5.9 6.0	Owi Island No. 1	Ishihara et al. (1981)
1983 Borah Peak Idaho	6.9	Goddard Ranch; Pence Ranch	Andrus (1994)

Table 3.2 (cont.) - Earthquakes and Sites Used in the SPT Database.

Earthquake (1)	Moment Magnitude (2)	Site (3)	Reference (4)
1986 Event LSST2 1986 Event LSST3 1986 Event LSST4 1986 Event LSST6 1986 Event LSST7 1986 Event LSST8 1986 Event LSST12 1986 Event LSST13 1986 Event LSST16 Taiwan	5.3 5.5 6.6 5.4 6.6 6.2 6.2 6.2 7.6	Lotung LSST Facility	Shen et al. (1991); EPRI (1992)
1987 Chiba-Toho-Oki Japan	6.5	Sunamachi	Ishihara et al. (1989)
1989 Loma Prieta California	7.0	Bay Bridge Toll Plaza; Bay Farm Island (Dike, South Loop Road); Port of Oakland; Port of Richmond	Stokoe et al. (1992); Mitchell et al. (1994)
		Coyote Creek; Salinas River (South)	Barrow (1983)
		Marina District (2, 3, 4, 5)	Kayen et al. (1990); Tokimatsu et al. (1991b)
		Moss Landing (Harbor Office, Sandholdt Road, State Beach)	Boulanger et al. (1995); Boulanger et al. (1997)
		Treasure Island Fire Station	de Alba et al. (1994)
		Treasure Island Perimeter (Approach to Pier, UM03, UM05, UM06, UM09)	Geomatrix Consultants (1990); Andrus et al. (1998a, 1998b)
1993 Kushiro-Oki Japan	8.3	Kushiro Port (2)	Iai et al. (1995)

Table 3.2 (cont.) - Earthquakes and Sites Used in the SPT Database.

Earthquake (1)	Moment Magnitude (2)	Site (3)	Reference (4)
1995 Hyogo-Ken Nanbu Japan	6.9	Hanshin Expressway 5 (3, 10, 14, 25, 29); Kobe-Nishinomiya Expressway (3, 17, 23, 28)	Hamada et al. (1995); Hanshin Expressway Corporation (1998)
		Port Island Downhole Array)	Shibata et al. (1996)
		Port Island (Common Factory)	Ishihara et al. (1998)
		Kobe Port (7C); Port Island (1C, 2C)	Inatomi et al. (1997)
		Kobe Port (LPG Tank Yard)	S. Yasuda (personal communication to R. D. Andrus, 1997)

cases it was difficult to determine whether or not the SPT for a particular site was performed using the 'standard' procedure. In some cases, uncorrected N-values were reported, and in some cases corrected $N_{1,60}$ values were reported. In this report, all uncorrected values were corrected using the correction procedure outlined by Robertson and Fear (1996). The correction procedure and sample calculations involved in the SPT analyses are presented in Chapter 5. If corrected values were reported in the literature, the reported values were used without additional corrections.

3.2.3 Case History

For the SPT database, a SPT case history is defined as a seismic event and an average blow count value through the critical layer paired up with an averaged V_S measurement. For example, Coyote Creek had four crosshole test arrays resulting in

four V_S measurements through the critical layer. However, only one SPT test was performed in the critical layer. Therefore, the same SPT value is paired with each of the four different V_S measurements resulting in four SPT case histories. In addition, Coyote Creek was subject to both the 1906 San Francisco Earthquake and the 1989 Loma Prieta Earthquake. Therefore, by combining the four SPT values with the two seismic events, a total of eight SPT case histories for the Coyote Creek site are produced. The procedure of pairing the SPT values with individual V_S measurements was implemented in order to keep a consistent case history number throughout the entire database. Combining the 24 seismic events and the reported SPT blow counts, a total of 183 case histories are obtained with 117 from the United States, 36 from Taiwan, 24 from Japan, and six from China.

3.2.4 Liquefaction Occurrence

The occurrence of liquefaction for a SPT case history remained consistent with the paired V_S case history. No changes were made to the liquefaction determination made by Andrus et al. (1999). The distribution of case histories with earthquake magnitude and liquefaction performance is shown in Figure 3.3. Of the 183 SPT case histories, 73 are liquefaction case histories and 110 are non-liquefaction
case histories.

3.2.5 Fines Content

The distribution of SPT case histories with earthquake moment magnitude and fines content is shown in Figure 3.4. Of the 183 case histories, 35 had average fines contents less than or equal to 5%, 92 had fines contents between 6% and 34%, and 56 had fines contents greater than or equal to 35%.

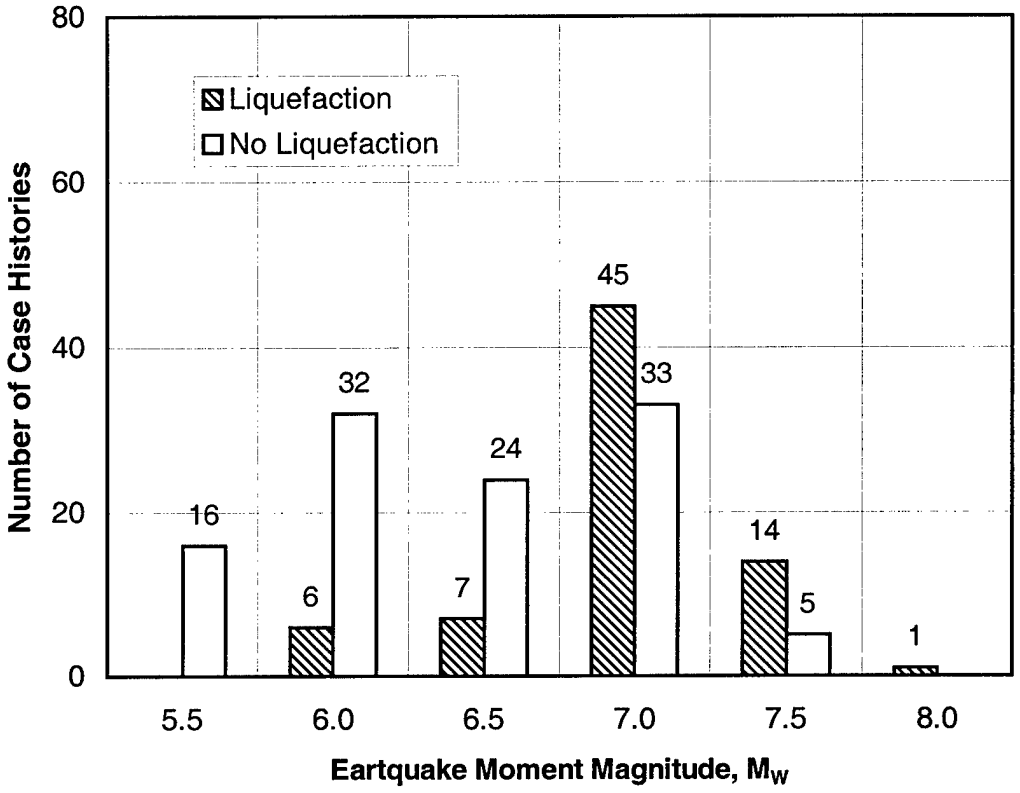

Fig. 3.3 – Distribution of Liquefaction and Non-Liquefaction Case Histories by Earthquake Magnitude for the SPT Database.

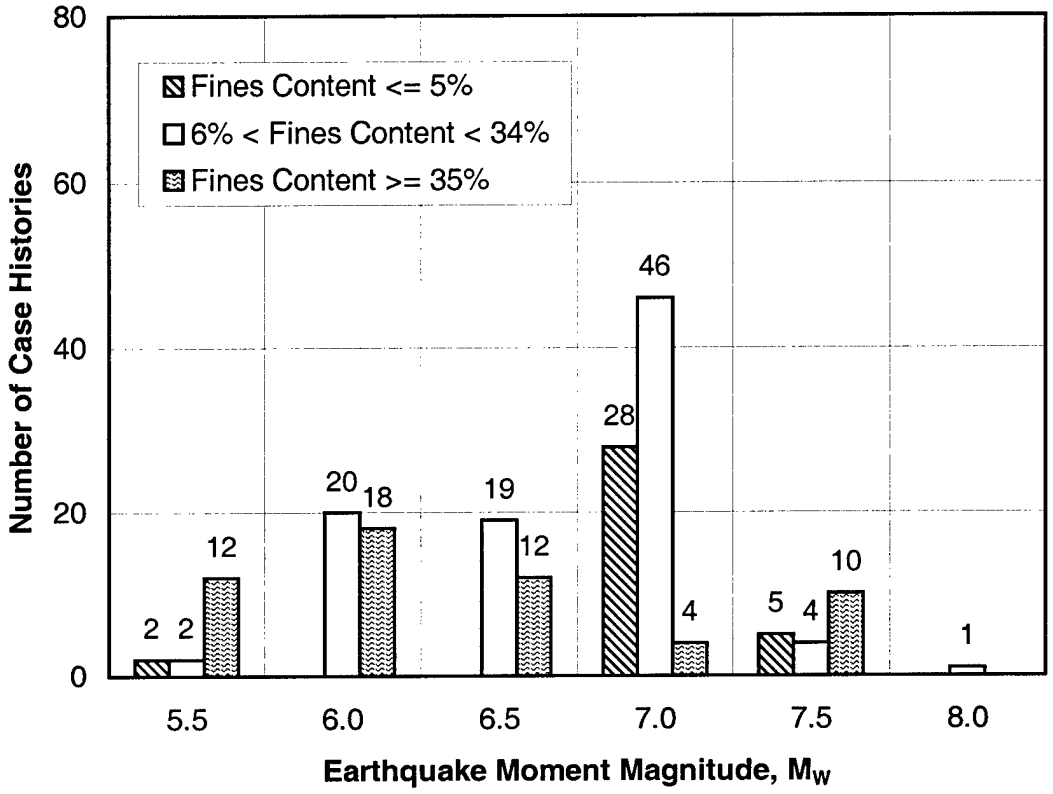

Fig. 3.4 – Distribution of SPT Case Histories by Earthquake Magnitude and Average Fines Content for the SPT Database.

3.2.6 Data Quality

Another key aspect in the description of the SPT database is the variability of the corrected blow count data through the critical layer for a particular case history. Once again, the variability of the SPT values in the critical layer was determined by calculating the coefficient of variability (CV). Equation 3.1, presented for the V_S sites, was applied to the SPT measurements in the critical layer for each SPT case history. A CV value of 50% was the initial base line for determining the quality of the data for a case history. Critical layers at sites that had a CV less than 50% through the critical layer were noted to be high quality data and sites that had a CV greater than 50% were marked as questionable. Of the 183 case histories, 167 exhibited a CV less than 50% and 16 exhibited a CV greater than 50%.

Some sites in the SPT database contain only one value within the critical layer. When this occurred, either only one averaged value was reported or only one value was obtained through testing. Of the 183 case histories, 36 had only one value and 147 had more than one value.

3.3 CPT DATABASE STATISTICS

3.3.1 Earthquake Magnitude and Location

The CPT database includes data from 61 sites and 12 earthquakes that have been previously investigated. Table 3.3 lists the sites, earthquakes, and references in the CPT database. Of the 12 earthquakes listed in Table 3.3, nine occurred in the United States, two occurred in Japan, and one occurred in China. Earthquake magnitudes for the 12 earthquakes ranged from 5.3 to 7.7, based on the moment magnitude scale

3.3.2 CPT Tip Resistance Measurement

The CPT test is known to be more consistent than the SPT test and has become very popular in the United States. Nonetheless, correction factors must be applied to the CPT data. In some cases, investigators reported CPT tip resistance values that were not corrected for overburden stress and/or were not normalized. In others, the investigators reported values that were normalized and corrected for overburden stress. As in the SPT database, if uncorrected values were reported, the values were corrected. The raw CPT data was corrected using the procedures described in Chapter 6. If normalized overburden stress corrected values were reported, these values were used in the database.

Table 3.3 - Earthquakes and Sites Used in the CPT Database.

Earthquake (1)	Moment Magnitude (2)	Site (3)	Reference (4)
1906 San Francisco California	7.7	Coyote Creek; Salinas River (North, South)	Barrow (1983)
1957 Daly City California	5.3	Marina District (2, 3, 4, 5)	Kayen et al. (1990)
1975 Haicheng China	7.3	Chemical Fiber; Construction Building; Fishery & Ship Building; Glass Fiber; Middle School; Paper Mill	Arulanandan et al. (1986)
1979 Imperial Valley California 1981 Westmorland California 1987 Elmore Ranch California 1987 Superstition Hills California	6.5 5.9 5.9 6.5	Heber Road (Channel fill, Point bar); Kornbloom; McKim; Radio Tower; Vail Canal; Wildlife	Bennett et al. (1981; 1984); Sykora & Stokoe (1982); Youd & Bennett (1983); Bierschwale & Stokoe (1984); Stokoe & Nazarian (1984); Dobry et al. (1992); Youd & Holzer (1994)
1980 Mid-Chiba Japan 1985 Chiba-Ibaragi-Kenkyo Japan	5.9 6.0	Owi Island No. 1	Ishihara et al. (1981; 1987)
1983 Borah Peak Idaho	6.9	Goddard Ranch; Pence Ranch	Andrus (1994)

Table 3.3 (cont.) - Earthquakes and Sites Used in the CPT Database.

Earthquake (1)	Moment Magnitude (2)	Site (3)	Reference (4)
1989 Loma Prieta California	7.0	Bay Bridge Toll Plaza; Bay Farm Island (Dike, South Loop Road); Port of Oakland; Port of Richmond	Mitchell et al. (1994)
		Coyote Creek; Salinas River (North, South)	Barrow (1983)
		Marina District (2, 3, 4, 5)	Kayen et al. (1990)
		Moss Landing (Harbor Office, Sandholdt Road, State Beach)	Boulanger et al. (1995); Boulanger et al. (1997)
		Santa Cruz (SC02, SC03, SC04, SC05, SC13, SC14)	Hryciw (1991); Hryciw et al. (1998)
		Treasure Island Fire Station	de Alba et al. (1994)
		Treasure Island Perimeter (Approach to Pier, UM03, UM05, UM06, UM09)	Hryciw (1991); Hryciw et al. (1998); Andrus et al. (1998a, 1998b)
1994 Northridge California	6.7	Rory Lane	Abdel-Haq & Hryciw (1998)

3.3.3 Case History

For the CPT database, case histories were defined using the same procedure as in the SPT database. A single CPT value for a particular site was paired with each V_S measurement reported at the site. Once again, this procedure was implemented in order to keep the case history numbers consistent throughout the entire combined database. Combining the 12 seismic events and the measured CPT values, a total of

147 case histories were obtained with 137 from the United States, four from Japan, and six from China. No CPT case histories are from Taiwan.

3.3.4 Liquefaction Occurrence

The occurrence of liquefaction for a CPT case history remained consistent with the paired V_S case history. No changes were made to the liquefaction determination made by Andrus et al. (1999). Figure 3.5 shows the distribution of case histories with earthquake magnitude and liquefaction performance. Of the 147 CPT case histories, 69 are liquefaction case histories and 78 are non-liquefaction case histories.

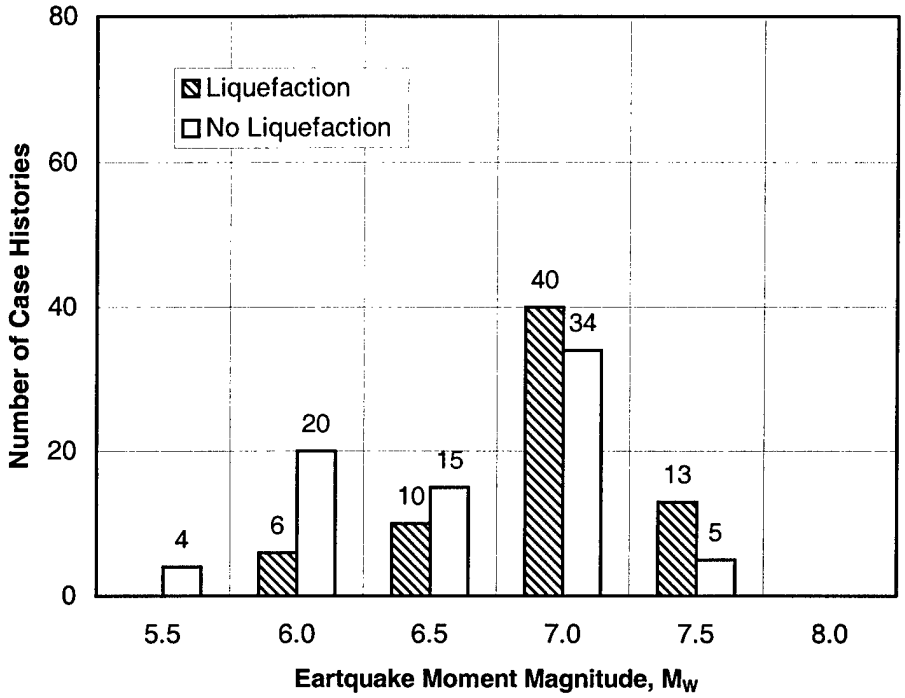

Fig. 3.5 – Distribution of Liquefaction and Non-Liquefaction Case Histories by Earthquake Magnitude for the CPT Database.

3.3.5 Fines Content

As with the V_S and CPT case histories, the average fines content of the soil in the critical layer was used as a site characteristic. Figure 3.6 shows the distribution of CPT case histories with earthquake moment magnitude and fines content. Of the 147 case histories, 37 had average fines contents less than or equal to 5%, 78 had fines contents between 6% and 34%, and 32 had fines contents greater than or equal to 35%.

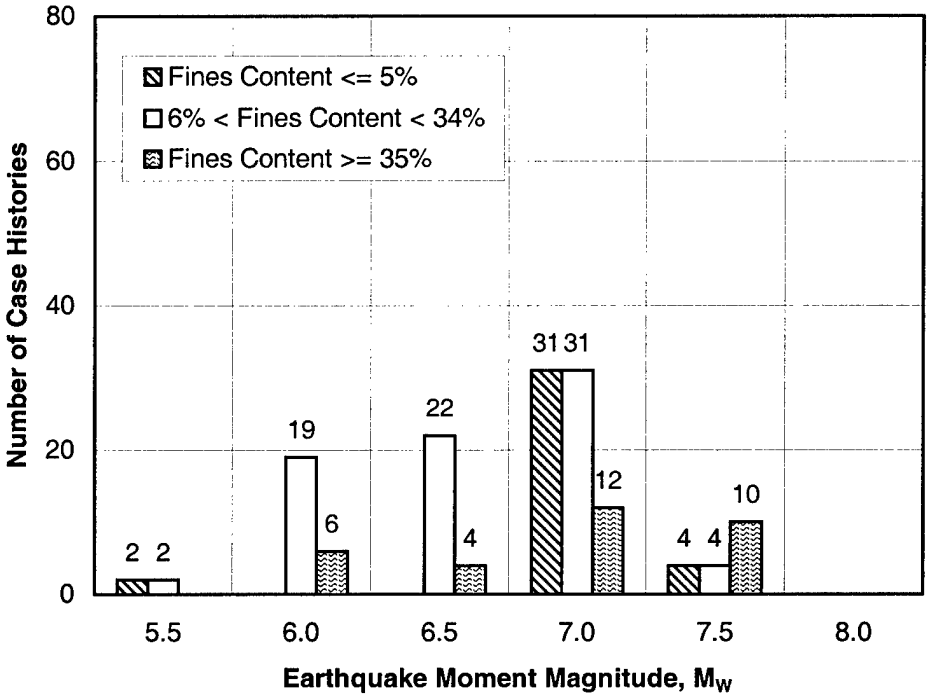

Fig. 3.6 – Distribution of Case Histories by Earthquake Magnitude and Average Fines Content for the CPT Database.

3.3.6 Data Quality

As in the V_S and SPT databases, the variability of the CPT data within the critical layer was considered a key factor in the determination of the data quality for a particular site. Once again, the variability of the CPT values in the critical layer

was determined by calculating the coefficient of variability (CV). Equation 3.1, presented for the V_S sites, was applied to the CPT measurements in the critical layer for each CPT case history. A calculated CV of 50% was the initial base line for determining the quality of the data for a site. Critical layers at sites that had a CV less than 50% through the critical layer were noted to be high quality data, and sites that had a CV greater than 50% were marked as questionable. Of the 147 case histories, 125 exhibited a CV less than 50% and 22 exhibited a CV greater than 50%.

Some sites in the CPT database contain only one value within the critical layer. This occurred when the author of the reference chose to only report one averaged value within the critical layer. Of the 183 case histories, 26 had only one CPT value and 121 had more than one reported value.

3.4 PRESENTATION OF DATA

All data collected from the sites listed in Table 3.1 and added to the combined database will be presented in a future geotechnical report by the same authors. The data are not presented because the purpose of this report is to merely present the conclusions drawn from the analysis of the database.

CHAPTER 4

SHEAR WAVE VELOCITY CASE HISTORIES

The case history data presented by Andrus et al. (1999), along with the boundary curves recommended by Andrus et al. (1999) are presented in this chapter. As noted in Chapter 3, no changes were made to the original database and no changes were made to the boundary curves dividing liquefaction conditions from non- liquefaction conditions.

4.1 CALCULATIONS REQUIRED FOR THE V_S DATABASE

4.1.1 Correcting the V_S Data

The overburden-stress corrected shear wave velocity (V_{S1}) measurements for all case histories were reported by Andrus et al. (1999) and used in this study as reported. Andrus et al. (1999) corrected shear wave velocity (V_S) to overburden-stress correct shear wave velocity (V_{S1}) using:

$$V_{S1} = V_S \{Pa/\sigma'_V)^{0.25} \qquad (4.1)$$

where

V_S = measured shear wave velocity in m/s,

σ'_V = effective overburden pressure in kPa, and

P_A = atmospheric pressure in kPa = 100 kPa.

4.1.2 Statistical Calculations Performed for V_S Case Histories

Since Andrus et al (1999) reported only one averaged overburden-stress corrected shear wave velocity for each case history, no additional statistical calculations were performed in this study for the V_S database.

4.2 PRESENTATION OF THE V_S CASE HISTORIES

A summary of the V_S case history data in terms of liquefaction behavior and fines content is presented in Table 4.1.

Table 4.1 – Summary of the 225 V_S Case Histories Reviewed in this Study.

	Number Of V_S Case Histories	% of V_S Case Histories within the Category	% of Total V_S Case Histories
Liquefaction Case Histories			
- Fines Content ≤ 5%	37	38.5	16.4
- Fines Content 6-34%	45	46.9	20
- Fines Content ≥ 35%	14	14.6	6.3
Total	**96**	**100**	**42.7**
Non-Liquefaction Case Histories			
- Fines Content ≤ 5%	17	13.2	7.6
- Fines Content 6-34%	57	44.2	25.3
- Fines Content ≥ 35%	55	42.6	24.4
Total	**129**	**100**	**57.3**

4.2.1 Entire V_S Case History Database

The entire V_S case history database is plotted in Figure 4.1. Overburden-corrected shear wave velocity in m/s is plotted on the horizontal axis and the equivalent $M_W = 7.5$ cyclic stress ratio is plotted on the vertical axis. The boundary curves between liquefaction and no liquefaction conditions that were recommended by Andrus et al. (1999) are also shown in the figure. There are a total of 225 case histories, with 96 liquefaction case histories and 129 non-liquefaction case histories. The liquefaction case histories are shown as solid symbols and the non-liquefaction case histories are shown as open symbols. As noted in Chapter 3, these case histories

cover earthquakes ranging in moment magnitude from 5.3 to 8.3. The scaling of earthquake magnitude in Figure 4.1 is discussed in Chapter 2, using the magnitude scaling factor given by Equation 2.3.

4.2.2 V_S Case Histories

Case histories with fines content $\leq 5\%$, fines content between 6 and 34%, and fines content $\geq 35\%$ are shown in Figures 4.2, 4.3, 4.4, respectively. The case histories are shown with the appropriate boundary curve in each respective figure. The liquefaction case histories have the case history number next to the individual data points. For clarity, the non-liquefaction data points are shown without case history numbers.

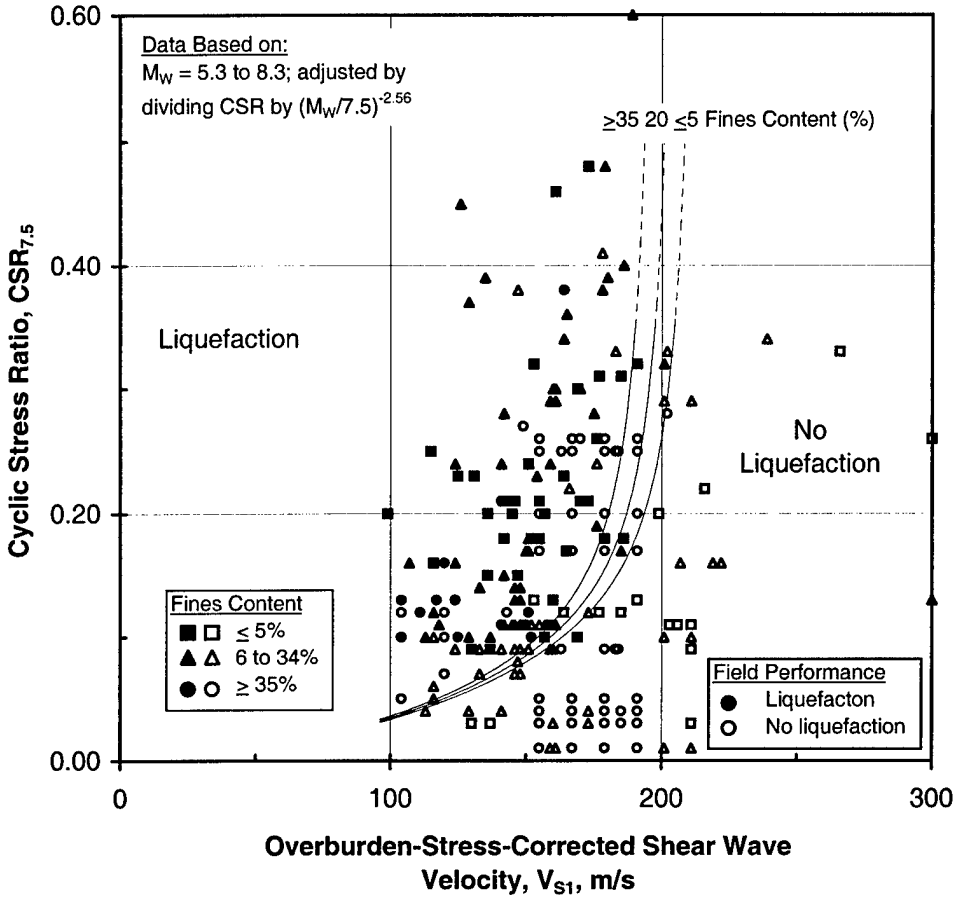

Fig. 4.1 - Average Overburden-Stress-Corrected Shear Wave Velocity through the Critical Layer from the Entire V_S Case History Database with the Andrus et al. (1999) Boundary Curves.

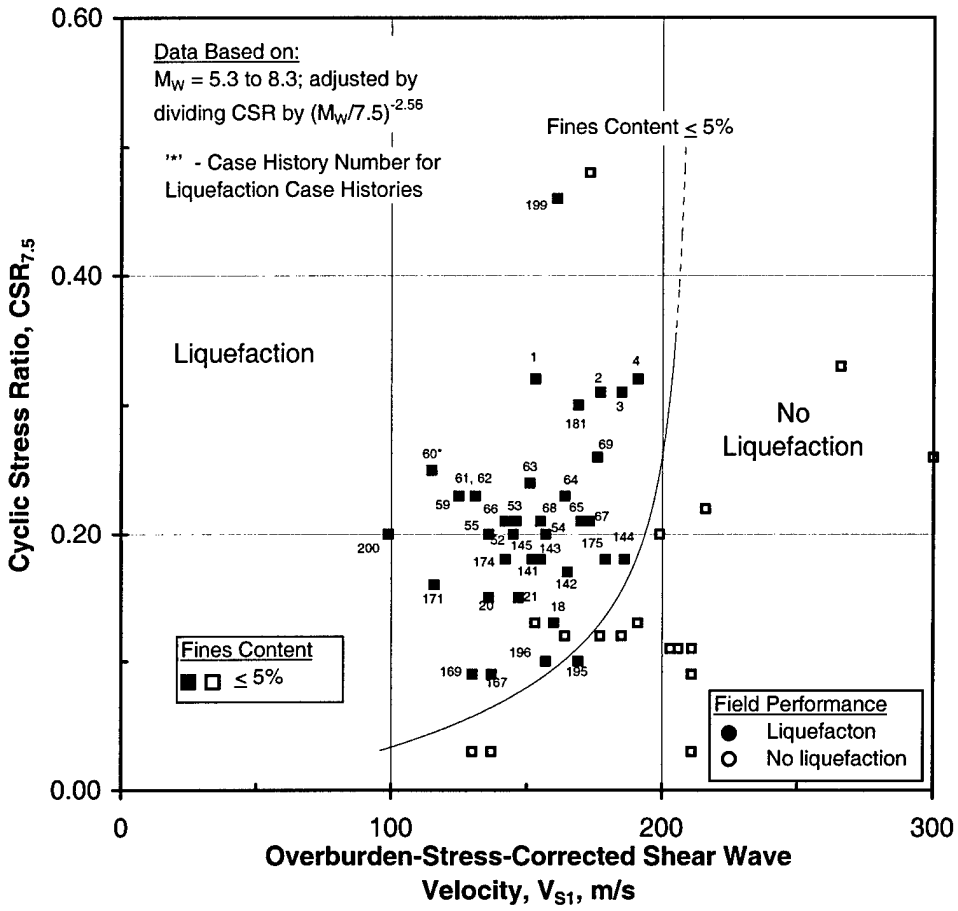

Fig. 4.2 - Average Overburden-Stress-Corrected Shear Wave Velocities for V_S Liquefaction Case Histories with Fines Content ≤ 5%.

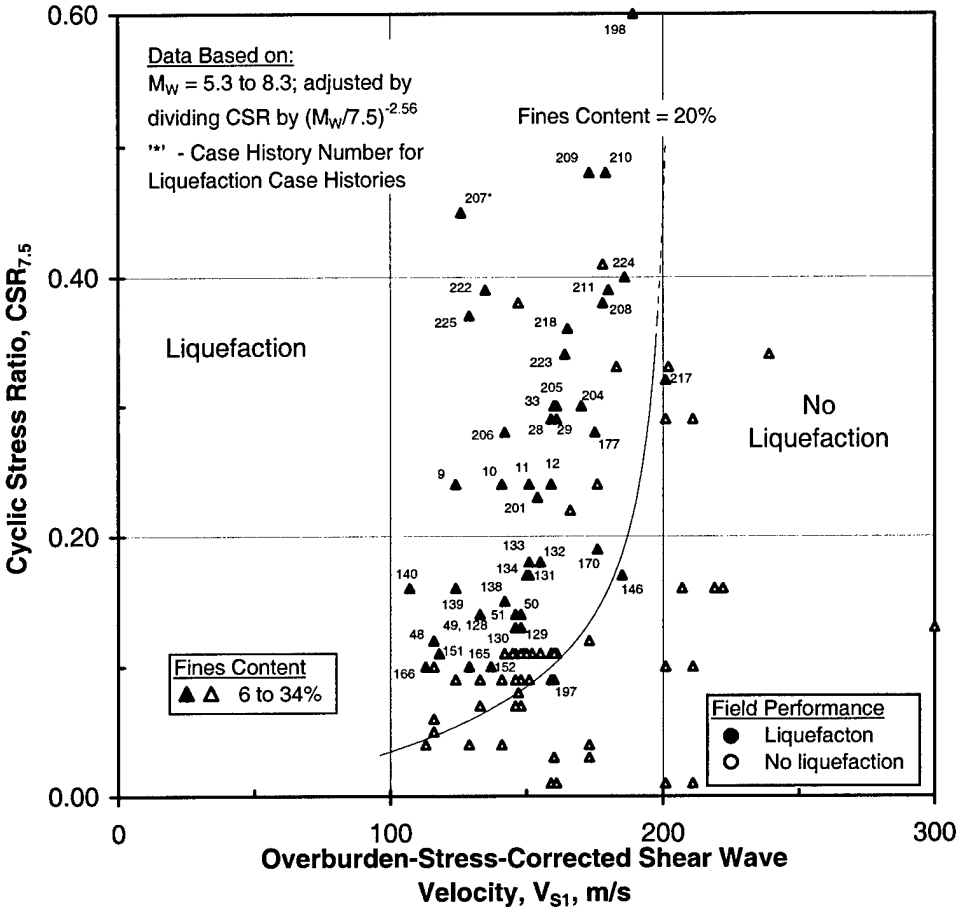

Fig. 4.3 - Average Overburden-Stress-Corrected Shear Wave Velocities for V_S Liquefaction Case Histories with Fines Content = 6% - 34%.

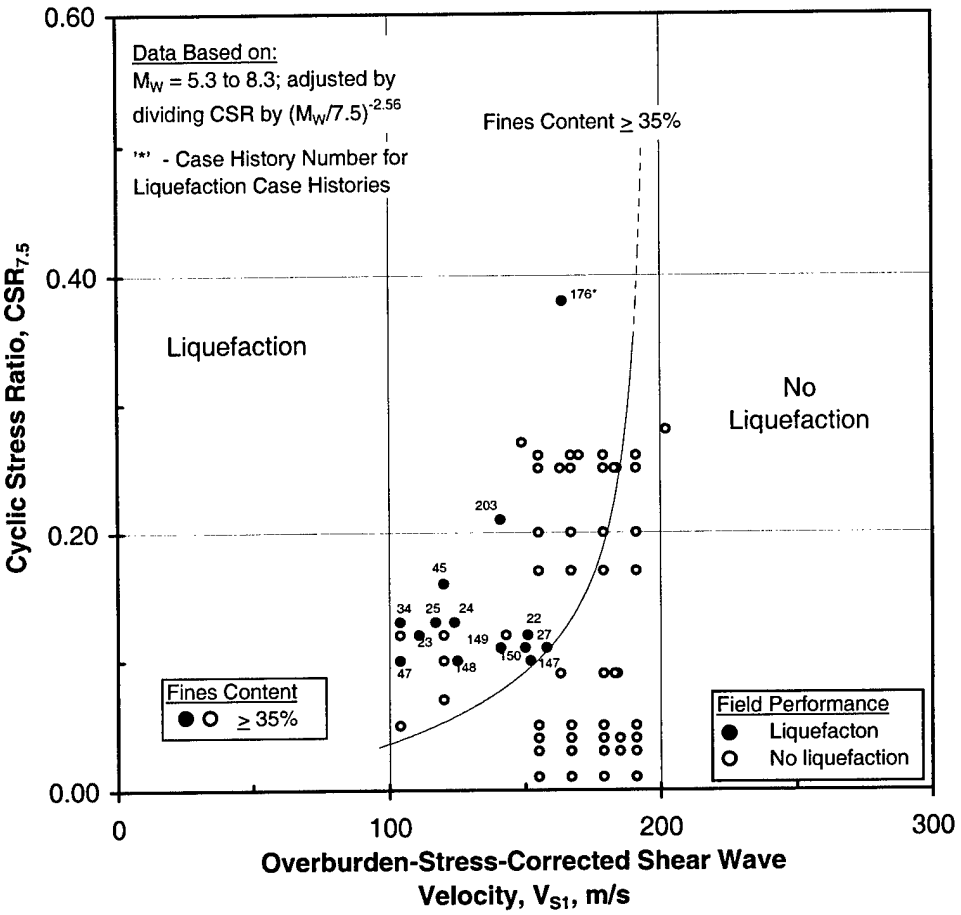

Fig. 4.4 - Average Overburden-Stress-Corrected Shear Wave Velocities for V_S Liquefaction Case Histories with Fines Content ≥ 35%.

4.3 ACCURACY OF THE V_S BOUNDARY CURVES

Table 4.2 lists the number of V_S liquefaction case histories that plotted on the 'Liquefaction' side of the boundary curves. In some cases, when a site did not liquefy, the case history plotted on the 'liquefaction' side of the boundary curve. The V_S boundary curves were drawn conservatively to encompass nearly all liquefaction case histories, and some non-liquefaction case histories. Therefore, it is expected that some of the non-liquefaction case histories plot on the liquefaction side of the boundary curves. In this study, the objective was to evaluate the curves in their ability to predict liquefaction for sites that did liquefy. In summary, of the 96 liquefaction case histories 93 plotted correctly yielding an accuracy of 96.9%.

Table 4.2 – Tabulation of How Well the V_S Boundary Curves were Able to Predict Liquefaction for Sites that Liquefied.

Fines Content	Number of Liquefaction Case Histories	Number Plotted Correctly	% Plotted Correctly
≤ 5%	37	36	97.3
6- 34%	45	43	95.6
≥35%	14	14	100.0
Total	**96**	**93**	**96.9**

The three liquefaction case histories that were misclassified by the V_S boundary were numbers 195, 197, and 217. In other words, these three V_S case histories were predicted to not liquefy by the V_S boundaries, when in reality, liquefaction was observed at the site. Case histories 195 and 197 had additional SPT and CPT data, but 217 only had additional SPT data. Case histories 195 and 197 are

from the United States, and case history 217 is from Japan. The average fines contents in the critical layer were 5%, 14%, and 10% respectively. As shown in Chapters 5, the SPT correlation agreed with the V_S correlation and did not plot case history 197 correctly. However, case histories 195 and 217 did plot correctly in the SPT correlation. As shown in Chapter 6, the two case histories with CPT data, 195 and 197, agreed with the V_S correlation and did not plot correctly.

CHAPTER 5

SPT CASE HISTORIES

5.1 CONSISTENCIES BETWEEN THE SPT AND V_S DATABASES

The SPT case histories had to be linked to the corresponding values within the V_S database. To accomplish this linkage, information concerning the critical layer and cyclic stress ratio were applied to the SPT database exactly as reported by Andrus et al. (1999).

5.2 CALCULATIONS REQUIRED FOR THE SPT DATABASE

The blow counts recorded during the SPT test (N-values) must be corrected in order to obtain 'standardized' values. Variations in testing procedures, equipment, and the experience of the personnel conducting the test should be properly taken into account before the values can be used in a liquefaction analysis. In this report, the first two were taken into account and the proper corrections were applied when necessary. Unfortunately, the experience of the personnel conducting the individual SPT tests was not reported and was impossible to quantify in this report. After the correction factors were applied to the N-values, statistical analyses of the data were conducted for each site within the critical layer. The following describes the calculations performed for case histories within the SPT database.

5.2.1 Correction Factors

The most important SPT correction accounts for the amount of energy delivered by the hammer to the drill pipe. The amount of energy is typically expressed as an energy ratio (ER), which is the percent of the theoretical free fall energy delivered by a particular hammer and release system. Actual values of ER depend on the type of hammer used and the method in which the hammer is released.

The actual values can be measured or can be estimated. Measured N-values are corrected to give equivalent values representing a hammer that delivers 60% of the maximum free-fall energy to the rods. According to Robertson and Fear (1996), values of the energy correction factor to modify SPT results (C_E = ER/60) can vary from 0.3 to 1.6, corresponding to field ER's from 20% to 100%. Other correction factors do not influence the results as much, but still must be taken into account. The other correction factors due to field effects are based on short rod lengths, borehole diameters not within the required standards, and the configuration of the sampler during testing. The factor based on the configuration of the sampler is applied only when the sampler being used has the ability to accept a liner, but the liner is not installed. The final correction factor corrects the N-value for overburden stress.

The equation to correct field N-values, after Robertson and Fear (1996), is:

$$N_{1,60} = N*C_N*C_E*C_B*C_R*C_S \qquad (5.1)$$

where

N = field N-value,

C_N = correction for overburden stress = $(Pa/\sigma_V')^{0.5} \leq 2.0$,

C_E = correction due to rod energy = ER/60,

C_B = correction for borehole diameter,

C_R = correction for rod length, and

C_S = correction for using a sampler without the liner.

The correction factors for borehole diameter, rod length, and sampler were originally recommended by Skempton (1986), and were modified by Robertson and Fear (1996). These factors are presented in Table 5.1.

Equation 5.1 was applied to all case histories that had uncorrected N-values reported in the reference literature. If the reference provided $N_{1,60}$ values, the corrected values were used in the liquefaction analysis as reported. For case

histories that had to be corrected, sometimes the author reported the value for ER and other times did not. If no ER was reported, the value for ER was assumed to be 60% for tests conducted in the United States, Taiwan, and China. According to Seed et al. (1986), an ER of 55% can be assumed for Japanese SPT test data. Therefore, for Japanese data in the SPT database that needed to be corrected, an ER equal to 55% was used. According to Seed et al. (1986), numerous corrections must be made due to variations in the manner the Japanese conduct the SPT. In lieu of additional correction factors, they found that using an ER equal to 55% took all these variables into account and produced acceptable results.

Table 5.1 – Recommended SPT Correction Factors (from Robertson and Fear, 1996).

Factor	Equipment Variable	Term	Correction
Energy Ratio	Safety Hammer	C_E	0.67 to 1.17
	Donut Hammer		0.50 to 1.00
Borehole Diameter	65 to 115 mm (2.5- 4.5 in)	C_B	1.0
	150 mm (6 in)		1.05
	200 mm (8 in)		1.15
Rod Length	> 30 m (>100 ft)	C_R	<1.0
	10 to 30 m (30 to 100 ft)		1.0
	6 to 10 m (20 to 30 ft)		0.95
	4 to 6 m (13 to 20 ft)		0.85
	3 to 4 m (10 to 13 ft)		0.75
Sampler	Standard Sampler	C_S	1.0
	Sampler without Liner		1.2

5.2.2 Statistical Calculations Performed for SPT Case Histories

After obtaining or calculating $N_{1,60}$ values for every case history, simple statistical analyses were performed for measurements within the critical layer. The statistical analysis involved calculations of the average value, minimum value, maximum value, standard deviation, and coefficient of variability. This information was used to judge the quality of the data and the uniformity of the critical layer. This information was also used to analyze the correlation boundary curves under different circumstances.

5.2.3 Removal of Data Due to Engineering Judgment

In certain cases, some of the data collected within the critical layer did not seem to represent the material in a layer that would be susceptible to liquefaction. In these instances the data were removed and were not included in the above statistical calculations. An example of this procedure is the following. The Bay Bridge Toll Plaza site, represents SPT case histories 131, 132, and 134. The investigators, Mitchell et al. (1994), reported six uncorrected N-values within the critical layer. The reported values, descending through the critical layer, were 28, 10, 5, 0, 8, and 41 blows per foot. Obviously, the portion of the critical layer represented by the four values in the middle of the layer seemed to be the most representative of the liquefiable portion of the layer. The N-values equal to 28 and 41 were obviously representative of a stiffer non-liquefiable portion of the layer. Therefore, the N-values representing the stiffer material were removed and not included in the statistical analysis of the critical layer. All case histories that had data removed are listed in Table 5.2. Of the 183 SPT case histories, 23 had data removed and 160 did not.

All soil profiles will be presented in a future geotechnical report by the same authors. The soil profiles will indicate the unrepresentative N-values and the depths at which they were reported.

Table 5.2 – Case Histories from the SPT Database that had SPT N-Values Removed from the Critical Layer due to Unrepresentative Material.

Number	Case History Number	Field Performance (LF or No LF)	Average Fines Content
1	13	No LF	8%
2	14	No LF	8%
3	27	LF	72%
4	32	No LF	75%
5	45	LF	75%
6	60	LF	5%
7	113	No LF	75%
8	124	No LF	75%
9	131	LF	9%
10	132	LF	9%
11	134	LF	9%
12	142	LF	5%
13	143	LF	5%
14	144	LF	5%
15	145	LF	5%
16	147	LF	57%
17	148	LF	57%
18	149	LF	57%
19	150	LF	57%
20	165	LF	8%
21	166	LF	8%
22	217	LF	10%
23	218	LF	10%

'LF' = Liquefaction

5.3 PRESENTATION OF THE SPT CASE HISTORIES

A summary of the SPT case history data in terms of liquefaction case histories and fines content is presented in Table 5.3.

Table 5.3 – Summary of the 183 SPT Case Histories Reviewed in this Study.

	Number Of SPT Case Histories	% of SPT Case Histories within the Category	% of Total SPT Case Histories
Liquefaction Case Histories			
- Fines Content $\leq$ 5%	22	30.1	12.1
- Fines Content 6-34%	39	53.4	21.3
- Fines Content $\geq$ 35%	12	16.4	6.6
Total	**73**	**100**	**39.9**
Non-Liquefaction Case Histories	17	13.2	7.1
- Fines Content $\leq$ 5%	57	44.2	29.0
- Fines Content 6-34%	55	42.6	24.0
- Fines Content $\geq$ 35%			
Total	**110**	**100**	**60.1**

5.3.1 Entire SPT Case History Database

The entire SPT case history database is shown in Figure 5.1. The $CSR_{7.5}$ values are the same ones used in the V_S database. The boundary curves recommended by Seed et al. (1985) are also plotted in the figure. There are a total of 183 case histories, with 73 liquefaction case histories and 110 non-liquefaction case histories. The liquefaction case histories are shown as solid symbols and the non-liquefaction case histories are shown as open symbols. Due to the linkage with the V_S database, some of the case histories within the SPT database have identical values of $N_{1,60}$ and $CSR_{7.5}$. Considering this 'overlap', the actual number of points shown is

reduced. Due to the 'overlap', there are only 116 individual data points representing the 183 case histories within the SPT database. Of the 116 data points, 56 represent the 73 liquefaction case histories and 60 represent the 110 non-liquefaction case histories.

In Figure 5.1, the average corrected blow count ($N_{1,60}$) in the critical layer is plotted on the horizontal axis and the equivalent cyclic stress ratio for $M_W = 7.5$ is plotted on the vertical axis. The minimum $N_{1,60}$ values within the critical layer are shown in Figure 5.2 and the maximum values in Figure 5.3. Obviously, the maximum $N_{1,60}$ values should not be used with the boundary curves because many liquefaction occurrences would be unconservatively predicted to not liquefy. On the other hand, when the minimum $N_{1,60}$ values in the SPT database are plotted, the values plot with a higher success than when the average values are used. Therefore, the minimum values are carried through this study and will be considered when correlations are made between the three methods in Chapter 7.

Proposed boundary curves dividing the liquefaction and non-liquefaction zones are also shown in Figures 5.1 through 5.3. These boundary curves are the ones proposed by Seed et al. (1985). They were selected because they are based on the fines content of the soil. The case histories within the SPT database only have recorded fines content values, not D_{50} values. Therefore, other proposed boundary curves could not be utilized for the SPT database in this report.

5.3.2 SPT Case Histories with Fines Content $\leq$ 5%

Case histories with fines content $\leq$ 5% are shown in Figures 5.4 and 5.5. In Figure 5.4, the average $N_{1,60}$ value within the critical layer is plotted along with a range bar extending to the minimum $N_{1,60}$ value within the critical layer. The same type of plot is presented in Figure 5.5 except that the range bar extends from the average value to the maximum $N_{1,60}$ value. The case histories are plotted with the appropriate boundary curve. The liquefaction case histories have the case history

number next to the individual data points. For clarity, the non-liquefaction data points are shown without case history numbers. It is obvious that, for a fines content $\leq 5\%$, use of minimum $N_{1,60}$ value only slightly improved the prediction success. Also, this improvement was observed to occur only for $CSR_{7.5}$ values below 0.20.

5.3.3 SPT Case Histories with Fines Content Between 6 and 34%

Case histories with fines content between 6 and 34% are shown in Figures 5.6 and 5.7. In Figure 5.6, the average $N_{1,60}$ value within the critical layer is plotted along with a range bar extending to the minimum $N_{1,60}$ value within the critical layer. The same type of plot is presented in Figure 5.7 except that the range bar extends from the average value to the maximum $N_{1,60}$ value. The case histories are plotted with the appropriate boundary curve. As before, the liquefaction case histories have the case history number next to the individual data points and the non-liquefaction data points are shown without case history numbers. Once again, the use of the minimum $N_{1,60}$ value improved the prediction only when the $CSR_{7.5}$ value was less than 0.20.

5.3.4 SPT Case Histories with Fines Content $\geq$ 35%

Case histories with fines content $\geq 35\%$ are shown in Figures 5.8 and 5.9. In Figure 5.8, the average $N_{1,60}$ value within the critical layer is plotted along with a range bar extending to the minimum $N_{1,60}$ value within the critical layer. The same type of plot is presented in Figure 5.9 except that the range bar extends from the average value to the maximum $N_{1,60}$ value. The case histories are plotted with the appropriate boundary curve.

Once again, the use of the minimum $N_{1,60}$ value improved the prediction only when the $CSR_{7.5}$ value was less than 0.20. It is obvious that, for all SPT case histories, the use of the minimum value only improved the prediction success when the $CSR_{7.5}$ value was less than 0.20.

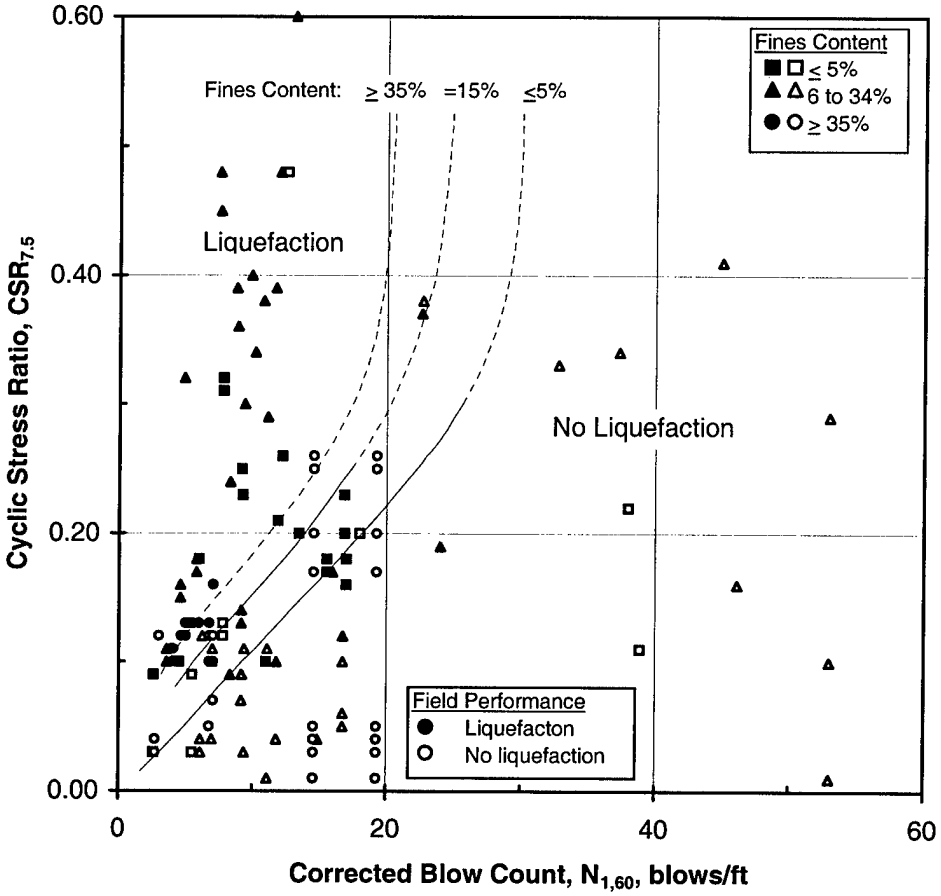

Fig. 5.1 - Average Corrected Blow Counts in the Critical Layer from the Entire SPT Case History Database with the Seed et al. (1985) Boundary Curves.

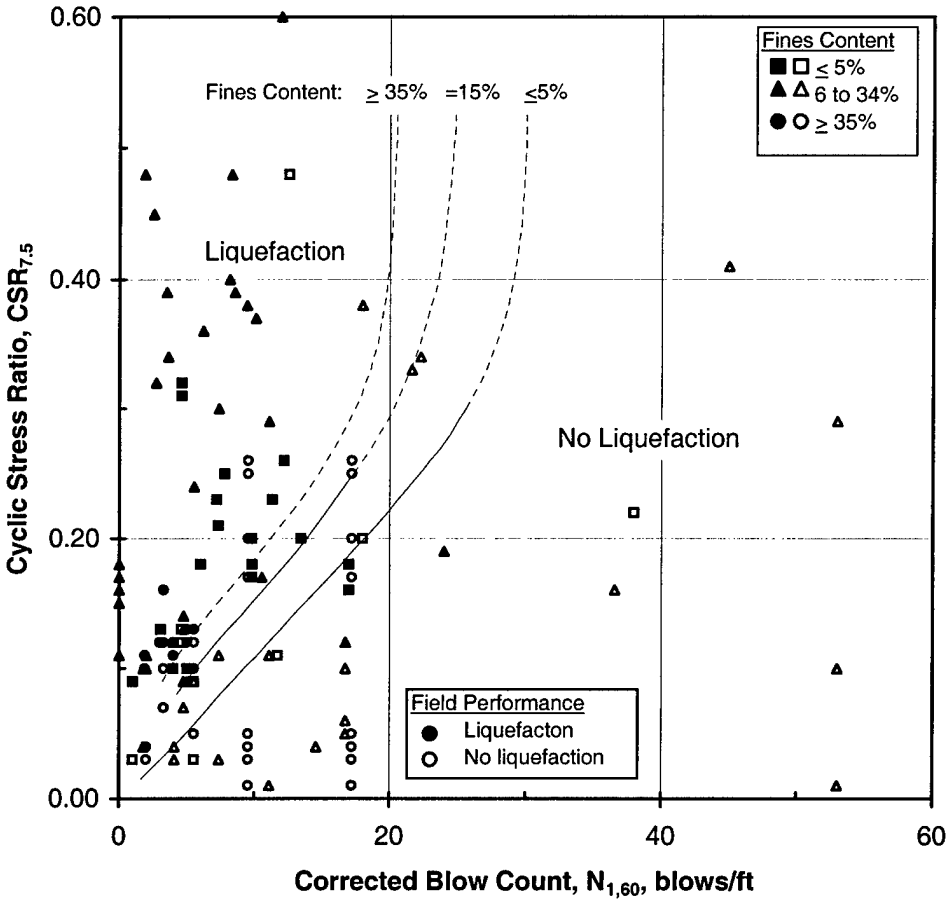

Fig. 5.2 - Minimum Corrected Blow Counts in the Critical Layer from the Entire SPT Case History Database with the Seed et al. (1985) Boundary Curves.

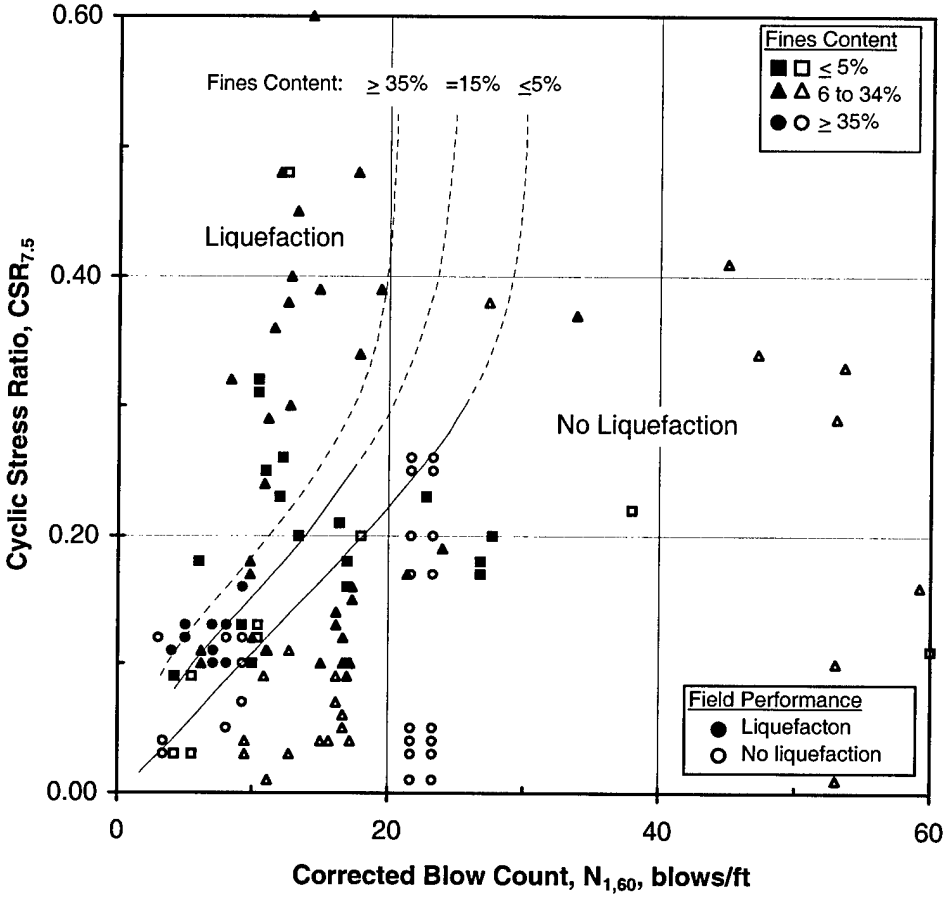

Fig. 5.3 - Maximum Corrected Blow Counts in the Critical Layer from the Entire SPT Case History Database with the Seed et al. (1985) Boundary Curves.

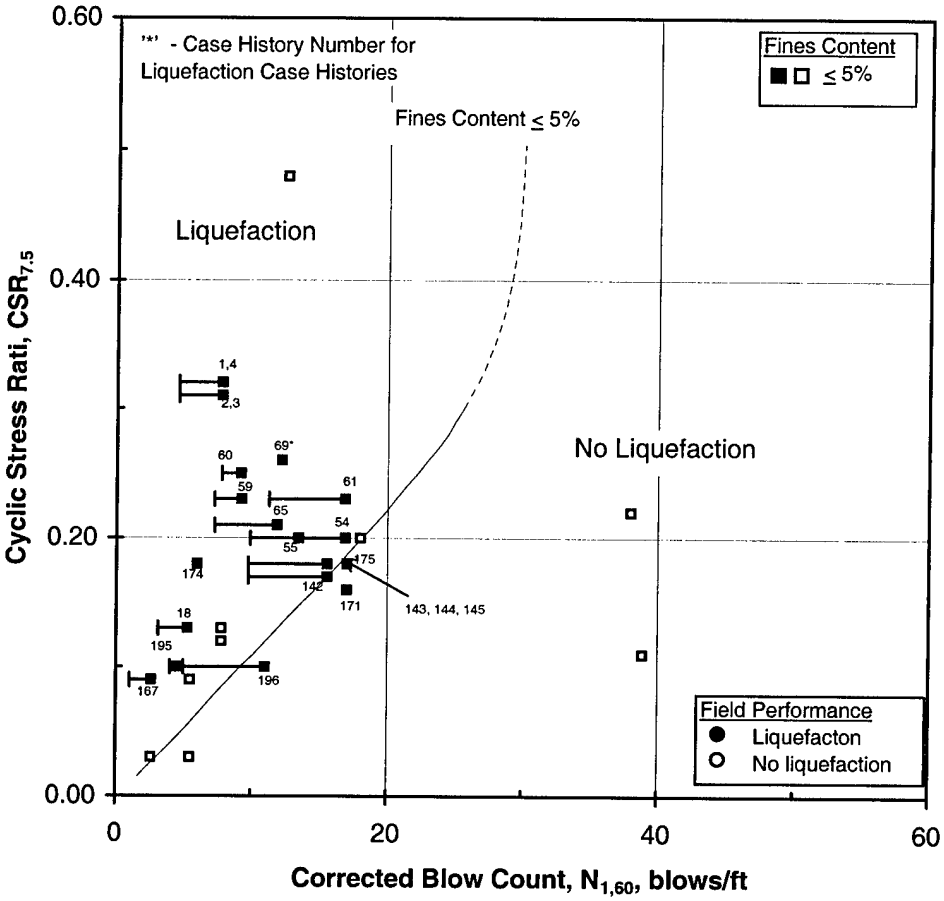

Fig. 5.4 - Average Corrected Blow Counts for SPT Liquefaction Case Histories with Fines Content $\leq$ 5% with Range Bar to the Minumum $N_{1,60}$ Value within the Critical Layer.

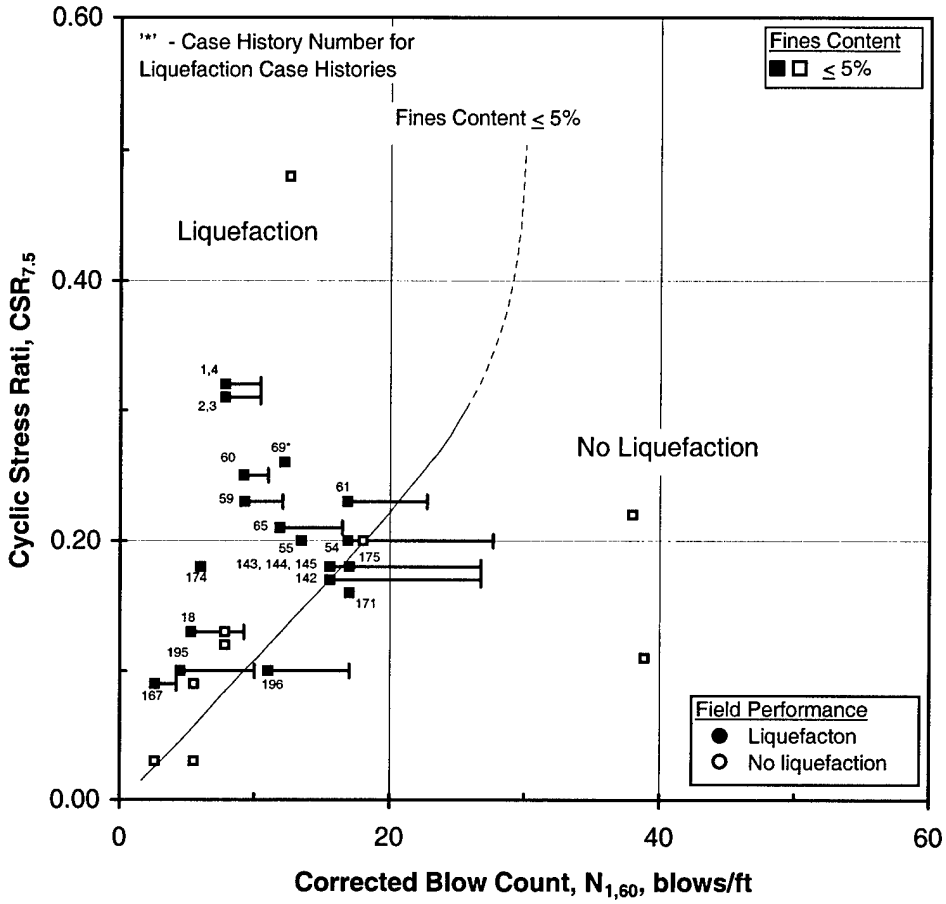

Fig. 5.5 - Average Corrected Blow Counts for SPT Liquefaction Case Histories with Fines Content ≤ 5% with Range Bar to the Maximum $N_{1,60}$ Value within the Critical Layer.

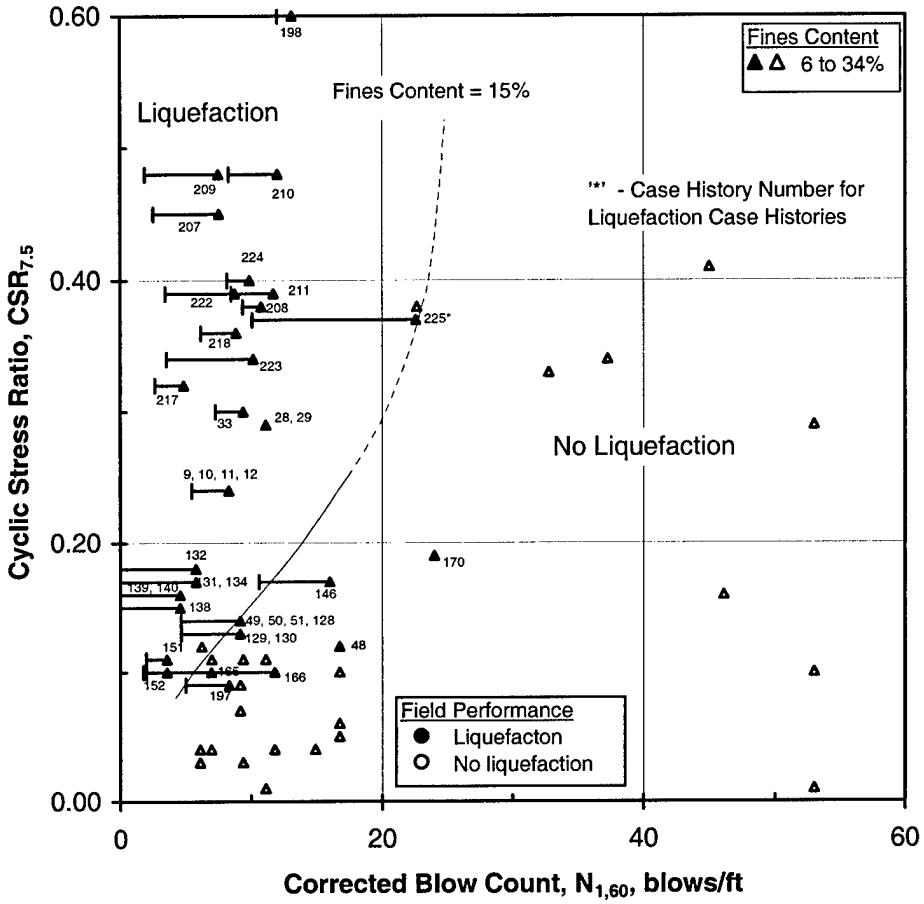

Fig. 5.6 - Average Corrected Blow Counts for SPT Liquefaction Case Histories with Fines Content = 6%-34% with Range Bar to the Minimum $N_{1,60}$ Value within the Critical Layer.

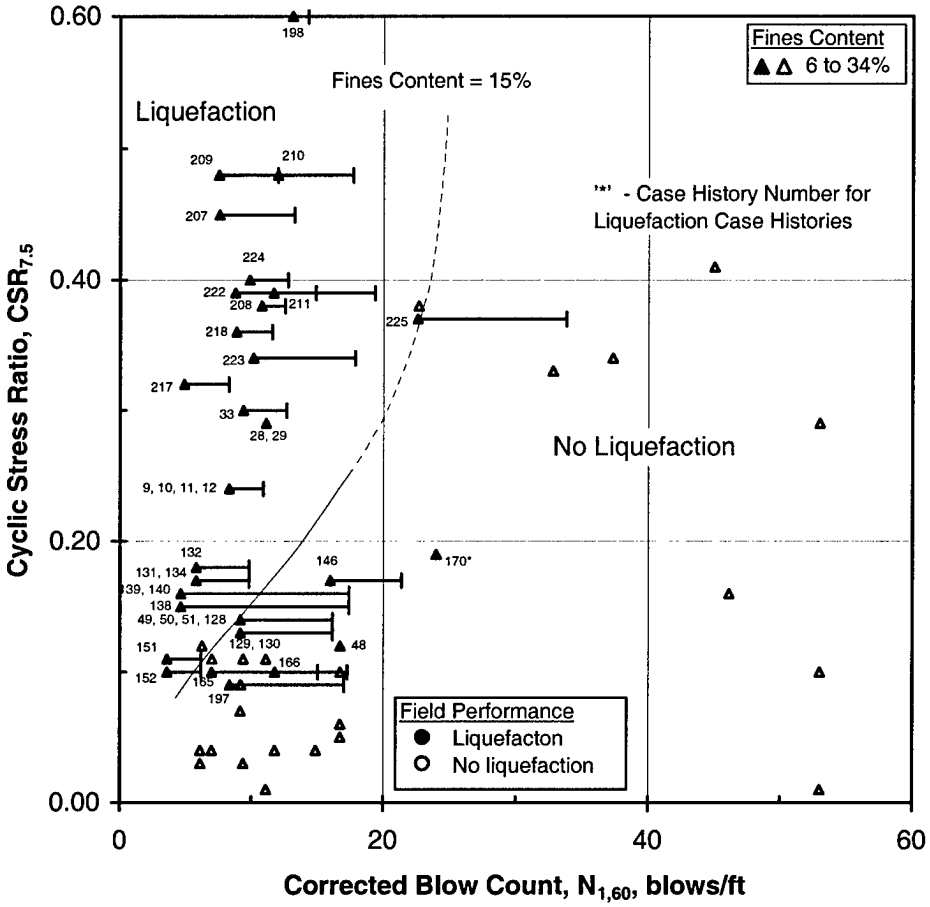

Fig. 5.7 - Average Corrected Blow Counts for SPT Liquefaction Case Histories with Fines Content = 6%-34% with Range Bar to the Maximum $N_{1,60}$ Value within the Critical Layer.

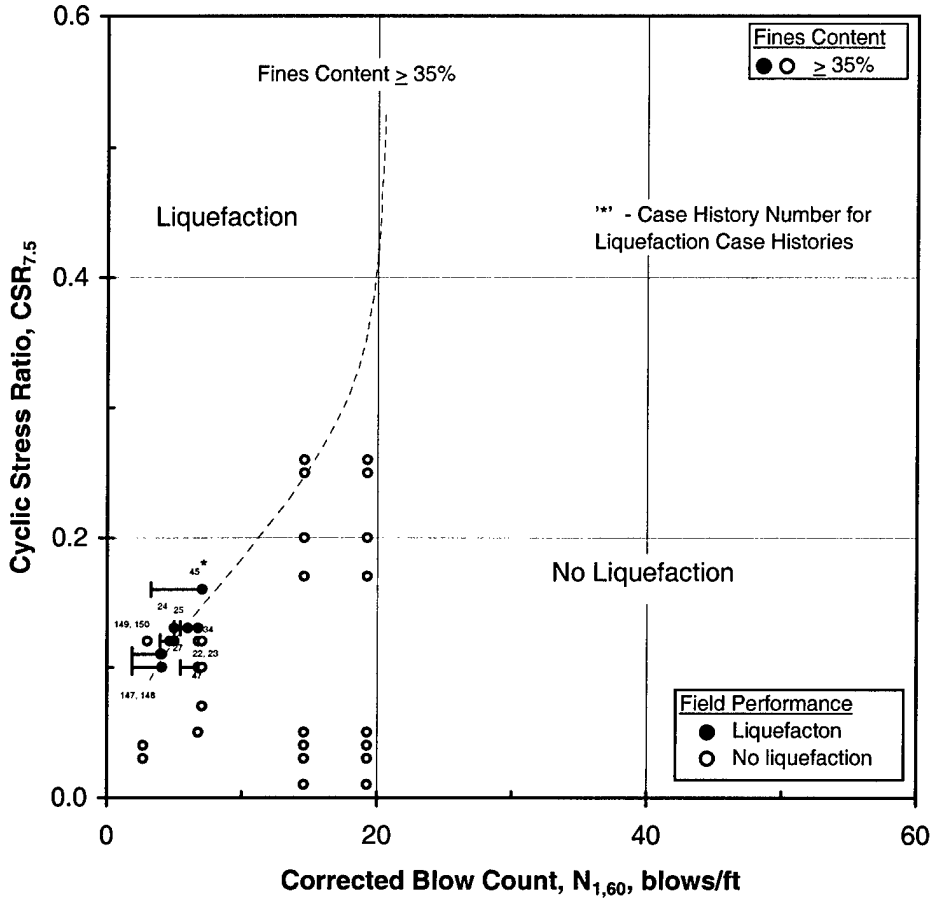

Fig. 5.8 - Average Corrected Blow Counts for SPT Liquefaction Case Histories with Fines Content ≥ 35 % with Range Bar to the Minimum $N_{1,60}$ Value within the Critical Layer.

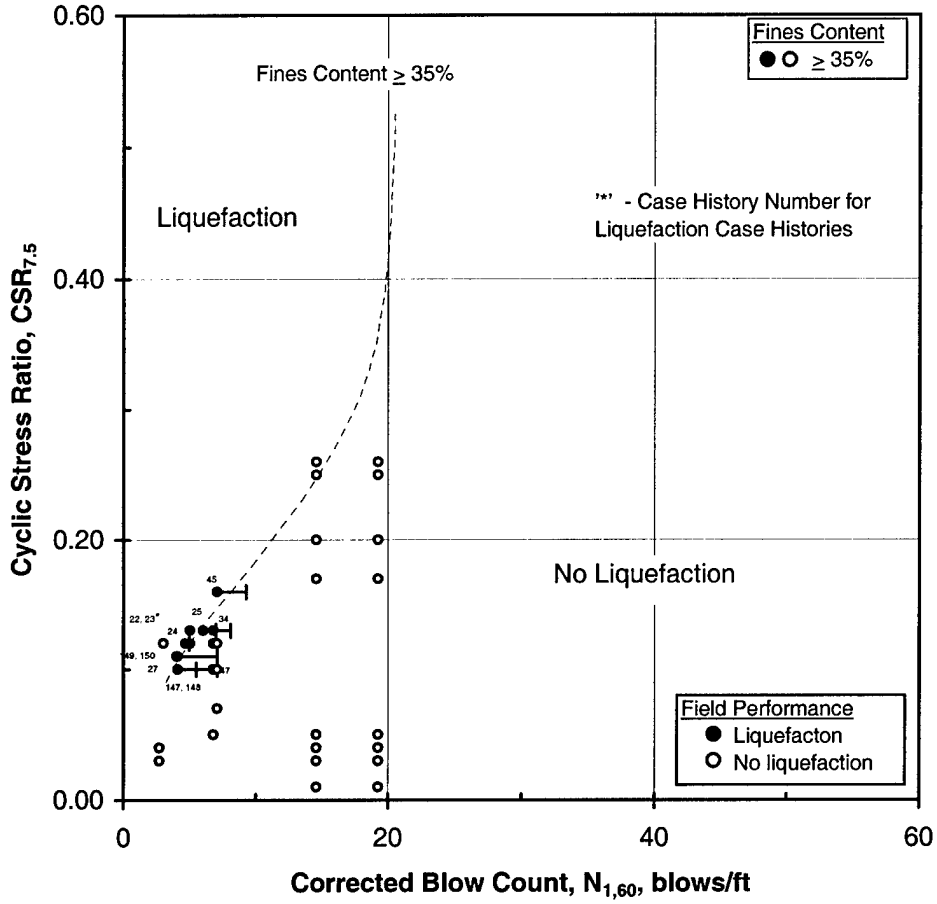

Fig. 5.9 - Average Corrected Blow Counts for SPT Liquefaction Case Histories with Fines Content ≥ 35 % with Range Bar to the Maximum $N_{1,60}$ Value within the Critical Layer.

5.4 ACCURACY OF THE SPT BOUNDARY CURVES

Table 5.4 lists the number of SPT liquefaction case histories that plotted on the correct side of the boundary curves using the average $N_{1,60}$ value. In some cases, when a site did not liquefy, the case history plotted on the 'liquefaction' side of the boundary curve. The SPT boundary curves were drawn conservatively to encompass nearly all liquefaction case histories, and some non-liquefaction case histories. Therefore, it is expected that some of the non-liquefaction case histories plot on the liquefaction side of the boundary curves. In this study, the objective was to evaluate the curves in their ability to predict liquefaction for sites that did liquefy. In summary, of the 73 liquefaction case histories, 54 plotted correctly yielding an accuracy of 74.0%.

Table 5.4 – Tabulation of How Well the SPT Boundary Curves Were Able to Predict Liquefaction for Sites that Liquefied.

Fines Content	Number of Liquefaction Case Histories	Number Plotted Correctly	% Plotted Correctly
≤ 5%	22	19	86.4
6- 34%	39	28	71.8
≥35%	12	7	58.3
Total	**73**	**54**	**74.0**

Of the 19 liquefaction case histories that were misclassified by the SPT boundaries, 13 plotted correctly when the minimum $N_{1,60}$ value was used in place of the average. Of the six case histories that did not plot correctly, four had only one $N_{1,60}$ value within the critical layer and can be ignored. Four out of the 19 exhibited

a coefficient of variability (CV) within the critical layer greater than 50%. The liquefaction case histories that did not plot correctly and key aspects that may have influenced the results of analysis are listed in Table 5.5.

Table 5.5 – SPT Liquefaction Case Histories that Plotted Incorrectly.

Number	Case History Number	Fines Content	No. of Values in the Average	Coeff. Of Variability < 50%?	Min. Plot Correctly ?
1	25	42%	2	Yes	Yes
2	34	35%	2	Yes	Yes
3	47	35%	2	Yes	No
4	48	13%	1	-	-
5	49	27%	5	Yes	Yes
6	50	27%	5	Yes	Yes
7	51	27%	5	Yes	Yes
8	128	27%	5	Yes	Yes
9	129	27%	5	Yes	Yes
10	130	27%	5	Yes	Yes
11	146	10%	2	Yes	Yes
12	147	57%	8	No	Yes
13	148	57%	8	No	Yes
14	166	8%	3	No	Yes
15	170	15%	1	-	-
16	171	2%	1	-	-
17	175	1%	1	-	-
18	196	5%	2	No	Yes
19	197	14%	3	Yes	No

CHAPTER 6

CPT CASE HISTORIES

6.1 CONSISTENCIES BETWEEN THE CPT AND V_S DATABASES

The CPT case histories within the CPT database had to be linked to the corresponding values within the V_S database. To accomplish this linkage, information concerning the critical layer and cyclic stress ratio were applied to the CPT database exactly as reported by Andrus et al. (1999).

6.2 CALCULATIONS REQUIRED FOR THE CPT DATABASE

As discussed in Chapter 2, CPT tip resistance values reported that were not already normalized and corrected have to be corrected and normalized to one atmosphere of overburden stress before the values can be used in the liquefaction hazard analysis. In addition, statistical analyses of the data were conducted for each site within the critical layer. The following describes the calculations that are required for case histories within the CPT database.

6.2.1 Correcting and Normalizing the CPT Data

The CPT test is a more consistent field test than the SPT test. Therefore, the values measured during the test require fewer corrections than the values measured during the SPT test. The equation to correct the measured tip resistance (q_C) to the overburden stress corrected tip resistance (q_{C1}) and then normalize this value using atmospheric pressure ($q_{c1,N}$) is (after Robertson and Fear, 1986):

$$q_{C1,N} = \{q_C / P_A\} * \{P_A / \sigma'_V\}^{0.5} \quad (6.1)$$

where

q_C = measured tip resistance in kPa,

σ'_V = effective overburden pressure in kPa, and

P_A = atmospheric pressure in kPa = 100 kPa.

Equation 6.1 was applied to all CPT case histories in the CPT database when values of q_c for a particular site were reported in the reference. If $q_{C1,N}$ values were provided in the reference, then no corrections were made and the data were used in the liquefaction analysis as reported.

6.2.2 Statistical Calculations Performed for CPT Case Histories

After obtaining or calculating $q_{C1,N}$ values for every case history, simple statistical analyses were performed for the site for $q_{C1,N}$ values within the critical layer. The statistical analysis involved calculations of the average value, minimum value, maximum value, standard deviation, and coefficient of variability. This information was used to judge the quality of the data and the uniformity of the critical layer. This information was also used to analyze the correlation boundary curves under different circumstances.

6.2.3 Removal of Data Due to Engineering Judgment

In certain cases, some of the data collected within the critical layer did not seem to represent the material in a layer that would be susceptible to liquefaction. In these instances the data were removed and were not included in the above statistical calculations. An example of this procedure is the following. The Radio Tower site represents CPT case histories 34, 47, 115, and 126. The investigators, Bierschwale and Stokoe (1984), reported five q_c values within the critical layer. The reported values, descending through the critical layer, were 10, 20, 38, 38, and 65 kg/cm^2.

Obviously, the portion of the critical layer represented by the four values in the top portion of the layer seemed to be the most representative of the liquefiable portion of the layer. The q_c value equal to 65 kg/cm^2 was obviously representative of a stiffer non-liquefiable portion of the layer. Therefore, the q_c value representing the stiffer material was removed and not included in the statistical analysis of the critical layer. All case histories that had data removed are listed in Table 6.1. Of the 147 CPT case histories, 40 had data removed and 107 did not.

All soil profiles will be presented in a future geotechnical report by the same authors. The soil profiles will indicate the unrepresentative q_c values and the depths at which they were reported.

Table 6.1 – Case Histories from the CPT Database that had q_c Values Removed from the Critical Layer due to Unrepresentative Material.

Number	Case History Number	Field Performance (LF or No LF)	Average Fines Content
1	1	LF	5%
2	2	LF	5%
3	3	LF	5%
4	4	LF	5%
5	5	No LF	44%
6	6	No LF	44%
7	7	No LF	44%
8	8	No LF	44%
9	9	LF	14%
10	10	LF	14%
11	11	LF	14%
12	12	LF	14%
13	22	LF	61%
14	24	LF	90%

'LF' = Liquefaction

Table 6.1 (cont.) – Case Histories from the CPT Database that had q_c Values Removed from the Critical Layer due to Unrepresentative Material.

Number	Case History Number	Field Performance (LF or No LF)	Average Fines Content
15	25	LF	42%
16	32	No LF	75%
17	39	LF	35%
18	45	LF	75%
19	47	LF	35%
20	55	LF	5%
21	66	LF	5%
22	67	LF	5%
23	69	LF	5%
24	113	No LF	75%
25	115	No LF	35%
26	124	LF	75%
27	126	No LF	35%
28	146	LF	10%
29	153	No LF	5%
30	154	No LF	5%
31	155	No LF	5%
32	156	No LF	5%
33	157	No LF	44%
34	158	No LF	44%
35	159	No LF	44%
36	160	No LF	44%
37	161	No LF	14%
38	162	No LF	14%
39	163	No LF	14%
40	164	No LF	14%

'LF' = Liquefaction

6.3 PRESENTATION OF THE CPT DATABASE

A summary of the CPT case history data in terms of liquefaction and fines content is presented in Table 6.2.

Table 6.2 – Summary of the 147 CPT Case Histories Reviewed in this Study.

	Number Of CPT Case Histories	% of CPT Case Histories within the Category	% of Total CPT Case Histories
Liquefaction Case Histories			
- Fines Content $\leq$ 5%	25	36.2	17.0
- Fines Content 6-34%	31	44.9	21.1
- Fines Content $\geq$ 35%	13	18.8	8.8
Total	**69**	**100**	**46.9**
Non-Liquefaction Case Histories			
- Fines Content $\leq$ 5%	25	15.4	8.1
- Fines Content 6-34%	31	60.3	32.0
- Fines Content $\geq$ 35%	13	24.3	13.0
Total	**78**	**100**	**53.1**

6.3.1 Entire CPT Case History Database

The entire CPT case history database is shown in Figure 6.1 plotted with the boundary curves recommended by Stark and Olson (1995). There are a total of 147 case histories with 69 liquefaction case histories and 78 non-liquefaction case histories. The liquefaction case histories are shown as solid symbols and the non-liquefaction case histories are shown as open symbols. Due to the linkage with the V_S database, some of the case histories within the CPT database have identical values of $q_{c1,N}$ and $CSR_{7.5}$. When evaluating this 'overlap', the actual number of

points shown is reduced. Due to the 'overlap', there are only 94 individual data points representing the 147 case histories within the CPT database. Of the 94 data points, 52 represent the 69 liquefaction case histories and 42 represent the 78 non-liquefaction case histories.

In Figure 6.1, the average normalized cone tip resistance ($q_{c1,N}$) in the critical layer is plotted on the horizontal axis and the equivalent cyclic stress ratio for $M_W = 7.5$ is plotted on the vertical axis. The minimum $q_{c1,N}$ values within the critical layer are shown in Figure 6.2 and the maximum values in Figure 6.3. Obviously, the maximum $q_{c1,N}$ values should not be used with the boundary curves because many liquefaction occurrences would be unconservatively predicted to not liquefy. On the other hand, when the minimum $q_{c1,N}$ values in the CPT database are plotted, the values plot with a higher success than when the average values are used. Therefore, the minimum values are carried through this study and will be considered when correlations are made between the three methods in Chapter 7.

Proposed boundary curves dividing the liquefaction and non-liquefaction zones are also shown in Figures 6.1 through 6.3. These boundary curves are the ones proposed by Stark and Olson (1995). They were selected because they are based on the fines content of the soil. The case histories within the CPT database only have recorded fines content values, not D_{50} values. Therefore, other proposed boundary curves could not be utilized for the CPT database in this report.

6.3.2 CPT Case Histories with Fines Content $\leq$ 5%

Case histories with fines content $\leq$ 5% are shown in Figures 6.4 and 6.5. In Figure 6.4, average $q_{c1,N}$ values within the critical layers along with a range bar extending to the minimum $q_{c1,N}$ values within the critical layer are shown. The same type of plot is presented in Figure 6.5 except that the range bar extends from the average $q_{c1,N}$ values to the maximum $q_{c1,N}$ values. The case histories are plotted with the appropriate boundary curve. The liquefaction case histories have the case history

number next to the individual data points. For clarity, the non-liquefaction data points are shown without case history numbers. It is obvious that, for a fines content $\leq 5\%$, use of minimum $q_{c1,N}$ value only slightly improved the prediction success. Also, this improvement was observed to only occur for $CSR_{7.5}$ values greater than 0.20.

6.3.3 CPT Case Histories with Fines Content Between 6 and 34%

Case histories with fines content between 6 and 34% are shown in Figures 6.6 and 6.7. In Figure 6.6, average $q_{c1,N}$ values within the critical layer along with a range bar extending to the minimum $q_{c1,N}$ values within the critical layer are shown. The same type of plot is presented in Figure 6.7 except that the range bar extends from the average value to the maximum $q_{c1,N}$ value. The case histories are plotted with the appropriate boundary curve. As before, the liquefaction case histories have the case history number next to the individual data points and the non-liquefaction data points are shown without case history numbers. In this data set, the use of the minimum $q_{c1,N}$ value improved the prediction only when the $CSR_{7.5}$ value was less than 0.20.

6.3.4 CPT Case Histories with Fines Content $\geq$ 35%

Case histories with fines content $\geq 35\%$ are shown in Figures 6.8 and 6.9. In Figure 6.8, average $q_{c1,N}$ values within the critical layer along with a range bar extending to the minimum $q_{c1,N}$ values within the critical layer are shown. The same type of plot is presented in Figure 6.9 except that the range bar extends from the average value to the maximum $q_{c1,N}$ value. The case histories are plotted with the appropriate boundary curve. Once again, the use of the minimum $q_{c1,N}$ value improved the prediction only when the $CSR_{7.5}$ value was less than 0.20. For most CPT case histories, the use of the minimum value only improved the prediction success when the $CSR_{7.5}$ value was less than 0.20.

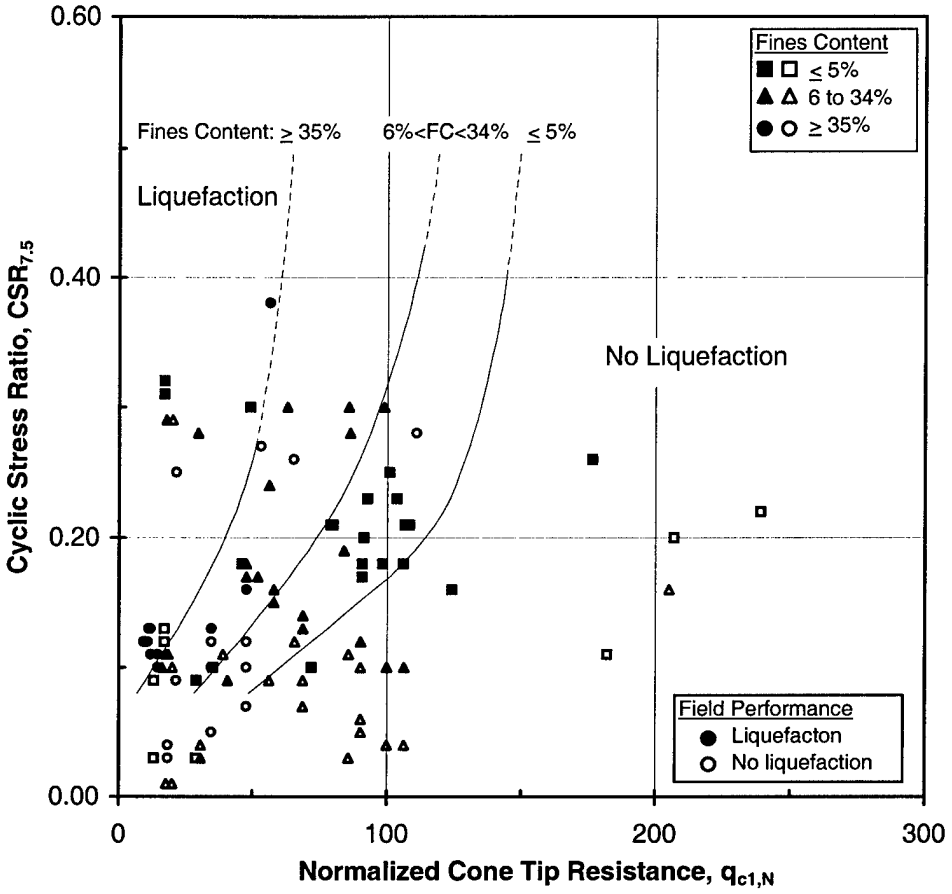

Fig. 6.1 - Average Normalized Cone Tip Resistance through the Critical Layer from the Entire CPT Case History Database with the Stark and Olson (1995) Boundary Curves.

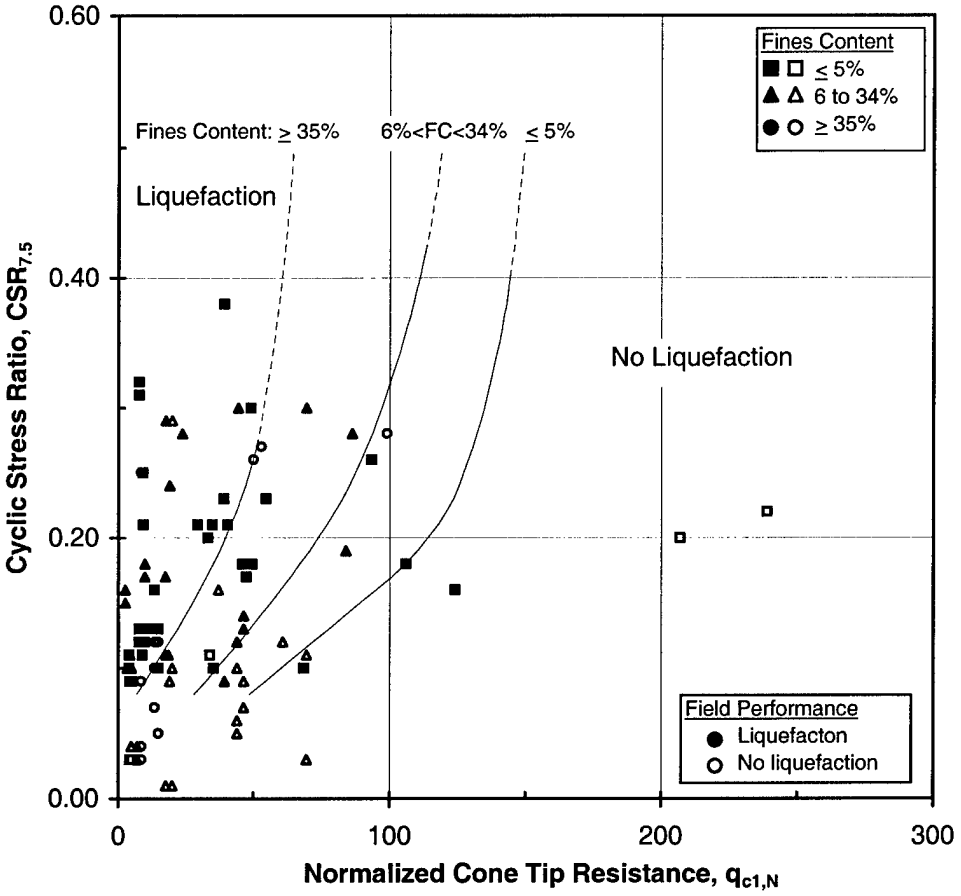

Fig. 6.2 - Minimum Normalized Cone Tip Resistance through the Critical Layer from the Entire CPT Case History Database with the Stark and Olson (1995) Boundary Curves.

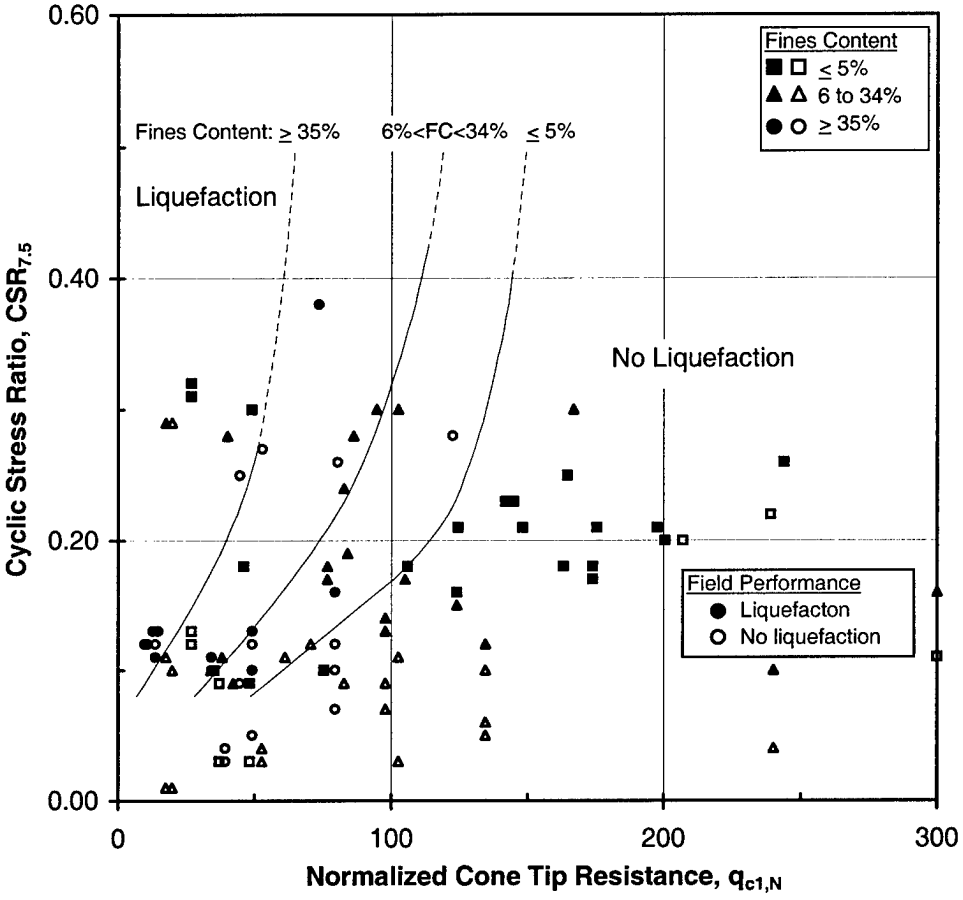

Fig. 6.3 - Maximum Normalized Cone Tip Resistance through the Critical Layer from the Entire CPT Case History Database with the Stark and Olson (1995) Boundary Curves.

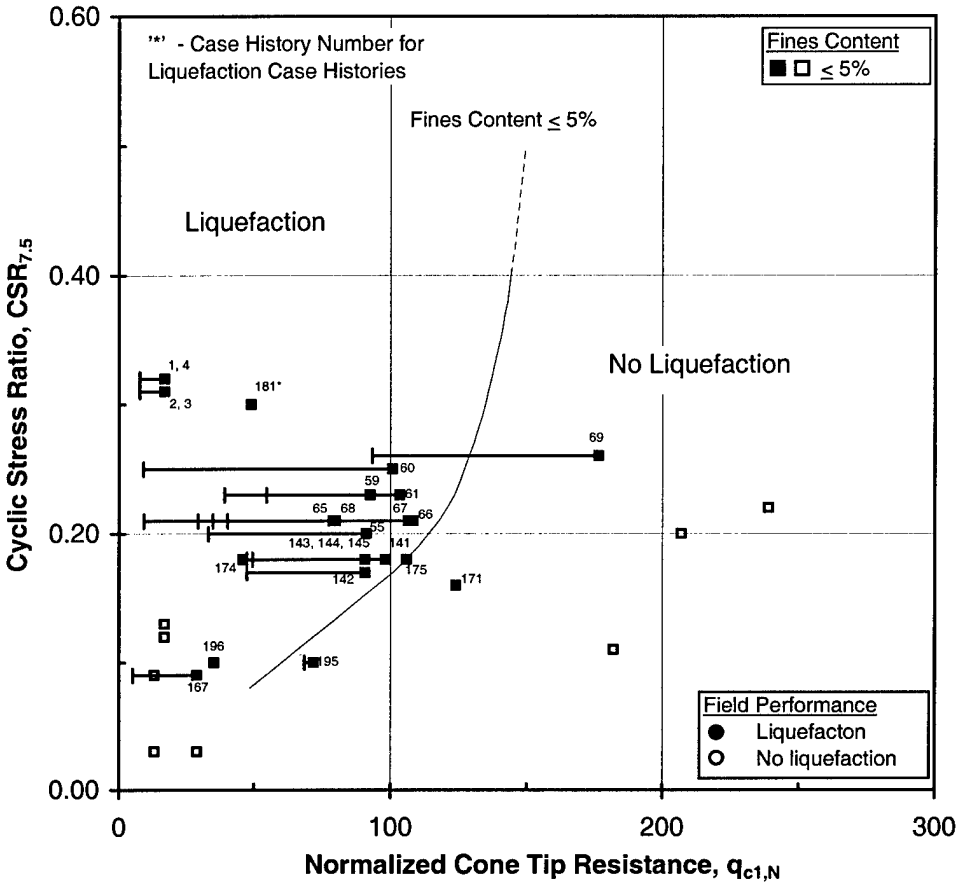

Fig. 6.4 - Average Normalized Cone Tip Resistance for CPT Liquefaction Case Histories with Fines Content ≤ 5% with Range Bar to the Minimum $q_{c1,N}$ Value within the Critical Layer.

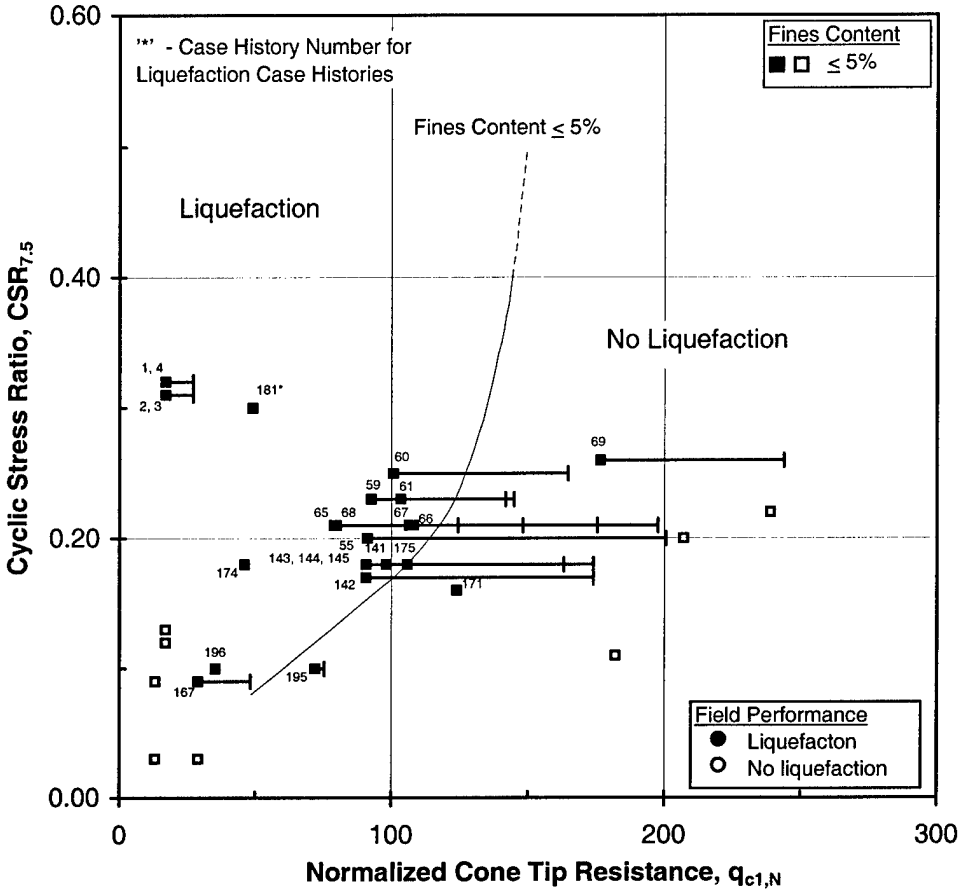

Fig. 6.5 - Average Normalized Cone Tip Resistance for CPT Liquefaction Case Histories with Fines Content ≤ 5% with Range Bar to the Maximum $q_{c1,N}$ Value within the Critical Layer.

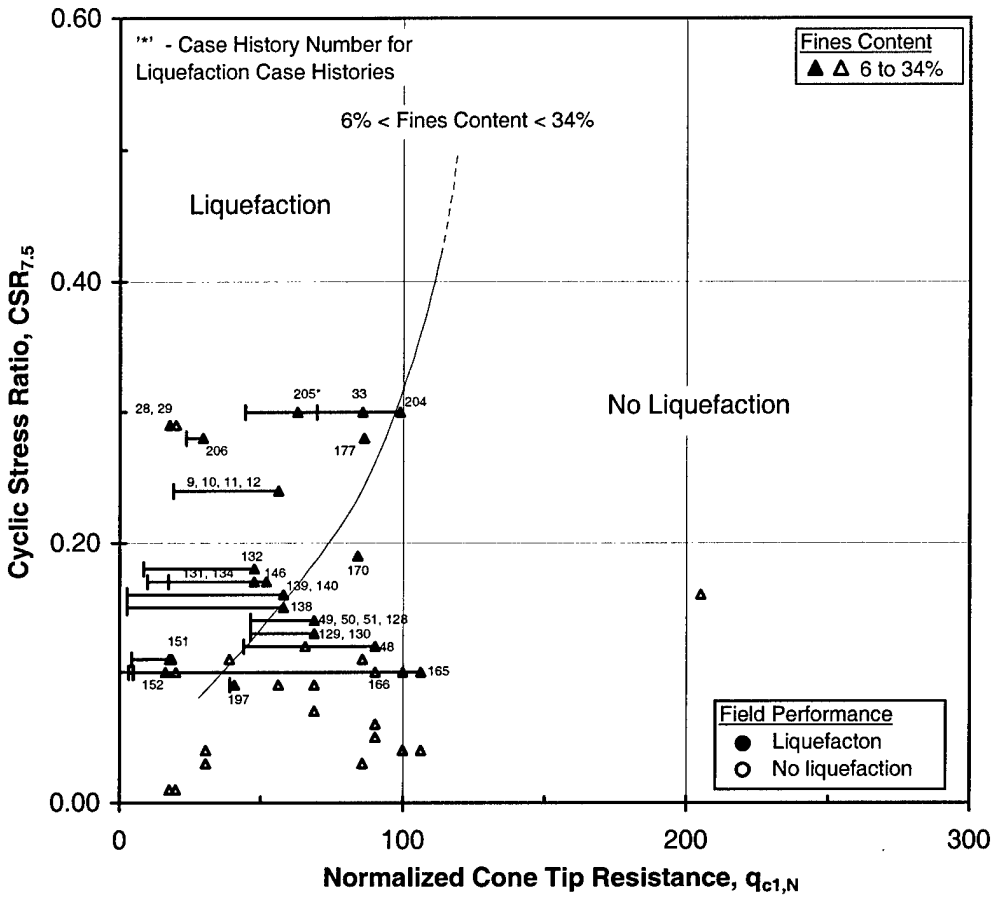

Fig. 6.6 - Average Normalized Cone Tip Resistance for CPT Liquefaction Case Histories with Fines Content = 6% - 34 % with Range Bar to the Minimum $q_{c1,N}$ Value within the Critical Layer.

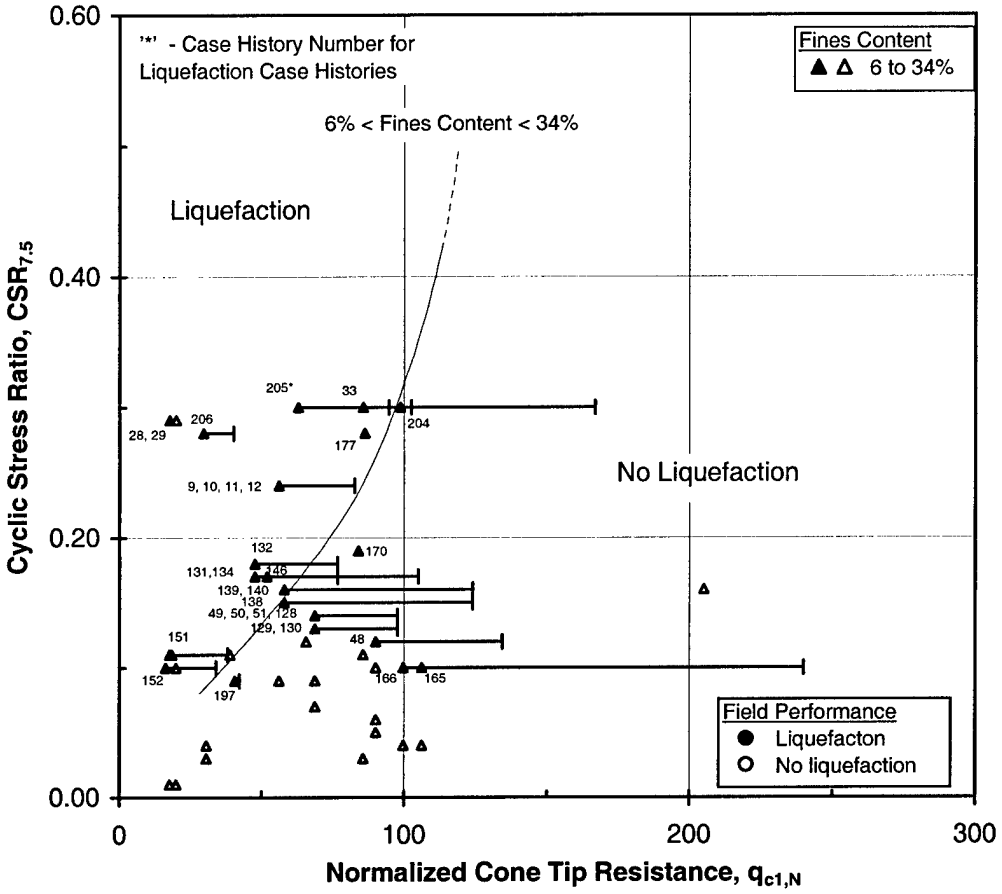

Fig. 6.7 - Average Normalized Cone Tip Resistance for CPT Liquefaction Case Histories with Fines Content = 6% - 34 % with Range Bar to the Maximum $q_{c1,N}$ Value within the Critical Layer.

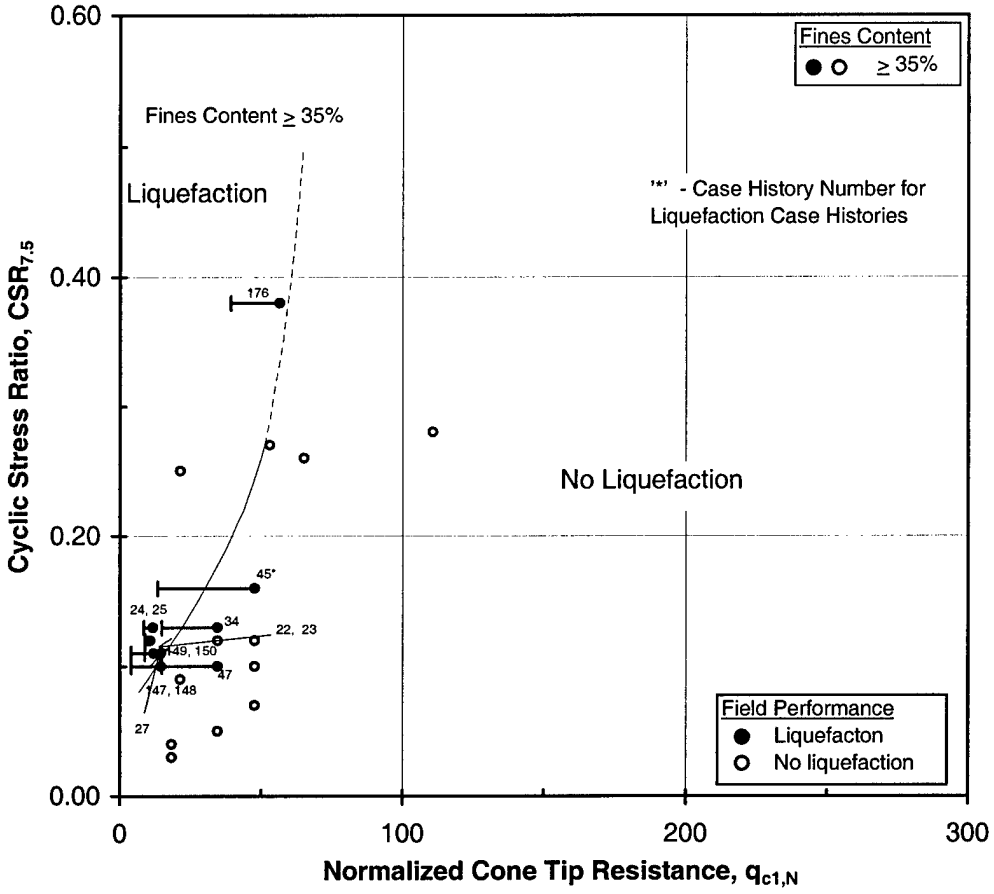

Fig. 6.8 - Average Normalized Cone Tip Resistance for CPT Liquefaction Case Histories with Fines Content $\geq$ 35 % with Range Bar to the Minimum $q_{c1,N}$ Value within the Critical Layer.

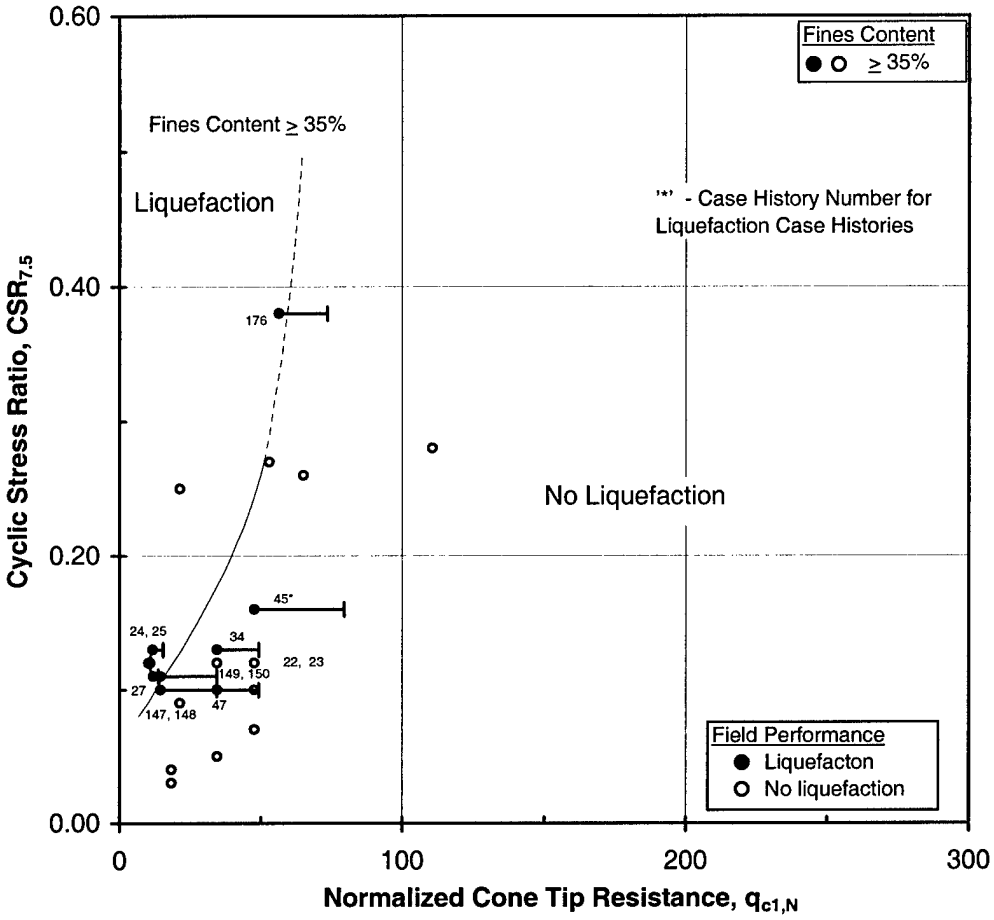

Fig. 6.9 - Average Normalized Cone Tip Resistance for CPT Liquefaction Case Histories with Fines Content ≥ 35 % with Range Bar to the Maximum $q_{c1,N}$ Value within the Critical Layer.

6.4 ACCURACY OF THE CPT BOUNDARY CURVES

Table 6.3 lists the number of CPT liquefaction case histories that plotted on the correct side of the boundary curves. In some cases, when a site did not liquefy, the case history plotted on the 'liquefaction' side of the boundary curve. The CPT boundary curves were drawn conservatively to encompass nearly all liquefaction case histories, and some non-liquefaction case histories. Therefore, it is expected that some of the non-liquefaction case histories plot on the liquefaction side of the boundary curves. In this study, the objective was to evaluate the curves in their ability to predict liquefaction for sites that did liquefy. In summary, of the 69 liquefaction case histories 50 plotted correctly yielding an accuracy of 72.5%.

Table 6.3 – Tabulation of How Well the CPT Boundary Curves Were Able to Predict Liquefaction for Sites that Liquefied.

Fines Content	Number of Liquefaction Case Histories	Number Plotted Correctly	% Plotted Correctly
≤ 5%	25	22	88.0
6- 34%	31	20	64.5
≥35%	13	8	61.5
Total	**69**	**50**	**72.5**

Of the 19 liquefaction case histories that were misclassified by the CPT boundaries, nine plotted correctly when the minimum $q_{c1,N}$ value was used in place of the average. Of the 10 case histories that did not plot correctly, two had only one $q_{c1,N}$ value within the critical layer and can be ignored. Four out of the 19 exhibited

a coefficient of variability (CV) within the critical layer greater than 50%. The liquefaction case histories that did not plot correctly and key aspects that may have influenced the results of analysis are listed in Table 6.4.

Table 6.4 – CPT Liquefaction Case Histories that Plotted Incorrectly.

Number	Case History Number	Fines Content	No. of Values in the Average	Coeff. Of Variability < 50%?	Min. Plot Correctly?
1	34	35%	4	Yes	Yes
2	45	75%	5	Yes	Yes
3	47	35%	4	Yes	Yes
4	48	13%	6	Yes	Yes
5	49	27%	5	Yes	No
6	50	27%	5	Yes	No
7	51	27%	5	Yes	No
8	69	5%	17	Yes	Yes
9	128	27%	5	Yes	No
10	129	27%	5	Yes	No
11	130	27%	5	Yes	No
12	147	57%	81	No	Yes
13	148	57%	81	No	Yes
14	165	8%	58	No	Yes
15	166	8%	58	No	Yes
16	170	15%	1	-	-
17	171	2%	1	-	-
18	195	5%	2	Yes	No
19	197	14%	2	Yes	No

CHAPTER 7

COMPARISON OF THE V_S, SPT, AND CPT CORRELATIONS

7.1 CONSISTENCIES BETWEEN THE DIFFERENT CORRELATIONS

7.1.1 Available Data for Case Histories in Database

Each of the 225 case histories contained in the database have at least one shear wave velocity measurement and the majority have at least one CPT and or SPT value. Table 7.1 shows the number of case histories and the type of data that is available.

Table 7.1 – Types of Field Measurements Available in the 225 Case Histories in the Database.

Type of Field Data Available	# of Case Histories	% of Total Case Histories	# of Liquefaction Case Histories	% of Liquefaction Case Histories
Only V_S	21	9.3	12	12.5
V_S and only SPT	56	25.0	15	15.6
V_S and only CPT	21	9.3	10	10.4
V_S, SPT, and CPT	127	56.4	59	61.5
Total	225	100.0	96	100.0

7.1.2 Consistencies and Inconsistencies Between the Three Correlations

Of the 59 liquefaction case histories that had V_S, CPT, and SPT data, 23 cases exhibited inconsistencies between the predictions (liquefaction or no liquefaction) of the three measurement types. In other words, at least one of the

three correlations predicted the site would not liquefy when in reality the site did liquefy. In terms of measurement types, three V_S, 19 SPT, and 19 CPT case histories plotted incorrectly. Only one case was plotted incorrectly for all three correlations, number 197. However, when comparing only the SPT and CPT correlations, 15 out of the 19 case histories that plotted incorrectly are the same. All liquefaction case histories that plotted incorrectly are given in Table 7.2.

Table 7.2 – Liquefaction Case Histories that Were Incorrectly Predicted to not Liquefy.

Case History Number	Fines Content	Country of Origin	Number of Data Points CPT Avg	Number of Data Points SPT Avg
a. For all three measurement types (V_S, SPT and CPT):				
197	14%	USA	2	3
b. For both the SPT and CPT measurements only:				
34	35%	USA	4	2
47	35%	USA	4	2
48	13%	USA	6	1
49	27%	USA	5	5
50	27%	USA	5	5
51	27%	USA	5	5
128	27%	USA	5	5
129	27%	USA	5	5
130	27%	USA	5	5
147	57%	USA	81	8

Table 7.2 (cont.) – Liquefaction Case Histories that Were Incorrectly Predicted to not Liquefy.

Case History Number	Fines Content	Country of Origin	Number of Data Points CPT Avg	Number of Data Points SPT Avg
b. For both the SPT and CPT measurements only (cont.):				
148	57%	USA	81	8
166	8%	USA	58	3
170	15%	USA	1	1
171	2%	USA	1	1
c. For both V_S and CPT measurements only:				
195	5%	USA	2	2
d. For both V_S and SPT measurements only:				
- None -				
e. For only SPT measurements:				
25	42%	China	2	2
146	10%	USA	28	2
175	1%	USA	1	1
196	5%	USA	1	3
f. For only V_S measurements:				
217	10%	Japan	n/a	14

Table 7.2 (cont.) – Liquefaction Case Histories that Were Incorrectly Predicted to not Liquefy.

Case History Number	Fines Content	Country of Origin	Number of Data Points CPT Avg	Number of Data Points SPT Avg
g. For only CPT measurements:				
45	75%	USA	5	3
69	5%	USA	17	1
165	8%	USA	58	4

7.2 CORRELATIONS BETWEEN V_S - SPT, V_S - CPT, AND CPT - SPT

7.2.1 V_S and SPT Correlation

An overall correlation between V_{S1} and $N_{1,60}$ values can be made by plotting the paired values from the entire corrected database together. The 183 case histories from this database that had both V_{S1} and $N_{1,60}$ values are plotted in Figure 7.1. The mean correlation curve presented by Andrus et al. (1999) and the mean correlation curve proposed in this report are also shown in the figure. The mean correlation curve was created by plotting a 'best fit' line through the data set. The equation of the line is:

$$V_{S1} = 113.4\ (N_{1,60})^{0.139} \qquad 7.1$$

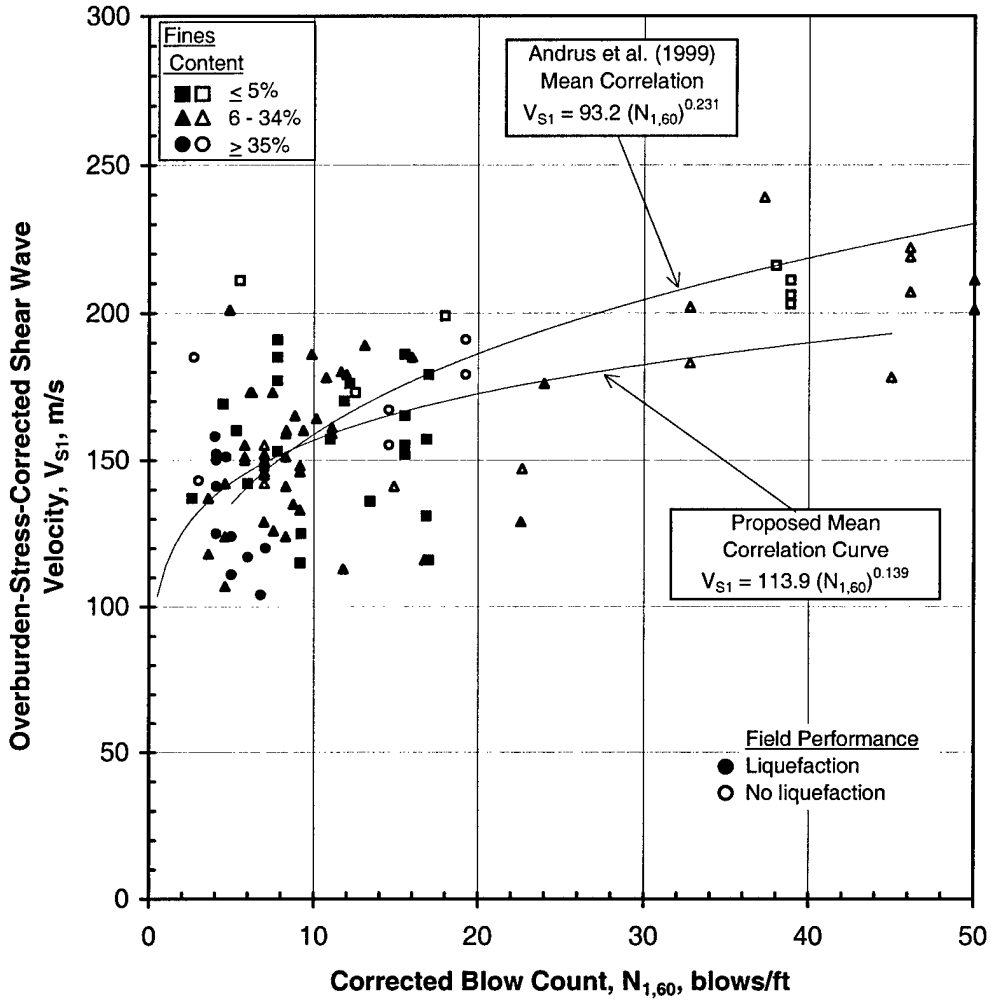

Fig 7.1 - Correlation Between V_{S1} and $N_{1,60}$ for All Case Histories Plotted with the Mean Correlation Curve Recommended by Andrus et al.(1999) and the Mean Correlation Curve Proposed in this Report.

The data, separated according to fines content, are presented in Figures 7.2, 7.3, and 7.4 for fines content $\leq 5\%$, 6 to 34%, and $\geq 35\%$, respectively. Mean correlation curves for all case histories and mean correlation curves for liquefaction and non-liquefaction case histories within the respective fines content ranges are also included in the figures.

In addition, Figures 7.2 – 7.4 display an implied curve derived from the V_S and SPT liquefaction boundary curves. These implied curves, which represent a correlation between V_{S1} and $N_{1,60}$ based on independently developed liquefaction correlations, were derived by plotting V_{S1} and $N_{1,60}$ values from the respective boundary curves with equal $CSR_{7.5}$ values. For example, consider the boundary curves for $\leq 5\%$ fines in Figures 4.2 and 5.4. At a $CSR_{7.5} = 0.20$, the boundary curves separating liquefaction from non-liquefaction correspond to $V_{S1} = 190$ m/s and $N_{1,60} = 18.5$ blows per foot. Hence, assuming both boundary curves are correct, we can infer this to mean that $N_{1,60} = 18.5$ blows per foot corresponds to $V_{S1} = 190$ m/s, which is one point on the implied curve in Figure 7.2. The implied curve for fines content $\leq 5\%$ is shown in Figure 7.2, the curve for fines content equal to 6 to 34% is shown in Figure 7.3, and the curve for fines content $\geq 35\%$ is shown in Figure 7.4.

In an ideal case, the implied curve would plot directly on the overall mean correlation curve for a respective fines content sub-category ($\leq 5\%$, 6-34%, or $\geq$ 35%). This would indicate that both liquefaction boundaries (V_{S1} and $N_{1,60}$) predict liquefaction with the same level of confidence. When the implied curve is above the mean correlation curve for the data, the V_S boundary is more conservative than the $N_{1,60}$ boundary. Conversely, when the implied curve is below the mean correlation curve, the $N_{1,60}$ boundary is more conservative than the V_{S1} boundary. This assumes that the mean $V_{S1} - N_{1,60}$ correlation shown is correct. However, the mean correlation is based on the relatively limited data within this database which shows considerable scatter about the mean correlation curve.

To understand where the V_S criteria is more conservative than the SPT criteria, consider $N_{1,60} = 20$ in Figure 7.2, which corresponds to $V_{S1} = 195$ m/s on the implied curve. That is, for $N_{1,60} = 20$ on the SPT boundary curve at $CSR_{7.5} = 0.21$ (Figure 5.4) the V_{S1} boundary curve in Figure 4.2 gives $V_{S1} = 175$ m/s. At $N_{1,60} = 20$ in Figure 7.2, the mean correlation curve gives $V_{S1} = 175$ m/s. At $CSR_{7.5} = 0.21$, $V_{S1} = 175$ m/s plots to the left of the boundary curve (at $V_{S1} = 195$ m/s) in Figure 4.2, which is on the conservative side of the boundary curve. Hence, when the mean correlation curve plots below the implied curve in Figure 7.2, we can infer that the V_{S1} criteria is more conservative (greater tendency to predict liquefaction when none occurs).

The plotted position of individual case histories can also be used to evaluate which boundary curve is more conservative. Case histories that plot directly on the implied curve indicate that both liquefaction boundary curves predict liquefaction with the same level of confidence. Case histories that plot below the implied curve indicate that, for the particular case history, the V_{S1} liquefaction boundary curve is more conservative than the $N_{1,60}$ liquefaction boundary curve. Conversely, case histories that plot above the implied curve indicate that the $N_{1,60}$ boundary curves are more conservative than the V_{S1} liquefaction boundary curves. For example, liquefaction case history 54 plots below the implied boundary in Figure 7.2. Referring back to Figures 4.2 and 5.4, both the V_S and SPT boundaries correctly predicted this case history to liquefy. However, for this case history there is a greater horizontal offset between the point representing case history 54 and the boundary curve in Figure 4.2 than in Figure 5.4. Therefore, for case history 54, the V_S boundary curve predicts liquefaction more conservatively than the SPT boundary curve. In general, the majority of the case histories plot below the implied curves indicating that the V_{S1} based liquefaction boundary curves are more conservative than the $N_{1,60}$ based boundary curves.

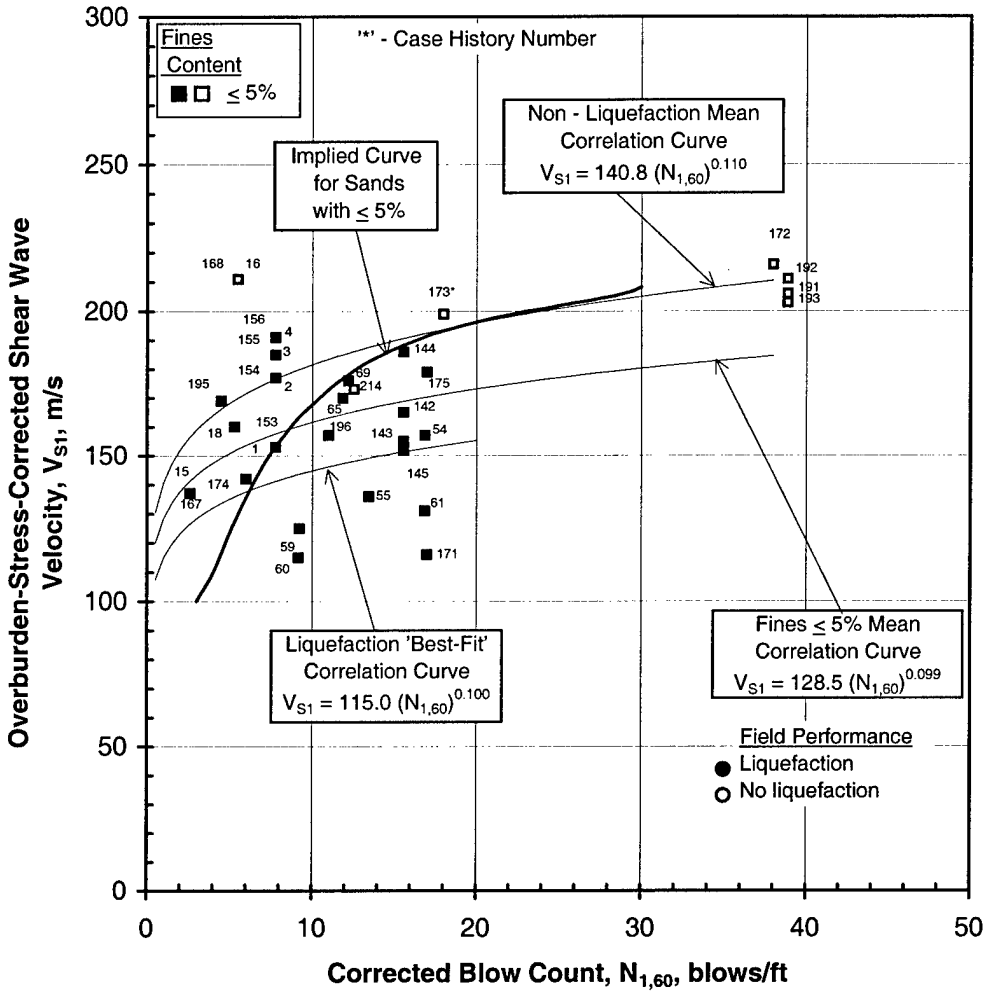

Fig 7.2 - Correlation Between V_{S1} and $N_{1,60}$ for Case Histories with Fines Content ≤ 5% Plotted with the Curve Implied by the Andrus et al. (1999) and Seed et al. (1985) Boundary Curves for Sands with ≤ 5% Fines and Various Correlation Curves for Case Histories with Fines ≤ 5%.

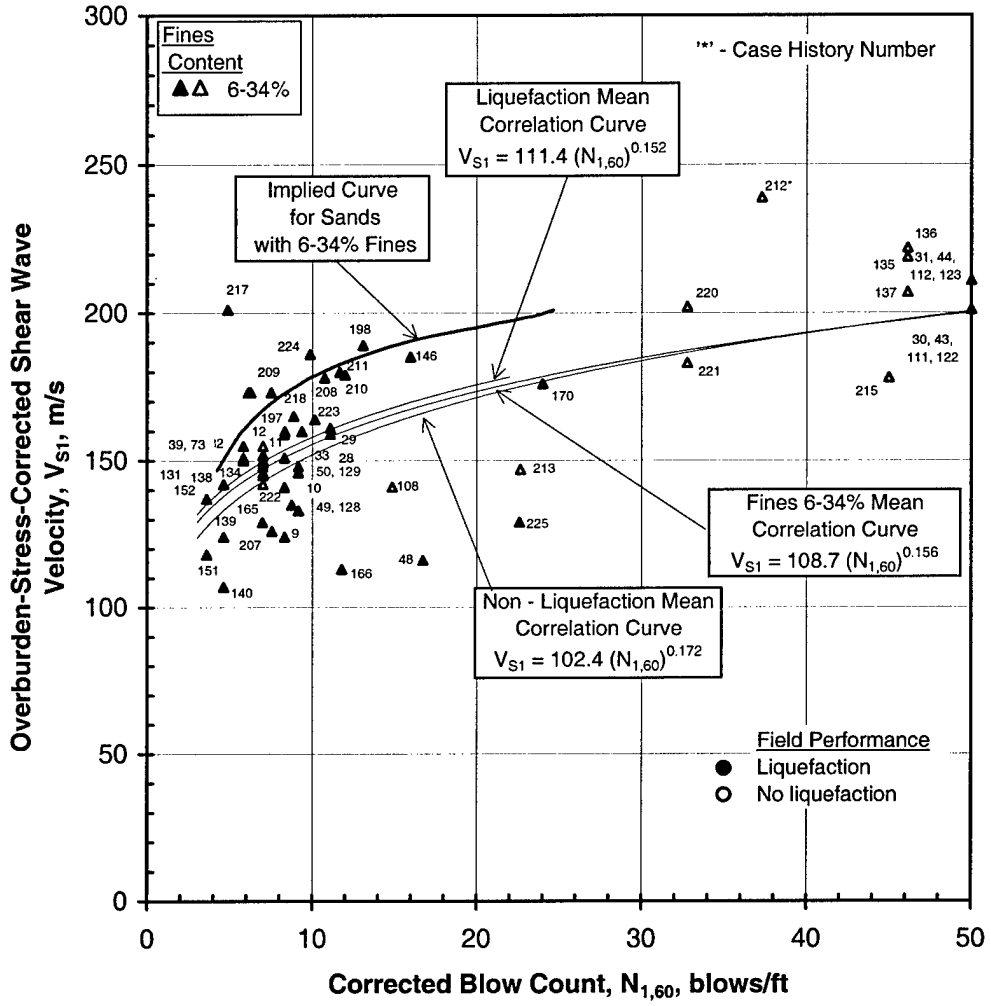

Fig 7.3 - Correlation Between V_{S1} and $N_{1,60}$ for Case Histories with Fines Content 6-34% Plotted with the Curve Implied by the Andrus et al. (1999) and Seed et al. (1985) Boundary Curves for Sands with 6-34% Fines and Various Mean Correlation Curves for Case Histories with Fines 6-34%.

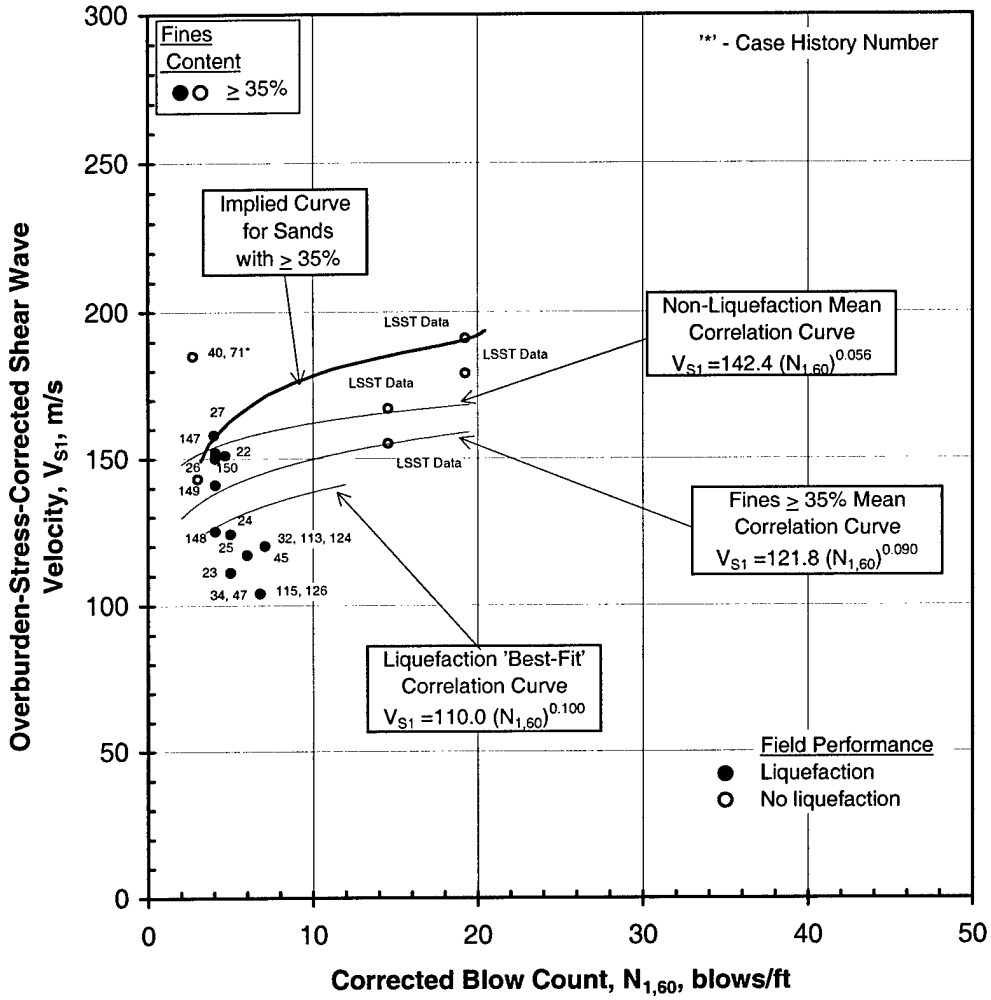

Fig 7.4 - Correlation Between V_{S1} and $N_{1,60}$ for Case Histories with Fines Content ≥ 35% Plotted with the Curve Implied by the Andrus et al. (1999) and Seed et al. (1985) Boundary Curves for Sands with ≥ 35% Fines and Various Mean Correlation Curves for Case Histories with Fines ≥ 35%.

7.2.2 V_S and CPT Correlation

A correlation between V_{S1} and $q_{c1,N}$ values can be made by plotting the paired values from the entire corrected database together. The 147 case histories from this database that had V_{S1} and $q_{c1,N}$ values are shown in Figure 7.5. The mean correlation curve presented by Andrus et al. (1999) and the mean correlation curve proposed in this report are also included in the figure. The mean correlation curve was created by plotting a 'best fit' line through the data set. The equation of the line is:

$$V_{S1} = 128.5\ (q_{c1,N})^{0.050} \qquad 7.2$$

The data, separated according to fines content, are presented in Figures 7.6, 7.7, and 7.8 for fines content $\leq 5\%$, 6 to 34%, and $\geq 35\%$, respectively. Mean correlation curves for all case histories and mean correlation curves for liquefaction and non-liquefaction case histories within the respective fines content ranges are also included in the figures.

In addition, Figures 7.6 - 7.8 display an implied curve derived from the V_S and CPT liquefaction boundary curves. These implied curves, which represent a correlation between V_{S1} and $q_{c1,N}$ based on independently developed liquefaction correlations, were derived by plotting V_{S1} and $q_{c1,N}$ values from the respective boundary curves with equal $CSR_{7.5}$ values. The implied curve for fines content $\leq 5\%$ is shown in Figure 7.6, the curve for fines content equal to 6 to 34% is shown in Figure 7.7, and the curve for fines content $\geq 35\%$ is shown in Figure 7.8. In an ideal case, the implied curve would plot directly on the overall mean correlation curve for a respective fines content sub-category ($\leq 5\%$, 6-34%, or $\geq 35\%$). This would indicate that both liquefaction boundaries (V_{S1} and $q_{c1,N}$) predict liquefaction with the same level of confidence. When the implied curve is above the mean correlation curve for the data, the V_S boundary is more conservative than the $q_{c1,N}$ boundary. Conversely, when the implied curve is below the mean correlation curve, the $q_{c1,N}$

boundary is more conservative than the V_{S1} boundary. This type of comparison is the same as described earlier in Section 7.2.1.

The plotted positions of individual case histories can also be used to evaluate which boundary curve is more conservative. Case histories that plot directly on the implied curve indicate that both liquefaction boundary curves predict liquefaction with the same level of confidence. Case histories that plot below the implied curve indicate, for the particular case history, that the V_{S1} liquefaction boundary curve is more conservative than the $q_{c1,N}$ liquefaction boundary curve. Conversely, case histories that plot above the implied curve indicate that the $q_{c1,N}$ boundary curves are more conservative than the V_{S1} liquefaction boundary curves. For example, liquefaction case history 60 plots below the implied boundary in Figure 7.6. Referring back to Figures 4.2 and 6.4, both the V_S and CPT boundaries correctly predicted this case history to liquefy. However, it is obvious for this case history, that there is a greater horizontal offset between the point representing case history 60 and the boundary curve in Figure 4.2 than in Figure 6.4. Therefore, for case history 60, the V_S boundary curve predicts liquefaction more conservatively than the CPT boundary curve. In general, the majority of the case histories plot below the implied curves indicating that the V_{S1} based liquefaction boundary curves are more conservative than the $q_{c1,N}$ based boundary curves.

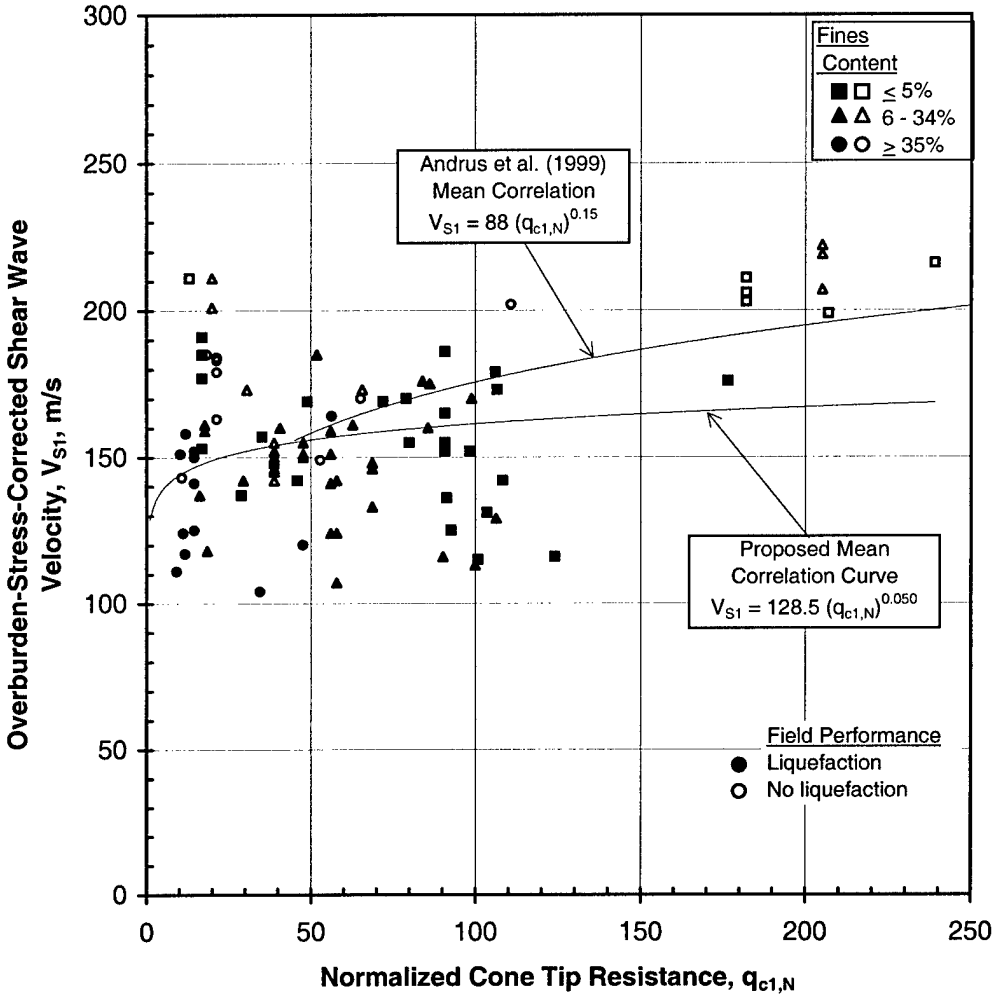

Fig 7.5 - Correlation Between V_{S1} and $q_{c1,N}$ for All Case Histories Plotted with the Mean Correlation Curve Recommended by Andrus et al.(1999) and the Mean Correlation Curve Proposed in this Report.

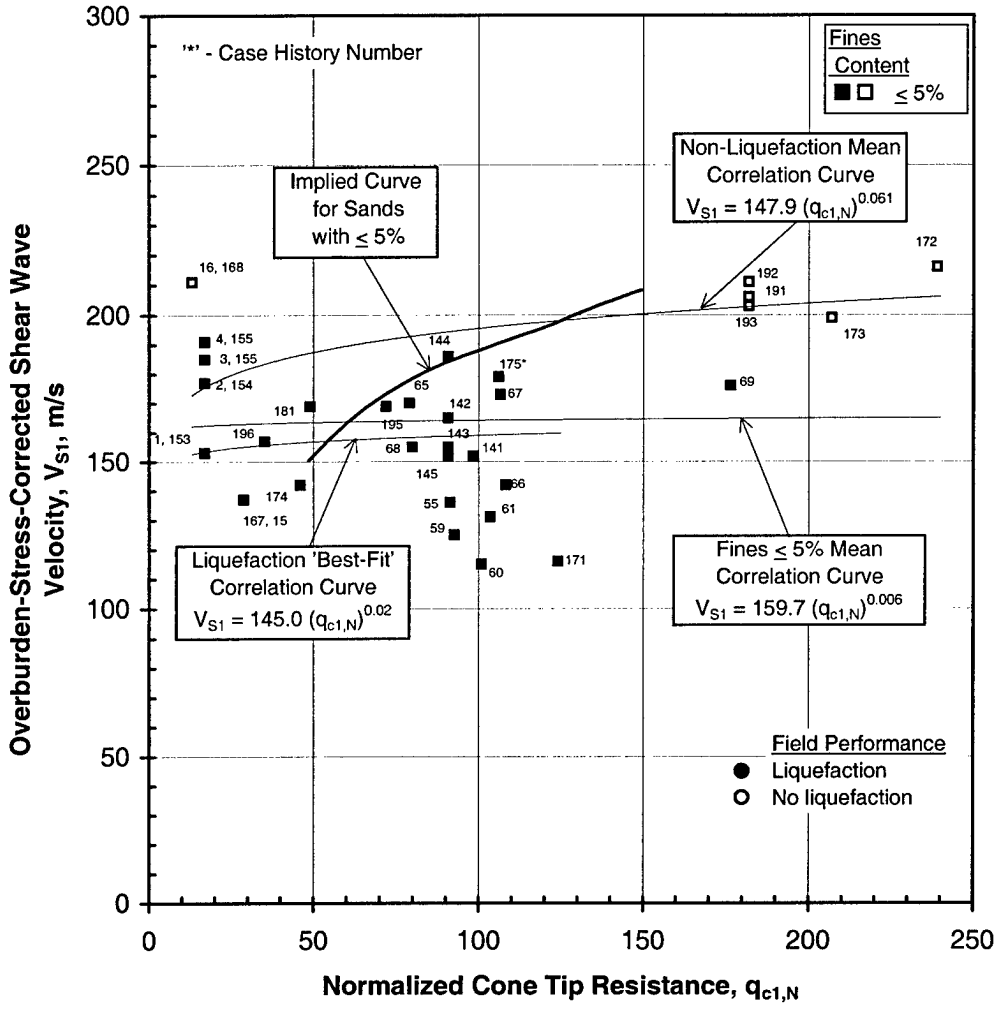

Fig 7.6 - Correlation Between V_{S1} and $q_{c1,N}$ for Case Histories with Fines Content ≤ 5% Plotted with the Curve Implied by the Andrus et al. (1999) and Stark and Olson (1995) Boundary Curves for Sands with ≤ 5% Fines, and Various Mean Correlation Curves for Case Histories with Fines ≤ 5%.

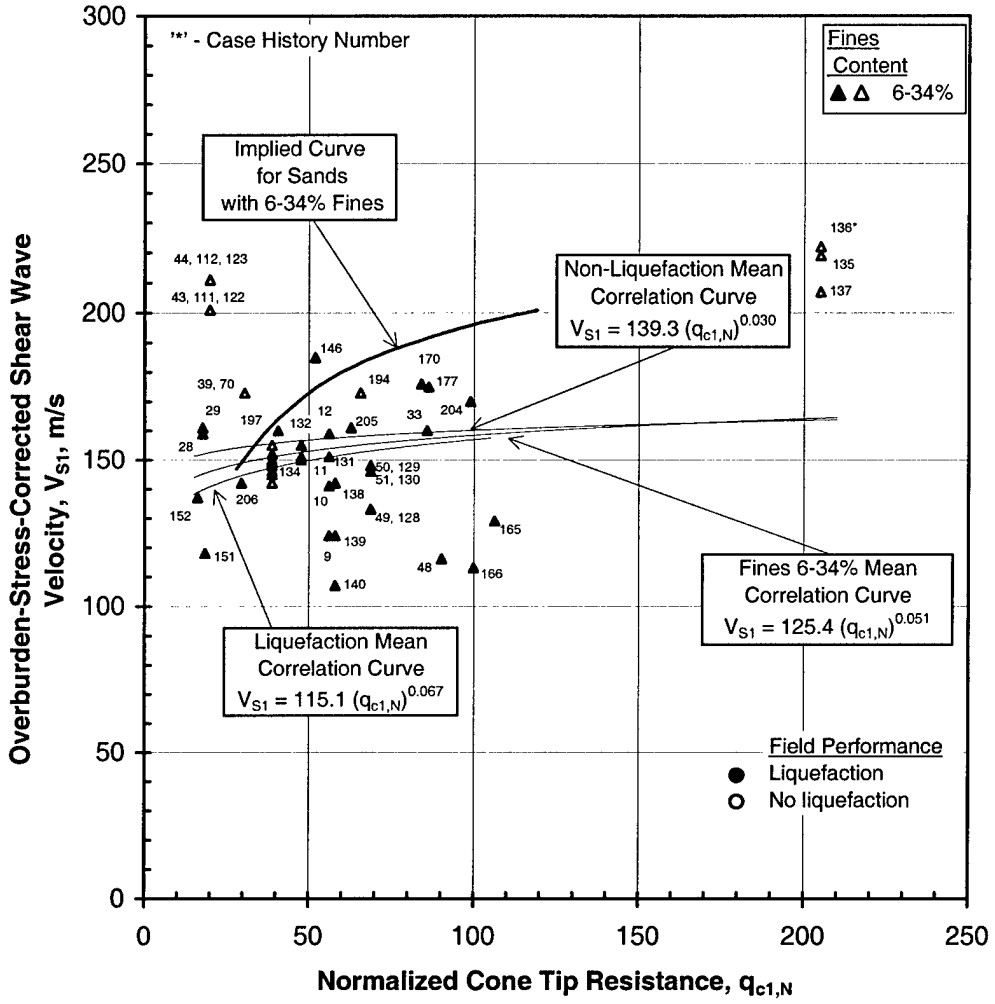

Fig 7.7 - Correlation Between V_{S1} and $q_{c1,N}$ for Case Histories with Fines Content 6-34% Plotted with the Curve Implied by the Andrus et al. (1999) and Stark and Olson (1995) Boundary Curves for Sands with 6-34% Fines and Various Mean Correlation Curves for Case Histories with Fines 6-34%.

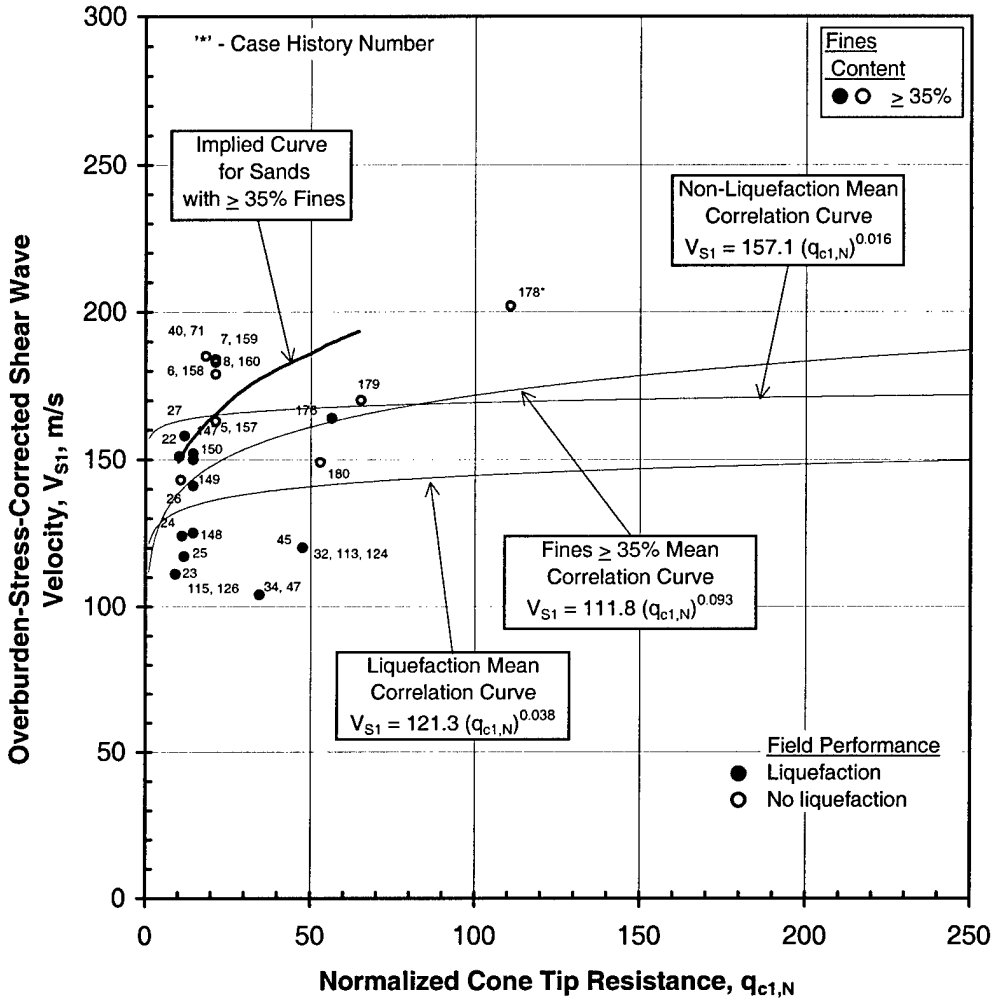

Fig 7.8 - Correlation Between V_{S1} and $q_{c1,N}$ for Case Histories with Fines Content ≥ 35% Plotted with the Curve Implied by the Andrus et al. (1999) and Stark and Olson (1995) Boundary Curves for Sands with ≥ 35% Fines and Various Mean Correlation Curves for Case Histories with Fines ≥ 35%.

7.2.3 CPT and SPT Correlation

A correlation between $q_{c1,N}$ and $N_{1,60}$ values can also be made by plotting the paired values from the entire corrected database together. The 126 case histories from the database that had $q_{c1,N}$ and $N_{1,60}$ values are shown in Figure 7.9. The mean correlation curve proposed in this report is also shown in the figure. The mean correlation curve was created by plotting a 'best fit' line through the data set. The equation of the line is:

$$q_{c1,N} = 5.0\ (N_{1,60})^{1.034} \qquad 7.3$$

The data, separated according to fines content, are presented in Figures 7.10, 7.11, and 7.12 for fines content $\leq$ 5%, 6 to 34%, and $\geq$ 35%, respectively. Mean correlation curves for all case histories and mean correlation curves for liquefaction and non-liquefaction case histories within the respective fines content ranges are also included in the figures.

In addition, Figures 7.10 – 7.12 display an implied curve derived from the CPT and SPT liquefaction boundary curves. These implied curves were derived by plotting $q_{c1,N}$ and $N_{1,60}$ values from the respective boundary curves with equal $CSR_{7.5}$ values. The implied curve for fines content $\leq$ 5% is shown in Figure 7.10, the curve for fines content equal to 6 to 34% is shown in Figure 7.11, and the curve for fines content $\geq$ 35% is shown in Figure 7.12. . In an ideal case, the implied curve would plot directly on the overall mean correlation curve for a respective fines content sub-category ($\leq$ 5%, 6-34%, or $\geq$ 35%). This would indicate that both liquefaction boundaries ($q_{c1,N}$ and $N_{1,60}$) predict liquefaction with the same level of confidence. When the implied curve is above the mean correlation curve for the data, the $q_{c1,N}$ boundary is more conservative than the $N_{1,60}$ boundary. Conversely, when the implied curve is below the mean correlation curve, the $N_{1,60}$ boundary is more conservative than the $q_{c1,N}$ boundary. This reasoning follows that described earlier in Section 7.2.1.

As in the other two correlations, V_S – SPT and V_S – CPT, the plotted positions of individual case histories can also be used to evaluate which boundary curve is more conservative. Case histories that plot directly on the implied curve indicate that both liquefaction boundary curves predict liquefaction with the same level of confidence. Case histories that plot below the implied curve indicate, for the particular case history, that the $q_{c1,N}$ liquefaction boundary curve is more conservative than the $N_{1,60}$ liquefaction boundary curve. Conversely, case histories that plot above the implied curve indicate that the $N_{1,60}$ boundary curves are more conservative than the $q_{c1,N}$ liquefaction boundary curves. For example, liquefaction case history 60 plots above the implied boundary in Figure 7.10. Referring back to Figures 5.4 and 6.4, both the SPT and CPT boundaries correctly predicted this case history to liquefy. However, it is obvious for this case history, that there is a greater horizontal offset between the point representing case history 60 and the boundary curve in Figure 5.4 than in Figure 6.4. Therefore, for case history 60, the SPT boundary curve predicts liquefaction more conservatively than the CPT boundary curve. Overall, the case histories plot equally on both sides of the implied curves indicating that the $q_{c1,N}$ based liquefaction boundary curves and the $N_{1,60}$ based boundary curves provide a similar level of confidence.

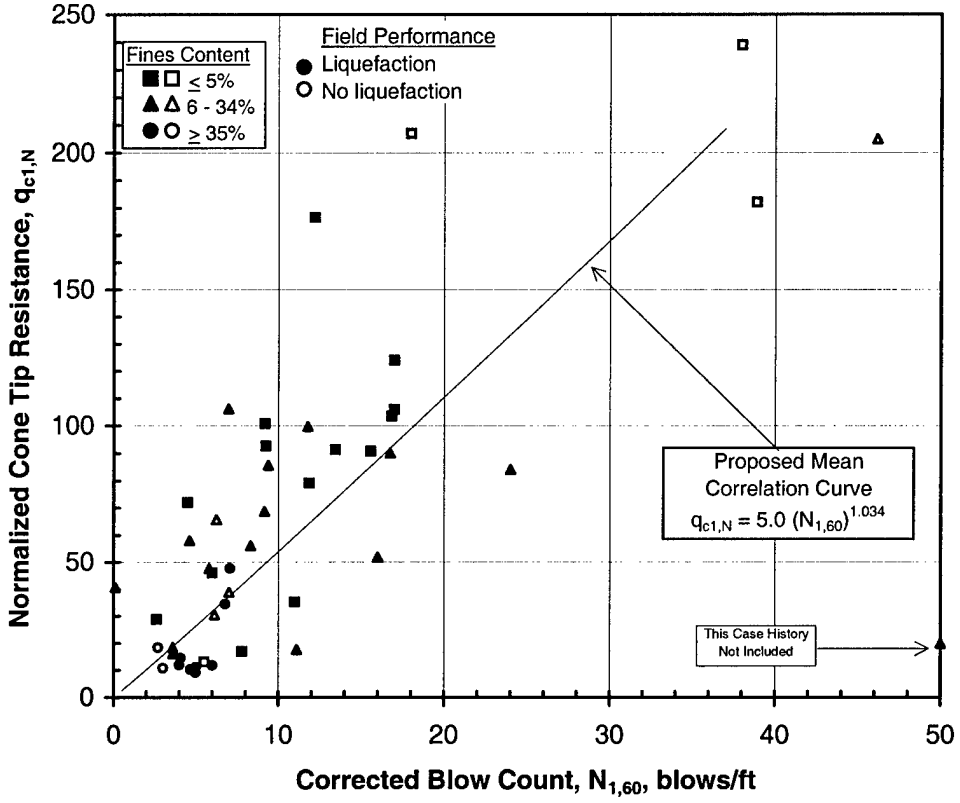

Fig 7.9 - Correlation Between $q_{c1,N}$ and $N_{1,60}$ for All Case Histories with the Mean Correlation Curve Proposed in this Report.

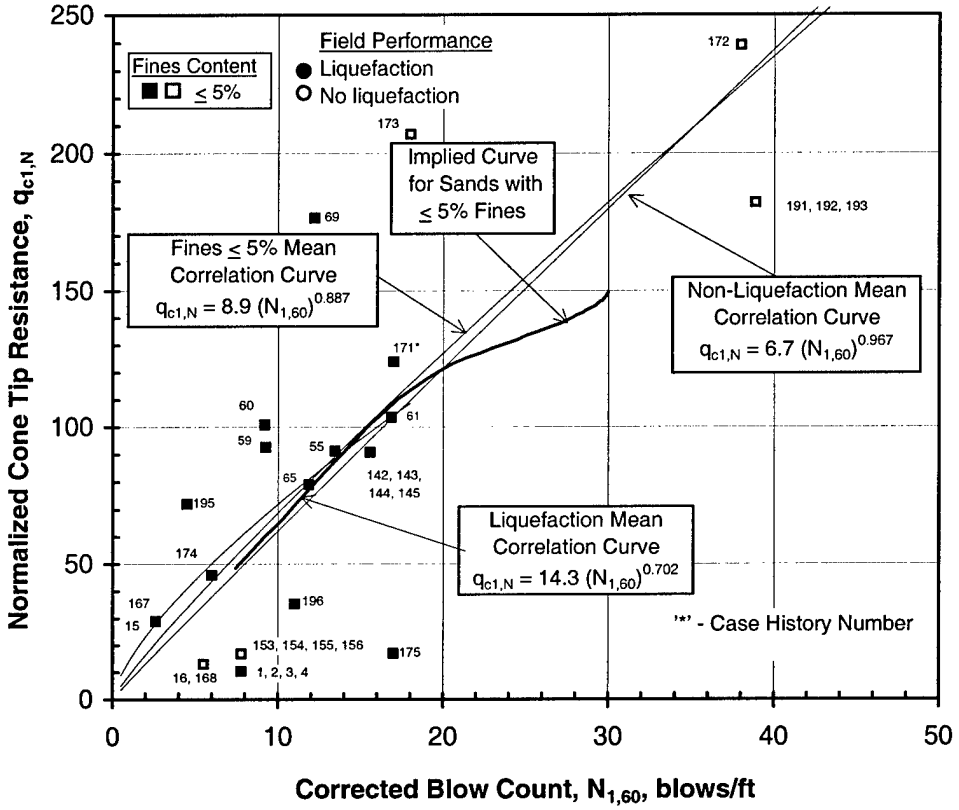

Fig 7.10 - Correlation Between $q_{c1,N}$ and $N_{1,60}$ for Case Histories with Fines Content ≤ 5% Plotted with the Curve Implied by the Seed et al. (1985) and Stark and Olson (1995) Boundary Curves for Sands with ≤ 5% Fines and Various Mean Correlation Curves for Case Histories with Fines < 5%.

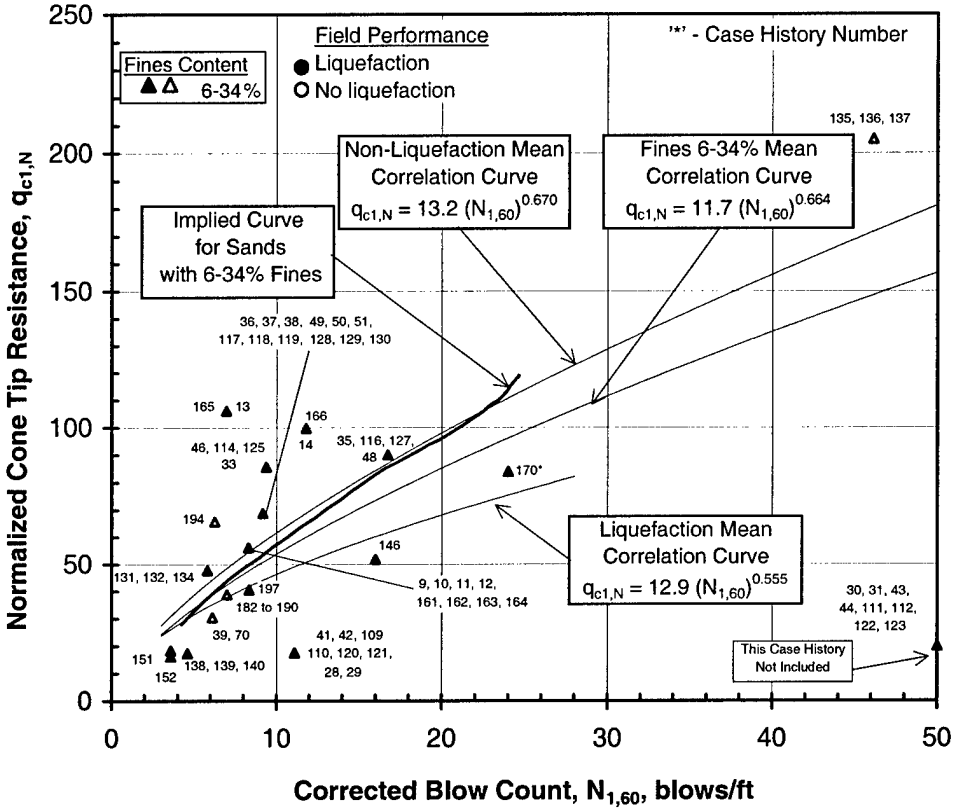

Fig 7.11 - Correlation Between $q_{c1,N}$ and $N_{1,60}$ for Case Histories with Fines Content 6-34% Plotted with the Curve Implied by the Seed et al. (1985) and Stark and Olson (1995) Boundary Curves for Sands with 6-34% Fines and Various Mean Correlation Curves for Case Histories with Fines 6-34%.

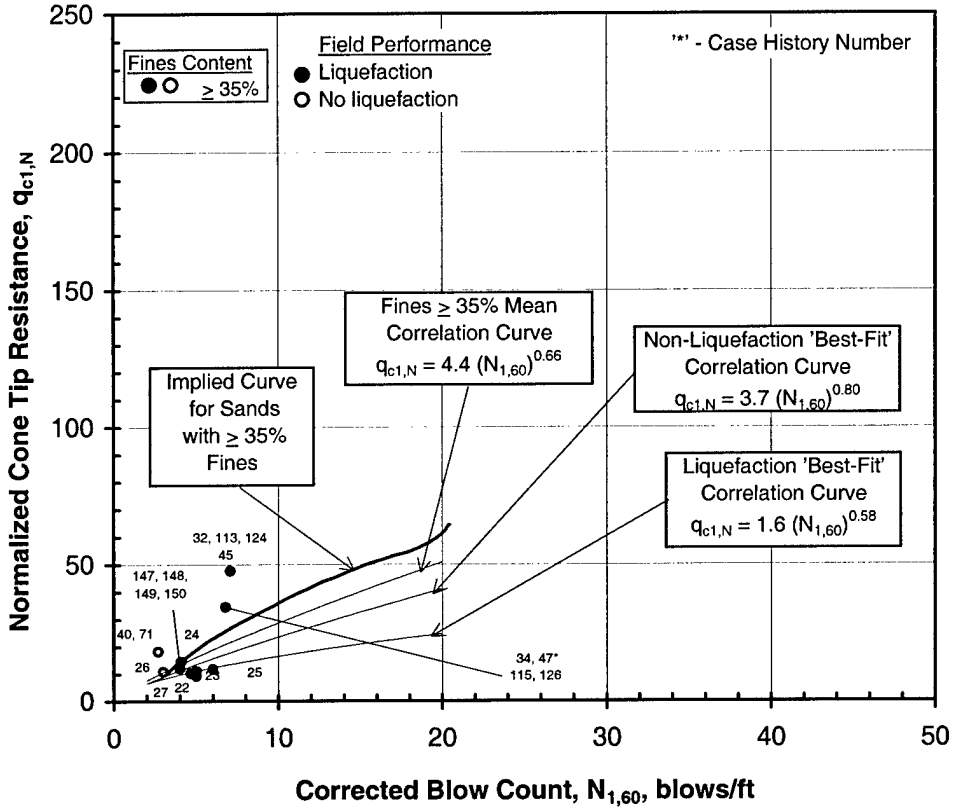

Fig 7.12 - Correlation Between $q_{c1,N}$ and $N_{1,60}$ for Case Histories with Fines Content ≥ 35% Plotted with the Curve Implied by the Seed et al. (1985) and Stark and Olson (1995) Boundary Curves for Sands with ≥ 35% Fines and Various Mean Correlation Curves for Case Histories with Fines > 35%.

7.2.4 Use of Minimum SPT and CPT Values

The V_S – SPT, V_S – CPT, and CPT – SPT case histories using the minimum $N_{1,60}$ and $q_{c1,N}$ values are shown in Figures 7.13, 7.14, and 7.15, respectively. In the figures, the minimum values for $N_{1,60}$ and $q_{c1,N}$ in the critical layer have simply been used in place of the average values. For the V_S – SPT and V_S – CPT correlation, the minimum values shifted all data points to the left, causing more of the case histories to plot above the implied boundary curves discussed earlier. This shifting indicates that the use of minimum $N_{1,60}$ and $q_{c1,N}$ values causes the $N_{1,60}$ and $q_{c1,N}$ liquefaction boundary curves to be more conservative than the V_{S1} liquefaction boundary curves. For the CPT – SPT correlation, the use of minimum values caused no noticeable change in the plotted positions of the case histories with respect to the implied boundary curves.

7.3 SUMMARY

An initial study of the consistency between predictions using the three liquefaction correlations (V_{S1}, $N_{1,60}$, and $q_{c1,N}$) was conducted. In this study, the prediction of no liquefaction when the site actually liquefied occurred three times for V_{S1} case histories, 19 times for $N_{1,60}$ case histories, and 19 times for $q_{c1,N}$ case histories. The V_{S1} correlations were correct the most often because the boundaries were established with this database. In fact, upon studying the other two correlations with $N_{1,60}$ and $q_{c1,N}$, the V_{S1} boundaries may be too conservative. Conversely, the V_{S1} boundaries may be correct and the $N_{1,60}$ and $q_{c1,N}$ may not be conservative enough. Nonetheless, the different correlations do not predict liquefaction potential with the same degree of confidence.

To be complete, a future study should be conducted that includes V_{S1} minimum values. The use of minimum $N_{1,60}$ and $q_{c1,N}$ values, in the respective correlations, indicated that the performance of the present liquefaction boundaries could be improved by simply replacing the average value with the minimum value.

Incorporating V_{S1} minimum values into the database may show all three methods exhibit more consistent results between the measurement types when the minimum values for all three methods are used.

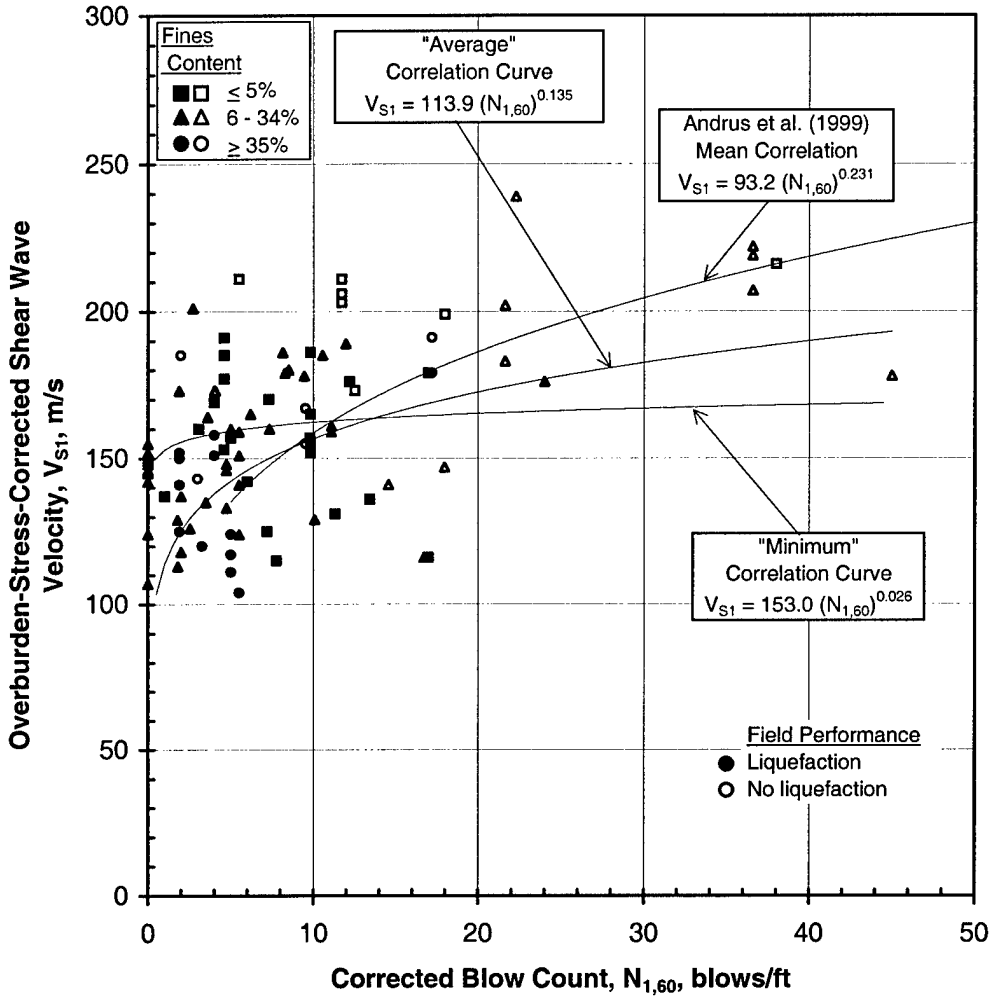

Fig 7.13 - Correlation Between Average V_{S1} and Minimum $N_{1,60}$ for All Case Histories Plotted with the Mean Correlation Curve Recommended by Andrus et al. (1999), the Mean Correlation Curve Based on Averages, and the Mean Correlation Curve Based on Minimums.

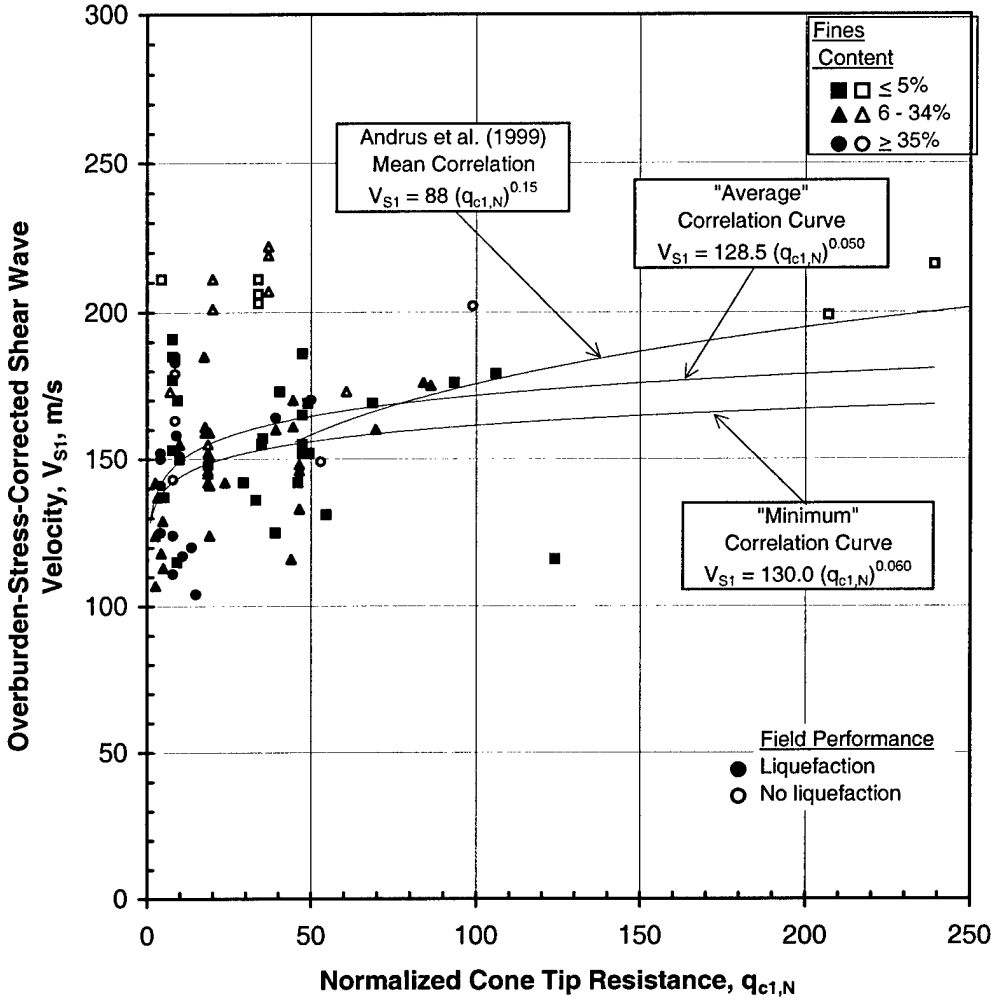

Fig 7.14 - Correlation Between Average V_{S1} and Minimum $q_{c1,N}$ for All Case Histories Plotted with the Mean Correlation Curve Recommended by Andrus et al. (1999), the Mean Correlation Curve Based on Averages, and the Mean Correlation Curve Based on Minimums.

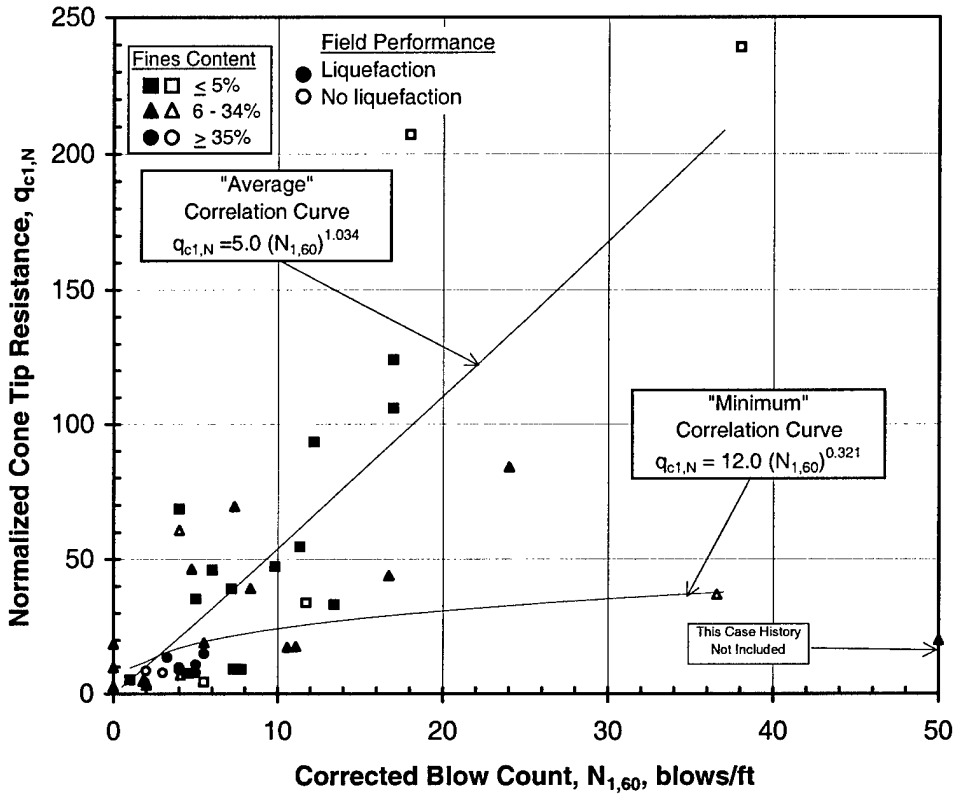

Fig 7.15 - Correlation Between Minimum $q_{c1,N}$ and Minimum $N_{1,60}$ for All Case Histories with the Mean Correlation Curve Based on Averages and the Mean Correlation Curve Based on Minimums.

CHAPTER 8

SUMMARY, CONCLUSIONS, AND RECOMMENDATIONS

8.1 SUMMARY

A study was undertaken to combine the V_S database compiled by Andrus et al. (1999) with all available SPT and CPT data from the same sites at which V_S measurements were made. The SPT and CPT data came from a wide range of sources, dating back to the early 1980s through the mid 1990s. For each V_S case history, the depth and thickness of the critical layer, the calculated equivalent $M_W = 7.5$ Cyclic Stress Ratio ($CSR_{7.5}$), and the determination of field liquefaction performance as reported by Andrus et al. (1999), were applied as to all corresponding SPT and CPT case histories. In all, the database is composed of 225 V_S case histories, 183 SPT case histories, and 147 CPT case histories.

Each case history with the corrected field values of V_{S1}, $N_{1,60}$, and/or $q_{c1,N}$ was plotted with the corresponding set of liquefaction boundary curves; that is, the V_{S1} for each case history was plotted versus the equivalent $CSR_{7.5}$ on one graph with the boundary between liquefaction and non-liquefaction case histories. Similar sets of $N_{1,60}$ and $q_{c1,N}$ data were plotted with the respective boundaries as well. With the data, each set of boundary curves was evaluated for accuracy. In addition, minimum and maximum values of $N_{1,60}$ and $q_{c1,N}$, for each SPT and CPT case history, were used in place of average values and plotted with the same set of boundary curves.

Finally, correlations were made between each of the three methods, V_S, SPT, and CPT, resulting in $V_{S1} - N_{1,60}$, $V_{S1} - q_{c1,N}$, and $q_{c1,N} - N_{1,60}$ correlation curves. These correlation curves were developed by plotting corresponding values from each case history and calculating the average mean correlation curve through the data points. Correlation curves were developed based on all case histories, case histories

with fines content $\leq$ 5%, case histories with fines content between 6 and 34%, and case histories with fines content $\geq$ 35%.

8.2 CONCLUSIONS

8.2.1 V_S Based Method

As stated earlier, all V_S case histories and the V_S boundary curves between liquefaction and non-liquefaction case histories were taken directly from Andrus et al. (1999). In summary, the V_S boundary curves, when applied to the V_S database, predicted liquefaction correctly for 93 out of the 96 liquefaction case histories, yielding an accuracy of about 97%. Obviously, the boundary curves were expected to perform well since the curves were established with this database. This report presented the case histories and boundary curves recommended by Andrus et al. (1999) for informational purposes and to display a comparison between the V_S based method and the SPT and CPT based methods. Therefore, no conclusions concerning the V_S boundary curves are made in this report. However, when the V_{S1} based method was compared with the corresponding $N_{1,60}$ and $q_{c1,N}$ based methods, the recommended boundaries from Andrus et al. (1999) appear to be too conservative. In other words, the V_S based method predicts liquefaction for a larger percentage of the sites that liquefied compared to the number of liquefaction sites that the SPT and CPT based methods predicted. The SPT and CPT based methods are discussed below.

8.2.2 SPT Based Method

The SPT boundary curves presented by Seed et al. (1985) were evaluated utilizing the SPT database. In summary, the SPT boundary curves predicted liquefaction correctly for 54 of the 73 liquefaction case histories in the SPT database, yielding an accuracy of about 74%. When the minimum $N_{1,60}$ value in the critical layer was used in place of the average $N_{1,60}$ value, the curves predicted 67 of the 73

SPT liquefaction case histories correctly, yielding an improved accuracy of about 92%. Based on the data in this report, it would appear that using the minimum $N_{1,60}$ value in the Seed et al. (1985) procedure will give a more reliable prediction of liquefaction. Four of the six incorrectly plotted case histories only had one reported value within the critical layer, so the minimum value was unknown and could not be evaluated. Even though the use of the minimum value improved the accuracy of the SPT boundary curves, two liquefaction case histories that did liquefy were still predicted to not liquefy.

8.2.3 CPT Based Method

The CPT boundary curves presented by Stark and Olson (1995) were evaluated utilizing the CPT database. In summary, the CPT boundary curves predicted liquefaction correctly for 50 of the 69 liquefaction case histories in the CPT database, when the average $q_{c1,N}$ in the critical layer was used yielding an accuracy of about 73%. When the minimum $q_{c1,N}$ value in the critical layer was used in place of the average $q_{c1,N}$ value, the curves plotted 59 of the 69 CPT liquefaction case histories correctly, yielding an improved accuracy of about 86%. As with the SPT criteria, the data in this report suggests that more reliable predictions are obtained if the minimum $q_{c1,N}$ value is used. Two of the ten incorrectly plotted case histories only had one reported value within the critical layer, so the minimum value was unknown and could not be evaluated. Even though the use of the minimum value improved the accuracy of the CPT boundary curves, eight liquefaction case histories that did liquefy were still predicted to not liquefy.

8.2.4 $V_{S1} - N_{1,60}$, $V_{S1} - q_{c1,N}$, and $q_{c1,N} - N_{1,60}$ Correlations

Mean correlation curves between $V_{S1} - N_{1,60}$, $V_{S1} - q_{c1,N}$, and $q_{c1,N} - N_{1,60}$ were developed and presented in Chapter 7. In addition, mean correlation curves for case histories with fines content $\leq$ 5%, between 6 and 34%, and $\geq$ 35% were also

Table 8.1 – Mean Correlation Curves for $V_{S1} - N_{1,60}$ Case Histories.

No.	Correlation	Equation	R^2 Value
1	**Entire Database**	$V_{S1} = 113.9\ (N_{1,60})^{0.139}$	0.30
	Fines Content ≤ 5%		
2	All Case Histories	$V_{S1} = 128.5\ (N_{1,60})^{0.099}$	0.14
3	Liquefaction Case Histories*	$V_{S1} = 115.0\ (N_{1,60})^{0.100}$	n/a
4	Non-Liquefaction Case Histories	$V_{S1} = 140.8\ (N_{1,60})^{0.110}$	0.56
	Fines Content 6 –34%		
5	All Case Histories	$V_{S1} = 108.7\ (N_{1,60})^{0.156}$	0.39
6	Liquefaction Case Histories	$V_{S1} = 111.4\ (N_{1,60})^{0.152}$	0.21
7	Non-Liquefaction Case Histories	$V_{S1} = 102.4\ (N_{1,60})^{0.172}$	0.51
	Fines Content ≥ 35%		
8	All Case Histories	$V_{S1} = 121.8\ (N_{1,60})^{0.090}$	0.10
9	Liquefaction Case Histories*	$V_{S1} = 110.0\ (N_{1,60})^{0.100}$	n/a
10	Non-Liquefaction Case Histories	$V_{S1} = 142.4\ (N_{1,60})^{0.056}$	0.08

'*' Correlation curves 'forced' to have the proper alignment.

Table 8.2 – Mean Correlation Curves for V_{S1} – $q_{c1,N}$ Case Histories.

No.	Correlation	Equation	R^2 Value
1	**Entire Database**	$V_{S1} = 128.5\ (q_{c1,N})^{0.050}$	0.05
	Fines Content ≤ 5%		
2	All Case Histories	$V_{S1} = 159.7\ (q_{c1,N})^{0.006}$	0.00
3	Liquefaction Case Histories*	$V_{S1} = 145.0\ (q_{c1,N})^{0.020}$	n/a
4	Non-Liquefaction Case Histories	$V_{S1} = 147.9\ (q_{c1,N})^{0.061}$	0.19
	Fines Content 6 –34%		
5	All Case Histories	$V_{S1} = 125.4\ (q_{c1,N})^{0.051}$	0.03
6	Liquefaction Case Histories	$V_{S1} = 115.1\ (q_{c1,N})^{0.067}$	0.07
7	Non-Liquefaction Case Histories	$V_{S1} = 139.3\ (q_{c1,N})^{0.030}$	0.01
	Fines Content ≥ 35%		
8	All Case Histories	$V_{S1} = 111.8\ (q_{c1,N})^{0.093}$	0.13
9	Liquefaction Case Histories	$V_{S1} = 121.3\ (q_{c1,N})^{0.038}$	0.02
10	Non-Liquefaction Case Histories	$V_{S1} = 157.1\ (q_{c1,N})^{0.016}$	0.01

'*' Correlation curves forced to have the proper alignment.

Table 8.3 – Mean Correlation Curves for $q_{c1,N} - N_{1,60}$ Case Histories.

No.	Correlation	Equation	R^2 Value
1	**Entire Database**	$q_{c1,N} = 5.0\ (N_{1,60})^{1.034}$	0.57
	Fines Content ≤ 5%		
2	All Case Histories	$q_{c1,N} = 8.9\ (N_{1,60})^{0.887}$	0.54
3	Liquefaction Case Histories	$q_{c1,N} = 14.3\ (N_{1,60})^{0.702}$	0.23
4	Non-Liquefaction Case Histories	$q_{c1,N} = 6.7\ (N_{1,60})^{0.967}$	0.76
	Fines Content 6 –34%		
5	All Case Histories	$q_{c1,N} = 11.7\ (N_{1,60})^{0.664}$	0.36
6	Liquefaction Case Histories	$q_{c1,N} = 12.9\ (N_{1,60})^{0.555}$	0.30
7	Non-Liquefaction Case Histories	$q_{c1,N} = 13.2\ (N_{1,60})^{0.670}$	0.34
	Fines Content ≥ 35%		
8	All Case Histories	$q_{c1,N} = 4.4\ (N_{1,60})^{0.660}$	0.22
9	Liquefaction Case Histories*	$q_{c1,N} = 1.6\ (N_{1,60})^{0.580}$	n/a
10	Non-Liquefaction Case Histories*	$q_{c1,N} = 3.7\ (N_{1,60})^{0.800}$	n/a

'*' Correlation curves forced to have the proper alignment.

developed. Equations for the mean correlation curves for $V_{S1} - N_{1,60}$, $V_{S1} - q_{c1,N}$, and $q_{c1,N} - N_{1,60}$ are presented in Tables 8.1, 8.2, and 8.3, respectively. The coefficient of determination, R^2, for each correlation is also shown in the tables.

8.2.4.1 Correlation Performance

In terms of overall correlation, the overall $q_{c1,N} - N_{1,60}$ correlation curve exhibited the highest R^2 value, 0.57, and the overall $V_{S1} - q_{c1,N}$ correlation curve exhibited the lowest value, 0.05. The sub-category correlation with the highest R^2 value was the $q_{c1,N} - N_{1,60}$ correlation curve for non-liquefaction case histories with fines content $\leq 5\%$ which had an R^2 value equal to 0.76. In a perfect correlation, the R^2 value would equal one. Obviously, obtaining a value of one between any of the three field measurements was not possible. Variations in measurement techniques and soil conditions would prevent this from ever happening for these cases. However, an R^2 greater than 0.6 indicates a 'strong' correlation (Devore, 1995) and the overall $q_{c1,N} - N_{1,60}$ correlation was almost in this range. Likewise, an R^2 less than 0.25 indicates a very 'weak' correlation (Devore, 1995) and the overall $V_{S1} - q_{c1,N}$ correlation was well within this range. In general, the correlation between $q_{c1,N} - N_{1,60}$ values was 'strong' and the correlation between $V_{S1} - q_{c1,N}$ values was very 'weak.' The correlation between $V_{S1} - N_{1,60}$ values was 'strong' for some sub-categories and 'weak' for others.

An interesting trend seen in the majority of correlations except one is that the liquefaction correlation curve plots 'beneath' the non-liquefaction curve. This evidence indicates that the liquefiable and non-liquefiable soils are inherently different. If liquefiable and non-liquefiable soils were the same, the two curves would line-up almost perfectly. The $V_{S1} - N_{1,60}$ correlation curves for fines content between 6 and 34%, the only instance where the liquefaction curve plotted 'above' the non-liquefaction curve, the two curves were almost identical (see Figure 7.3).

The overall trend indicates that liquefiable soils correlate between the three different field measurements differently than non-liquefiable soils.

8.2.4.2 Forced Correlations

The curves for liquefaction case histories with fines content $\leq 5\%$ and liquefaction case histories with fines content $\geq 35\%$ within the $V_{S1} - N_{1,60}$ correlation and the curve for liquefaction case histories with fines content $\leq 5\%$ within the $V_{S1} - q_{c1,N}$ correlation showed an inverse correlation. In other words, the slope of the mean correlation curve was negative. Obviously, this is impossible and in reality it is not the proper correlation curve. In these cases, the curve was 'forced' to have the proper alignment (positive slope). The reason for the negative slope was that there was not enough data in the particular sub-category to properly constrain the fit of the correlation curve.

The curves for liquefaction and non-liquefaction case histories with fines content $\geq 35\%$ within the $q_{c1,N} - N_{1,60}$ correlation also showed improper alignment. However, in these two cases, the slope of the line was positive but was nearly vertical. Once again, this does not make any sense and these two curves were also 'forced' to have the proper alignment. The reason for the improper alignment is also due to the lack of data.

8.3 RECOMMENDATIONS

To fully examine the case histories contained in the database, more V_S information is required. Without the minimum V_S values a true comparison between the three methods could not be made. When SPT and CPT minimum values were used, the performance of the current boundary curves was improved. The first recommendation is to expand the V_S database and correlate all three methods with minimum values.

The case histories in this database were evaluated based on the information concerning the critical layer reported by Andrus et al. (1999). The critical layer determination was based solely on the shear wave velocity profile relative to the calculated CSR. In general, V_S based soil profiles can miss thin layers of liquefiable material surrounded by stiffer non-liquefiable layers. On the other hand, the CPT test provides a more continuous soil profile and can detect the thin layers that V_S and SPT tests may not detect. If the CPT profile was used as the basis for the determining the critical layer, the results of this investigation may have been improved. A future study should be undertaken that bases the critical layer determination on the CPT profile.

The final recommendation is to incorporate laboratory studies of soil samples into the database. It is possible to measure V_S and q_c in the laboratory and CSR values can be estimated for laboratory conditions. This can be accomplished the easiest with a mini – CPT that has a cross-sectional tip area smaller than the standard 10 cm^2 tip. It would be interesting to see how laboratory measured values correlate with the field values presented in this report. Ideally, if the correlation was successful, laboratory studies could be used to augment the limited field case history database and develop improved field liquefaction criteria. However, as mentioned in Chapter 1, the key to any method is that the method be simple, inexpensive and most importantly, accurate.

BIBLIOGRAPHY

Abdel-Haq, A., and Hryciw, R. D. (1998). "Ground Settlement in Simi Valley Following the Northridge Earthquake," *Journal of Geotechnical and Geoenviornmental Engineering*, ASCE, Vol. 124, No. 1, pp. 80-89.

Andrus, R. D. (1994). "In Situ Characterization of Gravelly Soils That Liquefied in the 1983 Borah Peak Earthquake," *Ph. D. Dissertation*, The University of Texas at Austin, 533 p.

Andrus, R.D., and Stokoe, K. H., II (1997). "Liquefaction Resistance Based on Shear Wave Velocity," *NCEER Workshop on Evaluation of Liquefaction Resistance of Soils*, Technical Report NCEER-97-0022, T. L. Youd and I. M. Idriss, Eds., held 4-5 January 1996, Salt Lake City, UT, National Center for Earthquake Engineering Research, Buffalo, NY, pp. 89-128.

Andrus, R.D., Stokoe, K. H., II, Bay, J. A., and Chung, R. M. (1998a). "Delineation of Densified Sand at treasure Island by SASW Testing," *Geotechnical Site Characterization,* P. K. Robertson and P. W. Mayne, Eds., A. A. Balkema, Rotterdam, Netherlands, pp. 459-464.

Andrus, R. D., Stokoe, K. H., II, Chung, R. M., and Bay, J. A. (1998b). "Liquefaction Evaluation of Densified Sand at Approach to Pier 1 on Treasure Island, California, Using SASW Method," *NISTIR 6230*, National Institute of Standards and Technology, Gaithersburg, MD, 75 p.

Andrus, R. D., Stokoe, K. H., II, and Chung, R. M. (1999). "Draft Guidelines for Evaluating Liquefaction Resistance Using Shear Wave Velocity Measurements and Simplified Procedures," *NISTIR 6277*, National Institute of Standards and Technology, Gaithersburg, MD, 121 p.

Andrus, R. D., Stokoe, K. H., II, Bay, J. A., and Youd, T. L. (1992). "In Situ V_S of Gravelly Soils Which Liquefied," *Proceedings, Tenth World Conference on Earthquake Engineering*, held 19-24 July 1992, Madrid, Spain, A. A. Balkema, Rotterdam, Netherlands, pp. 1447-1452.

Andrus, R. D., and Youd, T. L. (1987). "Subsurface Investigation of a Liquefaction-Induced Lateral Spread, Thousand Springs Valley, Idaho," *Geotechnical Laboratory Miscellaneous Paper GL-97-8*, U.S. Army Engineer Waterways Experiment Station, Vicksburg, MS, 131 p.

Arulanandan, K., Yogachandran, C., Meegoda, N. J., Ying, L., and Zhaauji, S. (1986). "Comparison of the SPT, CPT, SV, and Electrical Methods of Evaluating Earthquake Induced Liquefaction Susceptibility in Ying Kou City During the Haicheng Earthquake," *Use of In Situ Tests in Geotechnical Engineering*, Geotechnical Special Publication No. 6, S. P. Clemence, Ed., ASCE, pp. 389-415.

Barrow, B. L. (1983). "Field Investigation of Liquefaction Sites in Northern California," *Geotechnical Engineering Thesis GT83-1*, The University of Texas at Austin, 213 p.

Bennett, M. J., Youd, T. L., Harp, E. L., and Wieczorek, G. F. (1981). "Subsurface Investigation of Liquefaction, Imperial Valley Earthquake, California, October 15, 1979," *Open-File Report 81-502*, U.S. Geological Survey, Menlo Park, CA, 83 p.

Bennett, M. J., McLaughlin, P. V., Sarmiento, J. S., and Youd, T. L. (1984). "Geotechnical Investigation of Liquefaction Sites, Imperial Valley, California," *Open-File Report 84-252*, U.S. Geological Survey, Menlo Park, CA.

Bennett, M. J., and Tinsley, J. C. (1995). "Geotechnical Data from Surface and Subsurface Samples Outside of and within Liquefaction-Related Ground Failure Caused by the October 17, 1989, Loma Prieta Earthquake, Santa Cruz and Monterey Counties, California," *Open-File Report 95-663*, U.S. Geological Survey, Menlo Park, CA.

Bierschwale, J. G., and Stokoe, K. H., II (1984). "Analytical Evaluation of Liquefaction Potential of Sands Subjected to the 1981 Westmorland Earthquake," *Geotechnical Engineering Report GR-84-15*, The University of Texas at Austin, 231 p.

Boulanger, R. W., Idriss, I. M., and Mejia, L. H. (1995). "Investigation and Evaluation of Liquefaction Related Ground Displacements at Moss Landing During the 1989 Loma Prieta Earthquake," *Report No. UCD/CGM-95/02*, University of California at Davis.

Boulanger, R. W., Mejia, L. H., Idriss, I. M. (1997). "Liquefaction at Moss Landing During Loma Prieta Earthquake," *Journal of Geotechnical and Geoenviornmental Engineering*, ASCE, Vol. 123, No. 5, pp. 453-467.

de Alba, P., Benoit, J., Pass, D. G., Carter, J. J., Youd, T. L., and Shakal, A. F. (1994). "Deep Instrumentation Array at the Treasure Island Naval Station," *The Loma Prieta, California, Earthquake of October 17, 1989—Strong Ground Motion*,

U.S. Geological Survey Professional Paper 1551-A, R. D. Borcherdt, Ed., U.S. Gov. Printing Office, Washington D.C., pp. A155-A168.
Devore, J. L. (1995). *Probability and Statistics for Engineering and the Sciences*, Fourth Edition, Duxbury Press, New York, NY.

Dobry, R., Baziar, M. H., O'Rourke, T. D., Roth, B. L., and Youd, T. L. (1992). "Liquefaction and Ground Failure in the Imperial Valley, Southern California During the 1979, 1981, and 1987 Earthquakes," *Case Studies of Liquefaction and Lifeline Performance During Past Earthquakes*, Technical Report NCEER-92-0002, T. O'Rourke and M. Hamada, Eds., National Center for Earthquake Engineering Research, Buffalo, NY, Vol. 2.

EPRI (1992). *Lotung Large-Scale Seismic Test Strong Motion Records*, EPRI NP-7496L, Electric Power Research Institute, Palo Alto, CA, Vols. 1-7.

Fuhriman, M. D. (1993). "Crosshole Seismic Tests at Two Northern California Sites Affected by the 1989 Loma Prieta Earthquake," *M.S. Thesis*, The University of Texas at Austin, 516 p.

Geomatrix Consultants (1990). "Results of Field Exploration and Laboratory Testing Program for Perimeter Dike Stability Evaluation Naval Station Treasure Island San Francisco, California," Project No. 1539.05, report prepared for U. S. Navy, Naval Facilities Engineering Command, Western Division, San Bruno, CA, Vol. 2.

Gibbs, J. F., Fumal, T. E., Boore, D. M., and Joyner, W. B. (1992). "Seismic Velocities and Geologic Logs from Borehole Measurements at Seven Strong-Motion Stations that Recorded the Loma Prieta Earthquake," *Open-File Report 92-287*, U.S. Geological Survey, Menlo Park, CA, 139 p.

Hanshin Expressway Public Corporation (1998). "The Hanshin Expressway Geological Database, Volume for Seismic Damage Reconstruction of Route No. 3, the Kobe Line, and Route No. 5, the Harbor Line," 224 p. (in Japanese).

Hamada, M., Isoyama, R., and Wakamatsu, K. (1995). *The 1995 Hyogoken-Nanbu (Kobe) Earthquake: Liquefaction, Ground Displacements and Soil Condition in Hanshin Area*, Waseda University, Tokyo, Japan, 194 p.

Hryciw, R. D. (1991). "Post Loma Prieta Earthquake CPT, DMT and Shear Wave Velocity Investigations of Liquefaction Sites in Santa Cruz and on Treasure Island," Final Report to the U.S. Geological Survey, Award No. 14-08-0001-G1865, University of Michigan at Ann Arbor, 68 p.

Hryciw, R. D., Rollins, K. M., Homolka, M., Shewbridge, S. E., and McHood, M. (1991). "Soil Amplification at Treasure Island During the Loma Prieta Earthquake," *Proceedings, Second International Conference on Recent Advances in Geotechnical Earthquake Engineering and Soil Dynamics*, S. Prakash, Ed., held 11-15 March 1991, St. Louis, MO, University of Missouri at Rolla, Vol. II, pp. 1679-1685.

Hryciw, R. D., Shewbridge, S. E., Kropp, A., and Homolka, M. (1998). "Postearthquake Investigation at Liquefaction Sites in Santa Cruz and on Treasure Island," *The Loma Prieta, California Earthquake of October 17, 1989—Liquefaction*, U.S. Geological Survey Professional Paper 1551-B, T. L. Holzer, Ed., U.S. Gov. Printing Office, Washington D.C., pp. B165-B180.

Iai, S., Morita, T., Kameoka, T., Matsunaga, Y., and Abiko, K. (1995). "Response of a Dense Sand Deposit During 1993 Kushiro-Oki Earthquake," *Soils and Foundations*, Japanese Society of Soil Mechanics and Foundation Engineering, Vol. 35, No. 1, pp. 115-131.

Idriss, I. M. (1998). "Evaluation of Liquefaction Potential, Consequences and Mitigation—An Update," Presentation notes for Geotechnical Society Meeting, held 17 February 1998, Vancouver, Canada.

Idriss, I. M. (1999). "An Update of the Seed-Idriss Simplified Procedure for Evaluating Liquefaction Potential," Presentation notes for Transportation Research Board Workshop on New Approaches to Liquefaction Analysis, held 10 January 1999, Washington D.C.

Inatomi, T., Zen, K., Toyama, S., Uwabe, T., Iai, S., Sugano, T., Terauchi, K., Yokota, H., Fujimoto, K., Tanaka, S., Yamazaki, H., Koizumi, T., Nagao, T., Nozu, A., Miyata, M., Ichii, K., Morita, T., Minami, K., Oikawa, K., Matsunaga, Y., Ishii, M., Sugiyana, M., Takasaki, N., Kobayashi, N., and Okashita, K. (1997). "Damage to Port and Port-related facilities by the 1995 Hyogoken-Nanbu Earthquake," *Technical Note No. 857*, Port and Harbour Research Institute, Yokosuka, Japan, 1762 p.

Ishihara, K., Shimizu, K., and Yamada, Y. (1981). "Pore Water Pressures Measured in Sand Deposits During an Earthquake," *Soils and Foundations*, Japanese Society of Soil Mechanics and Foundation Engineering, Vol. 21, No. 4, pp. 85-100.

Ishihara, K., Anazawa, Y., and Kuwano, J. (1987). "Pore Water Pressures and Ground Motions Monitored During the 1985 Chiba Ibaragi Earthquake," *Soils and Foundations*, Japanese Society of Soil Mechanics and Foundation Engineering, Vol. 27, No. 3, pp. 13-30.

Ishihara, K., Muroi, T., and Towhata, I. (1989). "In-situ Pore Water Pressures and Ground Motions During the 1987 Chiba-Toho-Oki Earthquake," *Soils and Foundations*, Japanese Society of Soil Mechanics and Foundation Engineering, Vol. 29, No. 4, pp. 75-90.

Ishihara, K., Karube, T. And Goto, Y. (1997). "Summary of the Degree of Movement of Improved Masado Reclaimed Land," *Proceedings, 24th JSCE Earthquake Engineering Symposium*, Japan Society of Civil Engineering, held 24-26 July1997, Kobe, Japan, Vol. 1, pp. 461-464 (in Japanese).

Ishihara, K. (1996). *Soil Behaviour in Earthquake Geotechnics*, Oxford University Press Inc., New York, NY.

Ishihara, K., Kokusho, T., Yasuda, S., Goto, Y., Yoshida, N., Hatanaka, M., and Ito, K. (1998). "Dynamic Properties of Masado Fill in Kobe Port Island Improved through Soil Compaction Method," Summary of Final Report by Geotechnical Research Collaboration Committee on the Hanshin-Awaji Earthquake, Obayashi Corporation, Tokyo, Japan.

Kayen, R. E., Liu, H. –P., Fumal, T. E., Westerland, R. E., Warrick, R. E., Gibbs, J. F., and Lee, H. J. (1990). "Engineering and Seismic Properties of the Soil Column at Winfield Scott School, San Francisco," *Effects of the Loma Prieta Earthquake on the Marina District San Francisco, California*, Open-file Report 90-253, U. S. Geological Survey, Menlo Park, CA, pp. 112-129.

Kayen, R.E., Mitchell, J. k., Seed, R. B., Lodge, A., Nishio, S., and Coutinbo, R. (1992). "Evaluation of SPT-, CPT-, and Shear Wave-Based Methods for Liquefaction Potential Assessment Using Loma Prieta Data," *Proceedings, Fourth Japan-U.S. Workshop on Earthquake Resistant Design of Lifeline Facilities and Countermeasures for Soil Liquefaction*, Technical Report NCEER-92-0019, M. Hamada and T. D. O'Rourke, Eds., held 27-29 May 1992, Honolulu, Hawaii, National Center for Earthquake Engineering Research, Buffalo, NY, Vol. 1, pp. 177-204.

Kokusho, T., Yoshida, Y., Nishi, K., and Esashi, Y. (1983a). *Evaluation of Seismic Stability of Dense Sand Layer (Part 1) – Dynamic Strength Charateristics of Dense Sand*, Report 383025, Electric Power Central Research Institute, Japan (in Japanese).

Kokusho, T., Yoshida, Y., Nishi, K., and Esashi, Y. (1983b). *Evaluation of Seismic Stability of Dense Sand Layer (Part 2) – Evaluation Method by Standard Penetration Test*, Report 383026, Electric Power Central Research Institute, Japan (in Japanese).

Kokusho, T., Tanaka, Y., Kudo, K., and Kawai, T. (1995a). "Liquefaction Case Study of Volcanic Gravel Layer during 1993 Hokkaido-Nansei-Oki Earthquake," *Third International Conference on Recent Advances in Geotechnical Earthquake Engineering and Soil Dynamics*, S. Prakash, Ed., held 2-7 March 1995, St. Louis, MO, University of Missouri at Rolla, Vol. 1, pp. 235-242.

Kokusho, T., Yoshida, Y., and Tanaka, Y. (1995b). "Shear Wave Velocity in Gravelly Soils with Different Particle Gradings," *Static and Dynamic Properties of Gravelly Soils*, Geotechnical Special Publication No. 56, M. D. Evans and R. J. Fragaszy, Eds., ASCE, pp. 92-106.

Kokusho, T., Tanaka, Y., Kawai, T., Kudo, K., Suzuki, K., Tohda, S., and Abe, S. (1995c). "Case Study of Rock Debris Avalanche Gravel Liquefied During 1993 Hokkaido-Nansei-Oki Earthquake," *Soils and Foundations*, Japanese Geotechnical, Vol. 35, No. 3, pp. 83-95.

Liao, S. S. C., and Whitman, R. V. (1986). "Overburden Correction Factors for SPT in Sands," *Journal of Geotechnical Engineering*, ASCE, Vol. 112, No. 3, pp. 373-377.

Lodge, A. L. (1994). "Shear Wave Velocity Measurements for Subsurface Characterization," *Ph. D. Dissertation*, University of California at Berkeley.

Mitchell, J. K., Lodge, A. L., Coutinho, R. Q., Kayen, R. E., Seed, R. B., Nishio, S., and Stokoe, K. H., II (1994). "In situ Test Results from Four Loma Prieta Earthquake Liquefaction Sites: SPT, CPT, DMT, and Shear Wave Velocity," *Report No. UCB/EERC-94/04*, Earthquake Engineering Research Center, University of California at Berkeley, 171 p.

Olsen, R. S. (1997). "Cyclic Liquefaction Based on the Cone Penetrometer Test," *NCEER Workshop on Evaluation of Liquefaction Resistance of Soils*, Technical Report NCEER-97-0022, T. L. Youd and I. M. Idriss, Eds., held 4-5 January 1996, Salt Lake City, UT, National Center for Earthquake Engineering Research, Buffalo, NY, pp. 225-276.

Redpath, B. B. (1991). "Seismic Velocity Logging in the San Francisco Bay Area," Report to the Electric Power Research Institute, Palo Alto, CA, 34 p.

Robertson, P. K., and Campanella, R. G. (1985). "Liquefaction Potential of Sands Using the CPT," ASCE, Vol. III, GT#, pp. 384-403.

Robertson, P. K., Woeller, D. J., and Finn, W. D. L. (1992). "Seismic Cone Penetration Test for Evaluating Liquefaction Potential Under Cyclic Loading," *Canadian Geotechnical Journal*, Vol. 29, pp. 686-695.

Robertson ,P. K., and Fear, C. E. (1996). "Soil Liquefaction and Its Evaluation Based on SPT and CPT," *Symposium on Recent Developments in Seismic Liquefaction Assessment*, held 12 April, 1996, Vancouver, B.C.,

Robertson, P. K., and Wride, C.E., (1997). "Cyclic Liquefaction and its Evaluation based on the SPT and CPT," *NCEER Workshop on Evaluation of Liquefaction Resistance of Soils*, Technical Report NCEER-97-0022, T. L. Youd and I. M. Idriss, Eds., held 4-5 January 1996, Salt Lake City, UT, National Center for Earthquake Engineering Research, Buffalo, NY, pp. 41-87.

Robertson, P. K., and Wride, C. E. (1998). "Evaluating Cyclic Liquefaction Potential Using the Cone Penetration Test," *Canadian Geotechnical Journal*, Vol. 35, No. 3, pp. 441-459.

Sato, K., Kokusho, T., Matsumoto, M., and Yamada, E. (1996). "Nonlinear Seismic Response and Soil Property During Strong Motion," *Soils and Foundations, Special Issue on Geotechnical Aspects of the January 17, 1995 Hyogoken-Nambu Earthquake*, Japanes Geotechnical Society, pp. 41-52.

Seed, H. B. (1979). "Soil Liquefaction and Cyclic Mobility Evaluation for Level Ground during Earthquakes," *Journal of Geotechnical Engineering Division*, ASCE, Vol. 105, GT2, pp. 201-255.

Seed, H. B (1983). "Earthquake-Resistant Design of Earth Dams." *Proceedings, Symposium on Seismic Design of Embankments and Caverns*, held 6-10 May 1983, Philadelphia, PA, ASCE, pp. 41-64.

Seed, H. B., and de Alba, P. (1986). "Use of SPT and CPT Tests for Evaluating the Liquefaction Resistance of Sands," *Proceedings, In Situ Tests*, ASCE, pp. 281-302.

Seed, H. B., and Idriss, I. M. (1971). "Simplified Procedure for Evaluating Soil Liquefaction Potential," *Journal of the Soil Mechanics and Foundations Division*, ASCE, Vol. 97, SMP, pp. 1249-1273.

Seed, H. B., and Idriss, I. M. (1982). *Ground Motions and Soil Liquefaction During Earthquakes*, Earthquake Engineering Research Institute, Berkeley, CA, 134 p.

Seed, H. B., Idriss, I. M., and Arango, I. (1983). "Evaluation of Liquefaction Potential Using Field Performance Data," *Journal of Geotechnical Engineering*, ASCE, Vol. 109, No. 3, pp. 458-482.

Seed, H. B., Tokimatsu, K., Harder, L. F., and Chung, R. M. (1985). "Influence of SPT Procedures in Soil Liquefaction Resistance Evaluations," *Journal of Geotechnical Engineering*, ASCE, Vol. 111, No. 12, pp. 1425-1445.

Seed, R. B., and Harder, L. F., Jr. (1990). "SPT-Based Analysis of Cyclic Pore Pressure Generation and Undrained Residual Strength," *Proceedings, H. Bolton Seed Memorial Symposium*, J. M. Duncan, Ed., BiTech Publishers, Vancouver, B. C., Vol. 2, pp. 351-376.

Shen, C. K., Li, X. S., and Wang, Z. (1991). "Pore Pressure Response During the 1986 Lotung Earthquakes," *Proceedings, Second International Conference on Recent Advances in Geotechnical Earthquake Engineering and Soil Dynamics*, S. Prakash, Ed., held 11-15 March 1991, St. Louis, MO, University of Missouri at Rolla, Vol. I, pp. 557-563.

Shibata, T. (1981). "Relations Between N-Value and Liquefaction Potential of Sand Deposits," *Proceedings, 16th Annual Convention of Japanese Society of Soil Mechanics and Foundation Engineering*, pp. 621-624 (in Japanese).

Shibata, T., Oka, F., and Ozawa, Y. (1996). "Characteristics of Ground Deformation Due to Liquefaction," *Soils and Foundations, Special Issue on Geotechnical Aspects of the January 17, 1995 Hyogoken-Nambu Earthquake*, japans Geotechnical Society, pp. 65-79.

Shibata, T., and Teparaska, W. (1988). "Evaluation of Liquefaction Potential of Soils Using Cone Penetration Tests," *Soils and Foundations*, Japanese Society of Soil Mechanics and Foundation Engineering,Vol. 28, pp. 49-60.

Stark, T. D., and Olson, S. M. (1995). "Liquefaction Resistance Using CPT and Field Case Histories," *Journal of Geotechnical Engineering*, ASCE, Vol. 121, No. 12, pp. 856-869.

Stokoe, K., H., II, Andrus, R. D., Bay, J., A., Fuhriman, M. D., Lee, N. J., and Yang, Y. (1992). "SASW and Crosshole Seismic Test Results from Sites that Did and Did not Liquefy During the 1989 Loma Prieta, California Earthquake," Geotechnical

Engineering Center, Department of Civil Engineering, The University of Texas at Austin.

Stokoe, K. H., II, and Nazarian, S. (1985). "Use of Rayleigh Waves in Liquefaction Studies," *Measurement and Use of Shear Wave Velocity for Evaluating Dynamic Soil Properties*, R. D. Woods, Ed., ASCE, pp. 1-17.

Stokoe, K. H., II, Nazarian, S., Rix, G. J., Sanchez-Salinero, I., Sheu, J. C., and Mok, Y. J. (1988a). "In Situ Seismic Testing of Hard-to-Sample Soils by Surface Wave Method," *Earthquake Engineering and Soil Dynamics II—Recent Advances in Ground-Motion Evaluation*, Geotechnical Special Publication No. 20, J. L. Von Thun, Ed., ASCE, pp. 264-289.

Stokoe, K. H., II, Andrus, R. D., Rix, G. J., Sanchez-Salinero, I., Sheu, J. C., and Mok, Y. J. (1988b). "Field Investigation of Gravelly Soils Which Did and Did not Liquefy During the 1983 Borah Peak, Idaho, Earthquake," *Geotechnical Engineering Report GR 87-1*, The University of Texas at Austin, 206p.

Stokoe, K. H., II, Roesset, J. M., Bierschwale, J. G., and Aouad, M. (1988c). "Liquefaction Potential of Sands from Shear Wave Velocity," *Proceedings, Ninth World Conference on Earthquake Engineering*, Tokyo, Japan, Vol. III, pp. 213-218.

Sykora, D. W., and Stokoe, K. H., II (1982). :Seismic Investigation of Three Heber Road Sites After 15 October, 1979 Imperial Valley Earthquake," *Geotechnical Engineering Report GR82-24*, The University of Texas at Austin, 76 p.

Tokimatsu, K., and Yoshimi, Y. (1983). "Empirical Correlation of Soil Liquefaction Based on SPT N-Value and Fines Content," *Soils and Foundations*, Japanese Society of Soil Mechanics and Foundation Engineering, Vol. 23, No. 4, pp. 56-74.

Tokimatsu, K., Kuwayama, S., and Tamura, S. (1991a). "Liquefaction Potential Evaluation Based on Rayleigh Wave Investigation and Its Comparison with Field Behavior," *Proceedings, Second International Conference on Recent Advances in Geotechnical Earthquake Engineering and Soil Dynamics*, S. Prakash, Ed., held 11-15 March 1991, St. Louis, MO, University of Missouri at Rolla, Vol. I, pp. 357-364.

Tokimatsu, K., Kuwayma, S., Abe, A., Nomura, S., and Tamura, S. (1991b). "Considerations to Damage Patterns in the Marina District During the Loma Prieta Earthquake Based on Rayleigh Wave Investigation." *Proceedings, Second International Conference on Recent Advances in Geotechnical Earthquake Engineering and Soil Dynamics*, S. Prakash, Ed., held 11-15 March 1991, St. Louis, MO, University of Missouri at Rolla, Vol. II, pp.1649-1654.

Tokimatsu, K., and Uchida, A. (1990). "Correlation Between Liquefaction Resistance and Shear Wave Velocity," *Soils and Foundations*, Japanese Society of Soil Mechanics and Foundation Engineering, Vol. 30, No. 2, pp. 33-42.

Yoshimi, Y., Tokimatsu, K., Kaneko, O., and Makihara, Y. (1984). "Undrained Cyclic Shear Strength of Dense Niigata Sand," *Soils and Foundations*, Japanese Society of Soil Mechanics and Foundation Engineering, Vol. 24, No. 4. pp. 131-145.

Yoshimi, Y., Tokimatsu, K., and Hosaka, Y. (1989). "Evalustion of Liquefaction Resistance of Clean Sands Based on High-Quality Undisturbed Samples," *Soils and Foundations*, Japanese Society of Soil Mechanics and Foundation Engineering, Vol. 29, No. 1, pp. 93-104.

Youd, T. L., and Noble, S. K. (1997). "Liquefaction Criteria Based on Statistical and Probabilistic Analyses," *NCEER Workshop on Evaluation of Liquefaction Resistance of Soils,*, Technical Report NCEER-97-00222, T. L. Youd and I. M. Idriss, Eds., held 4-5 January 1996, Salt Lake City, UT, National Center for Earthquake Engineering Research, Buffalo, NY, pp. 210-215.

Youd, T. L., and Bennett, M. J. (1983). "Liquefaction Sites, Imperial Valley, California," *Journal of Geotechnical Engineering*, ASCE, Vol. 109, No. 3, pp. 440-457.

Youd, T. L., Harp, E. L., Keefer, D. K., and Wilson, R. C. (1985). "The Borah Peak, Idaho Earthquake of October 28, 1983 – Liquefaction," *Earthquake Spectra*, Earthquake Engineering Research Institute, El Cerrito, CA, Vol. 2, No. 1, pp. 71-89.

Youd, T. L., and Holzer, T. L. (1994). :Piezometer Performance at Wildlife Liquefaction Site, California," *Journal of Geotechnical Engineering*, ASCE, Vol. 120, No. 6, pp. 975-995.

Youd, T. L., and Hoose, S. N. (1978). "Historic Ground failures in Northern California Triggered by Earthquakes," *U.S. Geological Survey Professional Paper993*, U.S. Government Printing Office, Washington D.C., 177 p.

Youd, T. L., and Idriss, I. M., eds. (1997). *NCEER Workshop on Evaluation of Liquefaction Resistance of Soils,*, Technical Report NCEER-97-00222, T. L. Youd and I. M. Idriss, Eds., held 4-5 January 1996, Salt Lake City, UT, National Center for Earthquake Engineering Research, Buffalo, NY, 276 p.

Youd, T. L., Idriss, I. M., Andrus, R. D., Arango, I., Castro, G., Christian, J. T., Dobry, R., Finn, W. D. L., Harder, L. F., Jr., Hynes, M. E., Ishihara, K., Koester, J. P., Liao, S. S. C., Marcuson, W. F., III, Martin, G. R., Mitchell, J. K., Moriwaki, Y., Power, M. S., Robertson, P. K., Seed, R. b., and Stokoe, K. H., II (1997). :Summary Report," *NCEER Workshop on Evaluation of Liquefaction Resistance of Soils,*, Technical Report NCEER-97-00222, T. L. Youd and I. M. Idriss, Eds., held 4-5 January 1996, Salt Lake City, UT, National Center for Earthquake Engineering Research, Buffalo, NY, pp. 1-40.

VITA

James Calvin Chrisley was born in Panama City, Florida on December 11, 1971, the son of Wiley L. Chrisley and Geraldine A. Chrisley. After completing his work at Hackettstown High School, Hackettstown, New Jersey, in 1990, he entered The United States Air Force Academy in Colorado Springs, Colorado. He received the degree of Bachelor of Science from The United States Air Force Academy in June, 1994. Upon graduation, he entered the United States Air Force as a Second Lieutenant and worked as a civil engineer. In August, 1998, he entered the Graduate School at The University of Texas.

Permanent Address: 30 Vienna Hills Road
Hackettstown , NJ 07840

This report was typed by the author.